BRL

MEMORANDUM REPORT NO. 1809

ATTENUATION OF PEAKED AIR SHOCK WAVES IN SMOOTH TUNNELS

by

George A. Coulter

November 1966

Distribution of this document is unlimited.

U. S. ARMY MATERIEL COMMAND
BALLISTIC RESEARCH LABORATORIES
ABERDEEN PROVING GROUND, MARYLAND

84

B A L L I S T I C   R E S E A R C H   L A B O R A T O R I E S

MEMORANDUM REPORT NO. 1809

NOVEMBER 1966

ATTENUATION OF PEAKED AIR SHOCK WAVES IN SMOOTH TUNNELS

George A. Coulter

Terminal Ballistics Laboratory

This work was partially supported by Defense Atomic Support Agency, NWER Sub-Task No. 13.111.

A B E R D E E N   P R O V I N G   G R O U N D,   M A R Y L A N D

B A L L I S T I C   R E S E A R C H   L A B O R A T O R I E S

MEMORANDUM REPORT NO. 1809

George A. Coulter/ilm
Aberdeen Proving Ground, Md.
November 1966

ATTENUATION OF PEAKED AIR SHOCK WAVES IN SMOOTH TUNNELS

ABSTRACT

The attenuation of shock-front pressure for peaked air shock waves was measured along straight, smooth-wall test sections of 1-, 2-, and 4-inch inside diameter shock tubes over travel distances up to 520-tunnel diameters. Shock overpressures between 50 and 450 psi for an ambient pressure of 1 atmosphere were produced by the use of helium, or by burning M-9 propellant in the driver sections of the shock tubes. The lengths of the shock tube driver sections were changed to vary the shape of the shock waveform which caused the shock front pressure to attenuate differently with distance. Pressure-time records are shown from piezoelectric pressure gages placed at ten test positions along the shock tube. The experimental peak shock pressures are compared to attenuation equations of the form:

$$P_s' = P_s\, e^{-[A(X/D)+K(X/t_1)]}$$

and

$$P_s' = P_s \left\{ \frac{1}{1 + \tan\left[\left(\frac{\pi}{2}\right)\left(\frac{X}{X + E}\right)\right]} \right\}^{e^{V(X/D)}} .$$

The parameter, t_1/D, (the shock waveform's initial slope intercept on the time axis divided by the tunnel diameter) is used to compare the shock front attenuation in the three shock tubes used.

TABLE OF CONTENTS

LIST OF TABLES

LIST OF FIGURES

LIST OF FIGURES (Contd)

LIST OF SYMBOLS

a	Sound speed
A	Viscous attenuation coefficient
α	Waveform parameter
D	Diameter of cylindrical tunnel
E	Rarefaction attenuation parameter
K	Integration function, $\left(\frac{1}{U_2} - \frac{1}{u_2 + a_2}\right)$
L_c	Driver or compression chamber length
P	Pressure
P_s	Shock overpressure, $(P_2 - P_1)$
P_s'	Shock overpressure after attenuation
t	Time
t_i	Slope intercept on the time axis of pressure-time records
t_{io}	Time intercept for input shockwave at $X = 0$
T	Temperature
τ	Positive duration of shock wave
u_2	Particle velocity behind shock wave
U_2	Shock front velocity
V	Viscous attenuation parameter
X	Distance along tunnel

LIST OF SYMBOLS (Contd)

<u>Subscripts</u>

o   Refers to parameters at X = 0

1   Refers to ambient conditions ahead of the shock

2   Refers to conditions behind the incident shock

<u>Superscripts</u>

'   Prime refers to conditions after shock wave travels X - distance along the tunnel

<u>Double Subscripts</u>

ij   Means ratio, e.g., $P_{ij} = P_i/P_j$

1. INTRODUCTION

The design engineer needs to be able to predict accurately the behavior of shock waves inside ventilation ducts and access passageways if he is to effectively design underground structures where blast valves and doors are to be used to protect against air blast from external bomb explosions. The present experiment was conducted to furnish data for that part of the problem concerned with the attenuation of the peak overpressure of the shock wave as it travels along a smooth duct or tunnel.

The present work extends the shock pressure range of previous work[1-7*] and shows how the attenuation of peak shock waves traveling in long smooth tunnels varies as a function of the pressure of the input shock wave and the steepness of the pressure-time waveform. The data obtained are compared to an attenuation equation of the form:

$$P_s' = P_s \, e^{-[A(X/D)+K(X/t_1)]} ,$$

where the first term in the exponent represents the viscous part of the attenuation[1] proportional to the travel distance in tunnel diameters, X/D. The second term describes the attenuation due to rarefaction catch-up at the shock front[5] which is proportional to distance of travel and inversely proportional to the time-axis intercept, t_1. The intercept is a measure of the steepness of the rarefaction pressure-time decay behind the shock front. The parameter, t_1, is used to compare various wave-shapes for different tunnel sizes.

The data are also compound to predictions from an empirically derived attenuation equation,

$$P_s' = P_s \left\{ \frac{1}{1 + \tan\left[\left(\frac{\pi}{2}\right)\left(\frac{X}{X + E}\right)\right]} \right\}^{e^{V(X/D)}} ,$$

where V and E are experimentally determined parameters.

---

* *Superscript numbers denote references which may be found on page 53.*

2. EXPERIMENTAL APPARATUS

The experimental apparatus may be divided into three major parts: (a) the shock tubes, (b) the pressure transducers, and (c) the recording system.

Three shock tubes of 1-, 2-, and 4-inch inside diameter, each with variable driver lengths, were used during the experiment. Descriptions of the shock tubes are given in Table I. The shock tubes were operated in a normal manner with either compressed helium or burning M-9 propellant[8] used in the driver section to break a diaphragm which initially separated the driver gas from air at 1 atmosphere of pressure in the test section. The driver pressure determined the input shock pressure in the test section, and the driver length determined the rarefaction steepness for the wave shape. The shock waves used during the test were controlled in this way.

The pressure-time profile of the shock wave was measured by pressure transducers threaded into the wall at positions along the test section. A schematic diagram of the 2-inch shock tube is given in Figure 1 and is representative of the other two shock tubes. Piezoelectric transducers with either ceramic or crystal elements were used in the test positions. The transducers were built at the BRL Shock Tube Facility and have been described in an earlier report.[9]

The transducer output from each test position was recorded by a multi-channel galvanometer-oscillograph system,[10] or on Polaroid film recorded by a Tektronix 565 oscilloscope with a Kistler Model 566 charge amplifier. A block diagram of the multi-channel recording system is shown in Figure 2.

3. RESULTS

Representative pressure-time traces recorded from the test positions along the 2-inch shock tube are shown in Figures 3 to 6. The dotted risetime lines have been added to make the traces easier to follow. The variation in rarefaction steepness of the wave shape at the input position

(1) follows the change in shock tube driver length. With travel distance along the test section, the traces also show a less steep decay and a longer total positive duration, τ. The time-axis intercept, t_i, is used as a measure of the steepness of the rarefaction decay behind the shock front. This idea is illustrated in Figure 7. A smaller time intercept (steep slope) causes greater shock front attenuation than does a larger time intercept (shallow slope).

Table II presents the measured attenuated values of peak pressure and time intercepts for representative input shock waves recorded from each of the shock tubes. Pressure-time traces and attenuation data from the entire test range of input shock pressures are presented in Appendices A and B. Graphs of peak pressure as a function of travel distance in tunnel diameters taken from the complete data tables in the Appendices are shown in Figures 8 through 16.

If the attenuation data are grouped according to the factor, t_i/D, it becomes possible to compare directly the data from the three different diameter sizes of the shock tubes. Both attenuation caused by rarefaction catch-up and that due to viscious effects from the tunnel wall are represented by t_i and D, respectively.

Combined plots are shown as a function of the factor, t_i/D, in Figures 17 through 19 in order of increasing input shock pressure used during the experiments. Figure 20 does show, however, weak dependence upon input pressure for a constant t_i/D. Use of the factor t_i/D in this manner should permit scaling to other tunnel sizes.

4. COMPARISON WITH THEORY

Clark[5] has shown that a peaked shock wave traveling along a smooth-wall tunnel should decrease in peak pressure with travel distance according to the relationship:

$$P'_{21} - 1 = (P_{21} - 1)e^{-[(K/t_i)+(1/CD)]X} \quad (1)$$

where P'_{21} is the shock pressure ratio remaining after a shock wave of

input pressure ratio, P_{21}, has traveled a distance, X, in a tunnel of diameter, D. Rewriting Equation (1) in terms of shock overpressure and rearranging by writing $A = 1/C$ gives:

$$P_s' = P_s \, e^{-[A(X/D)+K(X/t_1)]} , \qquad (2)$$

where P_s' is the remaining peak shock pressure after an input wave of pressure, P_s, travels a distance, X, in a smooth wall tunnel or duct of diameter, D.

The first term of the exponential of Equation (2) gives the viscous part of the attenuation where A is a coefficient equal to 1/C in Equation (1). Reference 1 has given A an average value of 24×10^{-4} with quite a wide range (20 percent) of scatter which probably hides any dependence upon D, P_{21}, P_1, or X/D which may be present.

Clark[11] has changed the viscous attenuation factor in Equation (1) to give an additional dependence upon the pressure ratio, P_{21}. The differential form is:

$$\frac{dP_{21}}{dx} = -\frac{A'}{D}\sqrt{\frac{P_{21}}{6 + P_{21}}}\,(P_{21} - 1) , \qquad (3)$$

as compared to the simpler form[5],

$$\frac{dP_{21}}{dx} = -\frac{A}{D}(P_{21} - 1) , \qquad (4)$$

where the A of Equation (4) has been replaced by $A'\sqrt{(P_{21})/(6 + P_{21})}$ in Equation (3). The constants of Reference 11 may be rearranged to give a value of $A = 19.46 \times 10^{-4}$ for $P_{21} = 1$, and at very large values of P_{21}, $A \rightarrow 51.48 \times 10^{-4}$.

An average value of $A = 20 \times 10^{-4}$ was obtained for a pressure ratio range of $P_{21} = 1.68$ to 27.5 during the present experiment by adding a longer 13-foot driver section to the 2-inch shock tube to give initially only viscous attenuation because the rarefaction wave had not overtaken the shock front at the measurement positions. References 5 and 6 report

values for A above 30×10^{-4} for similar pressure levels. Due to such large variations in the value of A, the intermediate average value of 24×10^{-4} given in Reference 1 will be used to compare the present results to the theory.

The second term in the exponential of Equation (2) gives the contribution to the attenuation caused by rarefaction catch-up. The K is plotted in Figure 21 as a function of shock overpressure, P_s. The time axis intercept, t_i, is measured from the given pressure-time waveform for the input shock wave at X = 0. As the peaked shock wave travels over the distance, X, in a tunnel, t_i will increase. Accordingly, the rate of attenuation with distance slows. It appears necessary to know how t_i increases in order to predict accurately the attenuation with distance.

Clark[5] has given expressions for the new time intercept and new positive duration after a travel of distance, X, in the tunnel:

$$t_i' = t_i + \frac{t_i}{\tau}\left[\frac{1}{a_1} - \frac{1}{U_2}\right]X \ , \tag{5}$$

and

$$\tau' = \tau + \left[\frac{1}{a_1} - \frac{1}{U_2}\right] \ . \tag{6}$$

The expansion factor in the bracket is plotted in Figure 22. The ratio of the time intercept to positive duration, t_i/τ, is a relative measure of the steepness of the rarefaction decay of the shock wave. For a simple exponential waveform (Friedlander), this ratio may be a constant as a shock wave travels along a tunnel but can, and usually does, increase with travel along a tunnel. Some variation in the ratio t_i/τ in Equation (5) is needed, or a new expression for t_i' is needed in order to make accurate attenuation predictions. A constant value of t_i/τ predicts too little pressure because, experimentally, the value of t_i/τ increases with travel distance in the tunnel, thus causing less attenuation than expected.

One way of predicting the ratio, t_1'/τ, along the tunnel is to divide the complex input waveform at X = 0 into simple exponentials of the form,

$$P(t) = P(o)\ e^{-\alpha t} \ . \tag{7}$$

Then an assumption is made that the ratio, t_1'/τ', at any distance, X, along the tunnel is related by Equation (8) to those regions corresponding to the two or more simple exponentials found in the input waveform:

$$\frac{t_1'}{\tau'} = \frac{1}{\alpha \tau_o} \ . \tag{8}$$

Figure 23 shows how a given input pressure-time waveform may be plotted[12] on semilog graph paper to determine these regions of simple exponentials. For waveforms not going to zero pressure, a value of τ_o may be found by replotting the waveform with time on the log axis of a semilog plot and extrapolating the curve to zero pressure. The crossing point on the time axis is then chosen to be τ_o. Values of the waveform parameter, α, are shown for each of the straight-line regions. Equation (8) may be used instead of Equation (5) above, if the given input waveform is a complex one.

Broh[13] has assumed an attenuation function which includes both viscous and rarefaction parts. He arrived at the function by dimensional analysis and the given boundary conditions, $P_s' = P_s$ at X = 0, and $P_s' = o$ at $X = \infty$. His function has the advantage that it does not use previous, stepwise predictions to arrive at a prediction for a given distance. Only the time intercept, t_1, for the initial wave at X = 0 and the tunnel diameter is used. The function may be written:

$$P_s' = P_s \left\{ \frac{1}{1 + t_\theta \cdot \left[\left(\frac{\pi}{2}\right)\left(\frac{X}{X + E}\right) \right]} \right\} e^{V(X/D)} \tag{9}$$

where V is an experimentally determined viscous attenuation parameter and E is an experimentally determined rarefaction attenuation parameter. These two parameters are plotted in Figures 24 and 25. Equation (9) also gives predicted values too small after distances of X/D > 150.

Examples of each of the prediction methods discussed are shown in Table III and Figure 26 for three representative sets of experimental data obtained.

5. CONCLUSIONS

The attenuation of peak shock waves traveling along test sections of 1-, 2-, and 4-inch shock tubes has been measured for initial input pressure ratios up to approximately 30. Similarly shaped plots of peak pressure as a function of travel distance in diameters, X/D, were obtained from the data through the pressure range tested. The data for a given value of starting shock-front pressure could be represented by a single attenuation versus travel distance plot if the values of t_i/D were the same. It seems possible, therefore, to represent many combinations of peaked shock waves and tunnel sizes by a single attenuation plot for like values of t_i/D.

In addition to being used in the scaling parameter, the time intercept, t_i, was found to be quite critical to accurate predictions of attenuation. The experimental data were found to agree fairly well with pressures calculated from the equations of Clark[5] and Broh[13], until the value of attenuated pressure reached a level corresponding to a change in the value of the ratio, t_i/τ'. A correction was made to Clark's prediction method by assuming $t_i'/\tau' = 1/\alpha\tau_o$, where $1/\alpha\tau_o$ is the shape parameter for regions of the input pressure-time record which obey the simple exponential $P(t) = P(o)\, e^{-\alpha t}$. The attenuation equation of Clark, Equation (2), gave better pressure predictions when the new values of t_i' were used in the calculations. No attempt was made to modify Broh's prediction method.

ACKNOWLEDGMENTS

The author wishes to thank Mr. Rodney Abrahams and Mr. William Matthews for assistance with the recording system used to acquire the experimental data.

GEORGE A. COULTER

TABLE I

SHOCK TUBE SPECIFICATIONS

Shock Tube	Description	Driver Lengths	Driver Gas, Diaphragm Material
1-inch ID. Maximum length approximately 44.5 feet.	Seamless, round, cold drawn, low carbon, mechanical steel tubing - 2" OD x 1/2" wall thickness. Slip-on forged steel flanges 1-1/2" pipe size, 6" OD, 150#. Sections bolted with 3/4" x 3" long bolts.	1", 3", and 9"	Helium 2SO Aluminum .032" thick .020" thick Mylar .020" thick .010" thick .005" thick
2-inch ID. Maximum length approximately 89 feet.	Seamless, round, cold drawn, low carbon, mechanical steel tubing - 3" OD x 1/2" wall thickness. Slip-on forged steel flanges 2-1/2" pipe size, 7"OD, 150#. Sections bolted with 3/4" x 3" long bolts.	2", 6", 18", and 13'	Helium or M-9 Propellant Burning 2SO Aluminum .064" thick .040" thick .032" thick .020" thick .010" thick
4-inch ID. Maximum length approximately 113 feet.	Seamless, round, cold drawn, low carbon, mechanical steel tubing - 5-1/2" OD x 3/4" wall thickness. Slip-on forged steel flanges 5" pipe size, 11" OD, 300#. Sections bolted with 7/8" x 4" long bolts.	4", 12", and 36"	Helium Soft Copper .048" thick 2SO Aluminum .092" thick .064" thick .040" thick .020" thick

TABLE II

SHOCK FRONT OVERPRESSURE AS A FUNCTION OF DISTANCE OF TRAVEL

Position No.	P_s, psi	X, ft.	$\frac{X}{D}$	t_1, ms	$\frac{t_1}{D}$, $\frac{ms}{in.}$	Remarks
1	191	0.83	10	Step		1"ID Shock Tube
2	192	2.08	25	0.90	.90	L_c = 9"
3	187	3.75	45	1.26		He - Air
4	147	5.83	70	1.31		
5	118	7.92	95	1.41		
6	98	10.00	120	1.99		
7	78	11.99	145	1.88		
8	38	22.50	270	3.85		
9	23	32.92	395	9.56		
10	14	43.33	520	-		
1	207	2.00	12	Step		2" ID Shock Tube
2	201	3.83	23	Step		L_c = 18"
3	203	8.00	48	1.67	.84	He - Air
4	160	12.17	73	2.20		
5	124	16.33	98	2.99		
6	104	20.50	123	3.66		
7	88	24.67	148	3.66		
8	44	45.50	273	7.59		
9	27	66.53	398	14.23		
10	16	87.17	523	-		
1	212	4.00	12	Step		4" ID Shock Tube
2	205	7.67	23	Step		L_c = 36"

TABLE II (Contd)

Position No.	P_s, psi	X, ft.	$\frac{X}{D}$	t_i, ms	$\frac{t_i}{D}$, $\frac{ms}{in.}$	Remarks
3	187	16.00	48	Step		He - Air
4	174	24.33	73	4.49	1.12	
5	148	32.67	98	4.92		
6	116	41.00	123	5.59		
7	94	49.33	148	7.59		
8	-	57.67	173	-		
9	38	66.00	198	-		
10	35	99.33	298	-		
11	33	108.33	325	-		
1	183	0.83	10	0.41	0.41	1" ID Shock Tube
2	142	2.08	25	0.62		L_c = 3"
3	100	3.75	45	1.13		He - Air
4	71	5.83	70	1.49		
5	60	7.92	95	1.80		
6	43	10.00	120	2.42		
7	46	11.99	145	2.67		
8	22	22.50	270	5.97		
9	15	32.92	395	28.3		
10	10	43.33	520	-		
1	203	2.00	12	Step		2" ID Shock Tube
2	188	3.83	23	0.70	0.35	L_c = 6"
3	102	8.00	48	1.26		He - Air

TABLE II (Contd)

Position No.	P_s, psi	X, ft.	$\frac{X}{D}$	t_1, ms	$\frac{t_1}{D}$, $\frac{ms}{in.}$	Remarks
4	77	12.17	73	2.46		
5	61	16.33	98	2.93		
6	58	20.50	123	3.40		
7	41	24.67	148	3.82		
8	22	45.50	273	11.34		
9	15	66.53	398	15.85		
10	10	87.17	523	-		
1	195	4.00	12	Step		4" ID Shock Tube
2	177	7.67	23	1.94		L_c = 12"
3	119	16.00	48	2.84		He - Air
4	84	24.33	73	3.93		
5	68	32.67	98	4.77		
6	54	41.00	123	6.44		
7	41	49.33	148	8.96		
8	38	57.67	173	10.46		
9	30	66.00	198	-		
10	18	99.33	298	-		
11	17	108.33	325	-		
1	157	0.83	10	0.34	0.34	1" ID Shock Tube
2	88	2.08	25	0.46		L_c = 1"
3	59	2.75	45	0.83		He - Air
4	43	5.83	70	1.56		

TABLE II (Contd)

Position No.	P_s, psi	X, ft.	$\frac{X}{D}$	t_i, ms	$\frac{t_i}{D'}$, $\frac{ms}{in.}$	Remarks
5	33	7.92	95	4.15		
6	28	10.00	120	5.56		
7	27	11.99	145	7.11		
8	16	22.50	270	19.3		
9	12	32.92	395	-		
10	9	43.33	520	-		
1	154	2.00	12	.42	.21	2" ID Shock Tube
2	104	3.83	23	.75		L_c = 2"
3	59	8.00	48	1.30		He - Air
4	44	12.17	73	2.15		
5	31	16.33	98	3.49		
6	28	20.50	123	4.16		
7	22	24.67	148	5.36		
8	13	45.50	273	10.48		
9	8	66.53	398	27.91		
10	6.4	87.17	523	-		
1	142	4.00	12	.91	.25	4" ID Shock Tube
2	103	7.67	23	1.50		L_c = 4"
3	58	16.00	48	2.67		He - Air
4	43	24.33	73	3.61		
5	33	32.67	98	5.87		
6	26	41.00	123	8.39		
7	22	49.33	148	11.1		
8	19	57.67	173	13		
9	16	66.00	198	24		
10	10.6	99.33	298	-		
11	10.1	108.33	325	-		

TABLE III

COMPARISON OF DATA WITH THEORY

Experimental Data				Theory-Clark, Ref. 5			Theory, Brdh, Ref. 13			Theory, Ref. 5, Modified			Remarks
$\frac{X}{D}$	P_s, psi	t_1, ms	τ, ms	P_s, psi	t_1, ms	τ, ms	P_s, psi	E, ft	V	P_s, psi	t_1, ms	τ, ms	
48	203	1.67	11	203	1.67	11.0	203	13.5	14.6×10^{-4}	203	1.48	11	$\frac{t_{io}}{D} = .84 \frac{ms}{in.}$,
73	160	2.20		166	2.08	12.7	144			164	1.84		
98	124	2.99		139	2.49	15.2	116			135	2.18		D = 2"
123	104	3.66		117	2.90	17.7	97			112	3.67		
148	88	3.66		100	3.29	20.0	82			97	4.13		$T_1 = 20^oC$
273	44	7.59		45	5.15	31.4	39			49	6.33		
398	27	14.23		22	6.59	40.1	18			27	13.1		P_1 = 14.8 psi
523	16	—		12	7.63	46.4	7.2			16.6	15.2		
23	188	0.70	4.8	188	0.70	4.8	188	5.45	8.6×10^{-4}	188	0.60	4.8	$\frac{t_{io}}{D} = .35 \frac{ms}{in.}$,
48	102	1.26		127	1.08	7.4	102			120	0.93		
73	77	2.46		92	1.43	9.8	75			82	2.21		D = 2"
98	61	2.93		69	1.64	12.0	60			67	2.43		
123	58	3.40		53	1.92	14.1	49			54	2.41		$T_1 = 22^oC$
148	41	3.82		41	2.17	15.9	40			43	2.77		
273	22	11.34		11	3.31	24.3	19			21	7.89		P_1 = 14.8 psi
398	15	15.85		4.3	3.88	28.4	9.2			12	9.59		
523	10	—		2.3	4.16	35.5	4.5			6.8	12.92		
12	154	0.42	1.8	154	0.42	1.8	154	3.46	5.9×10^{-4}	154	0.38	1.8	$\frac{t_{io}}{D} = .21 \frac{ms}{in.}$,
23	104	0.75		115	0.67	2.9	96			112	0.61		
48	59	1.30		70	1.22	5.2	59			65	1.68		D = 2"
73	44	2.15		50	1.71	7.4	44			49	2.32		
98	31	3.49		37	2.12	9.1	34			39	3.70		$T_1 = 22^oC$
123	28	4.16		28	2.50	10.8	28			33	4.39		
148	22	5.36		22	2.80	11.9	23			28	5.02		P_1 = 14.9 psi
273	13	10.48		7.4	4.28	18.1	11			13.2	7.89		
398	8	27.91		3.5	5.01	21.2	6.2			7.4	9.77		
523	6.4	—		2.1	5.39	22.9	3.3			5.6	11.05		

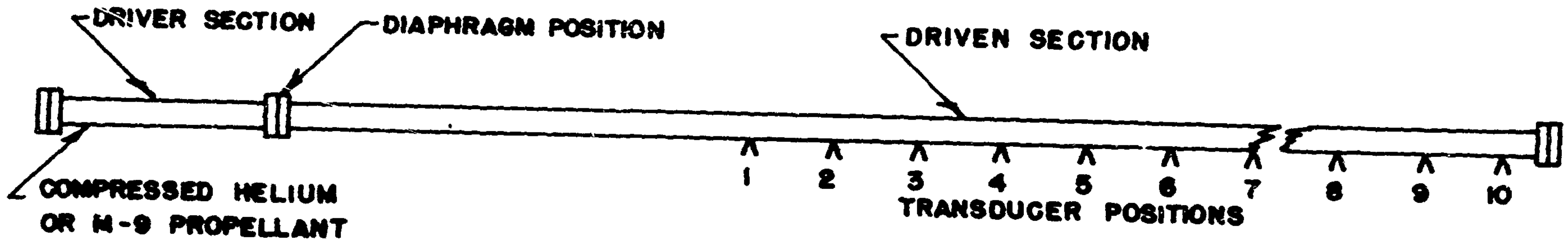

DRIVER LENGTHS
2 IN
6 IN
18 IN
13 FT

POSITIONS	X, FT	X/D, DIA
1	2	12
2	3.83	23
3	8.00	48
4	12.17	73
5	16.33	98
6	20.50	123
7	24.67	148
8	45.50	273
9	66.33	398
10	87.17	523

FIG. 1 SCHEMATIC OF 2-INCH ID SHOCK TUBE

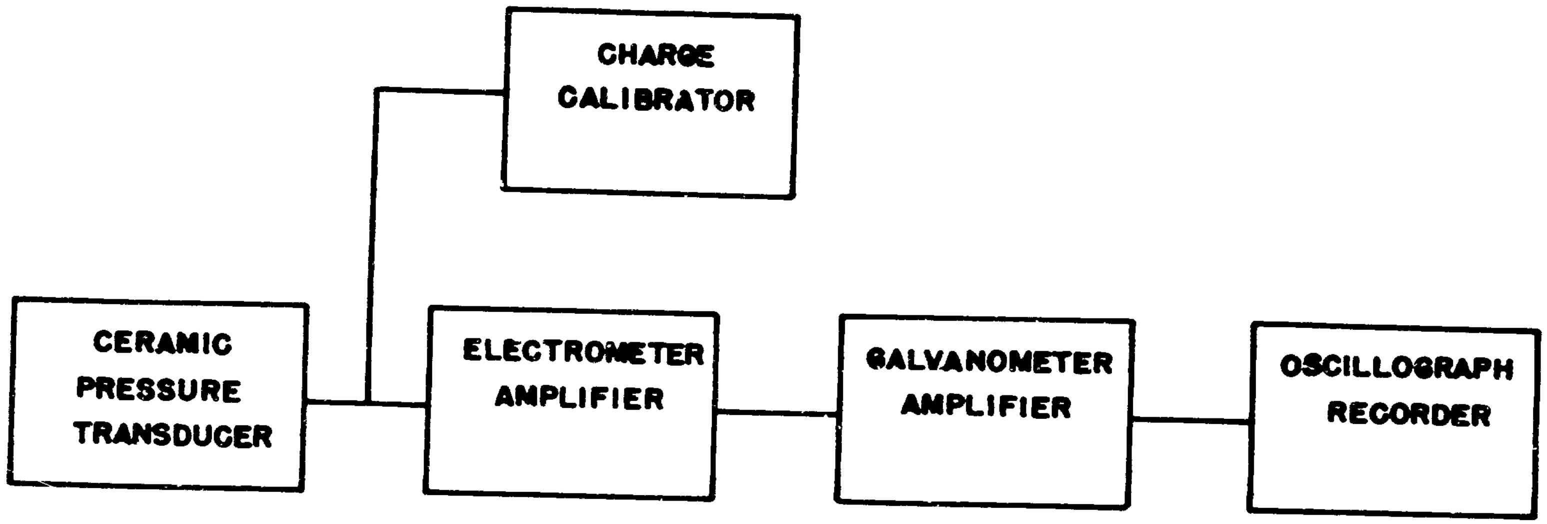

FIG. 2 BLOCK DIAGRAM OF RECORDING SYSTEM

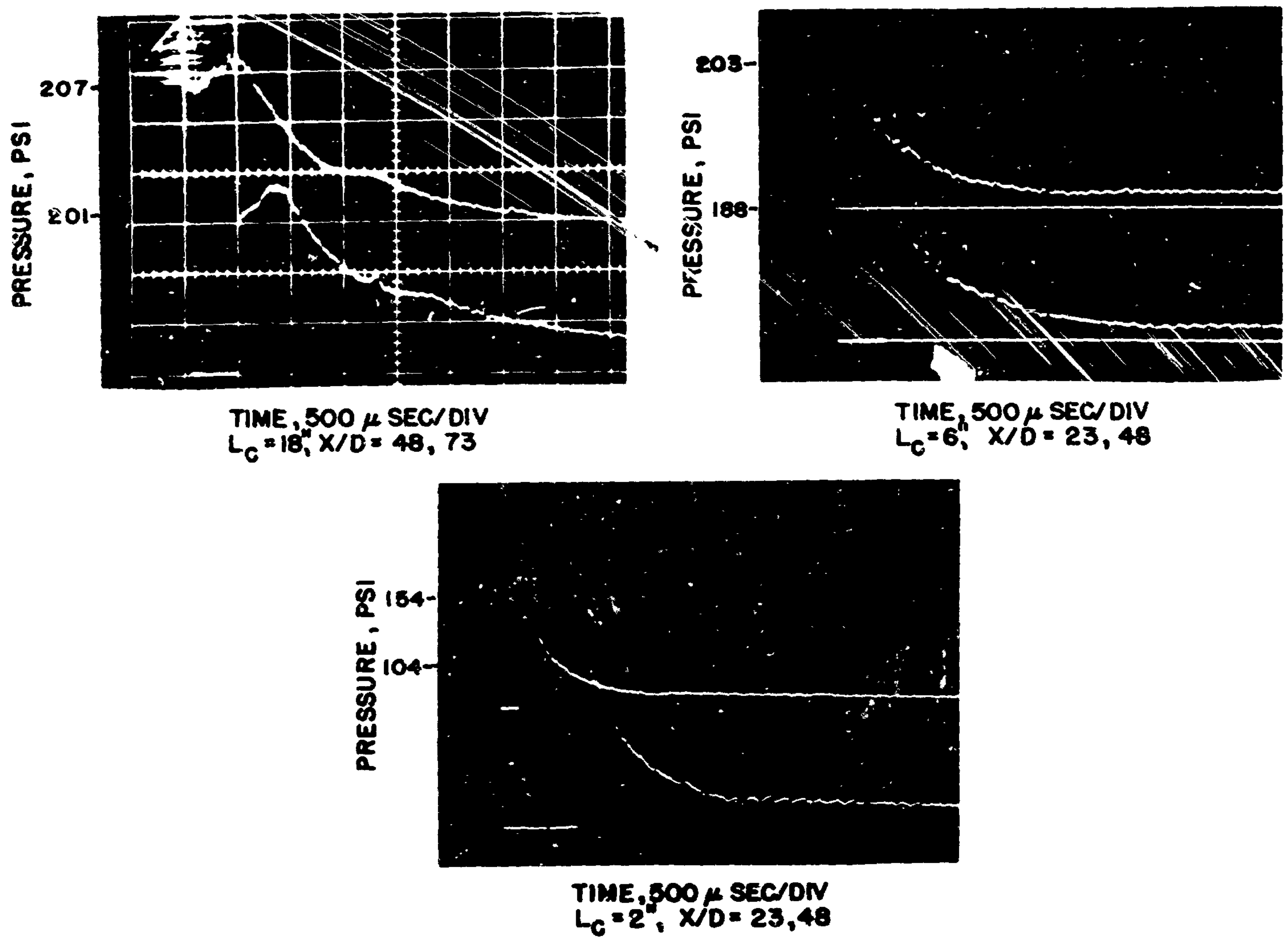

FIG. 3 PRESSURE - TIME RECORDS FROM 2-INCH SHOCK TUBE - HELIUM DRIVER

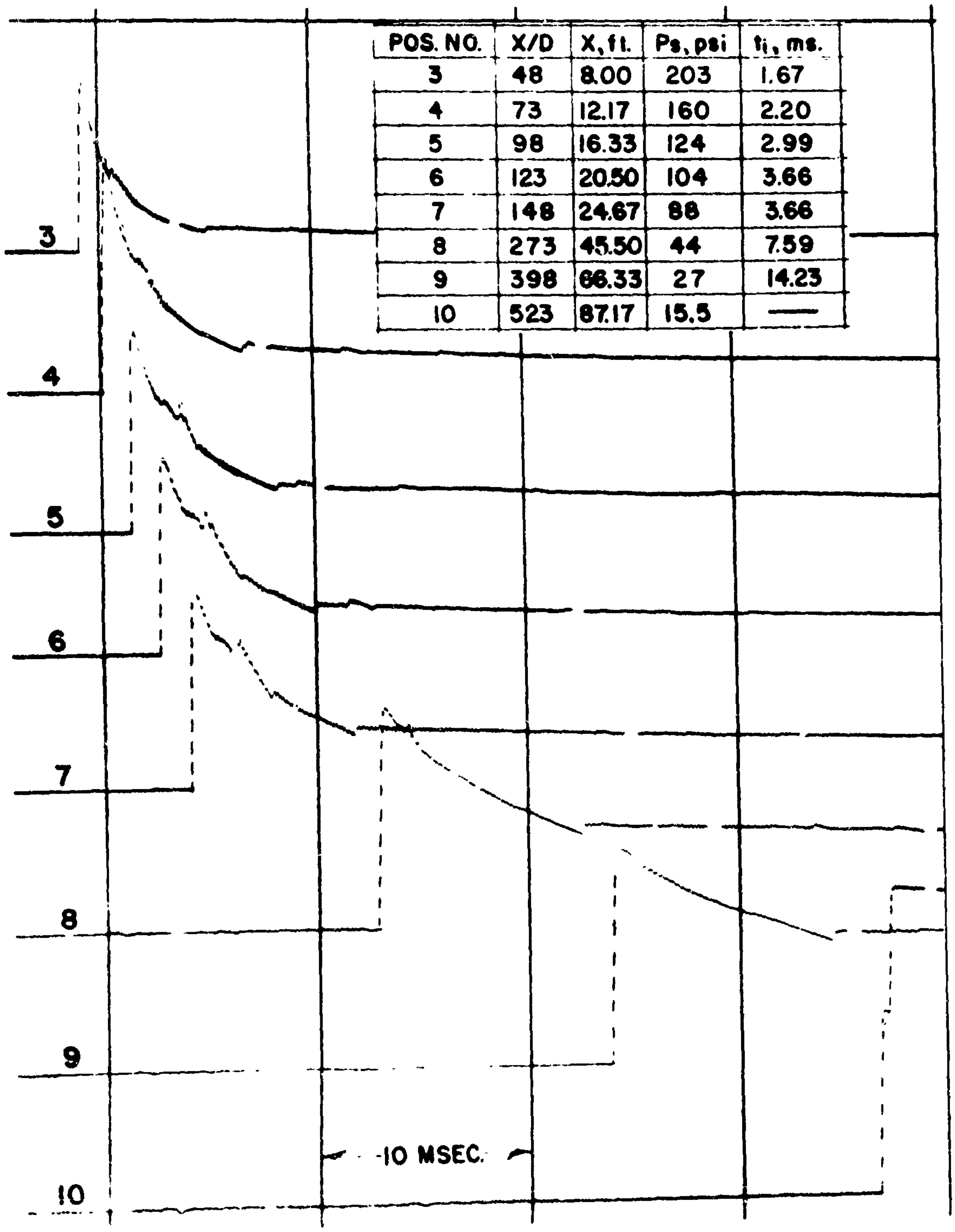

POS. NO.	X/D	X, ft.	Ps, psi	t_i, ms.
3	48	8.00	203	1.67
4	73	12.17	160	2.20
5	98	16.33	124	2.99
6	123	20.50	104	3.66
7	148	24.67	88	3.66
8	273	45.50	44	7.59
9	398	66.33	27	14.23
10	523	87.17	15.5	—

FIG. 4 PRESSURE-TIME RECORDS FROM 2-INCH SHOCK TUBE - L_c = 18 INCHES

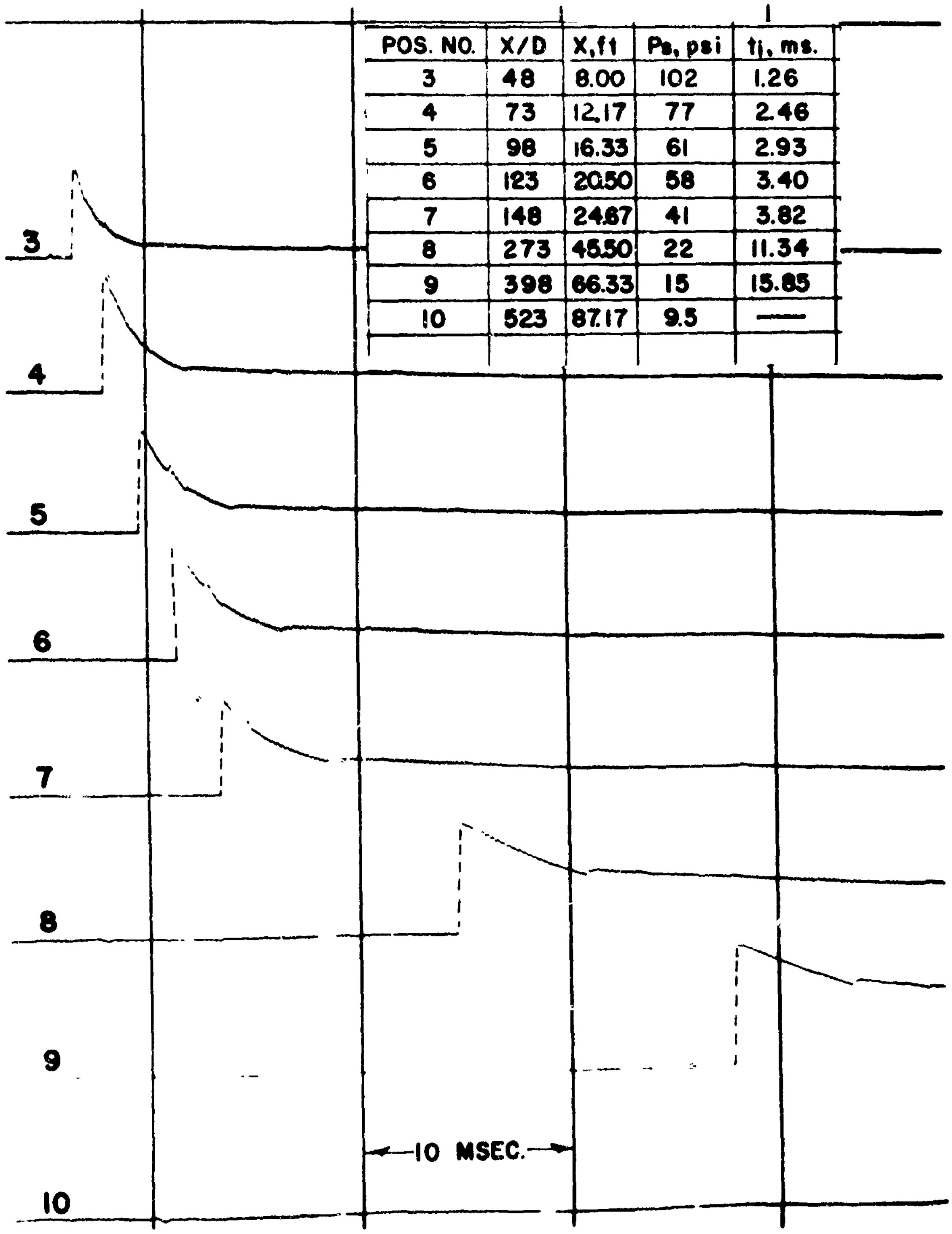

POS. NO.	X/D	X,ft	Ps, psi	ti, ms.
3	48	8.00	102	1.26
4	73	12.17	77	2.46
5	98	16.33	61	2.93
6	123	20.50	58	3.40
7	148	24.67	41	3.82
8	273	45.50	22	11.34
9	398	66.33	15	15.85
10	523	87.17	9.5	—

FIG. 5 PRESSURE-TIME RECORDS FROM 2-INCH SHOCK TUBE - $L_c = 6$ INCHES

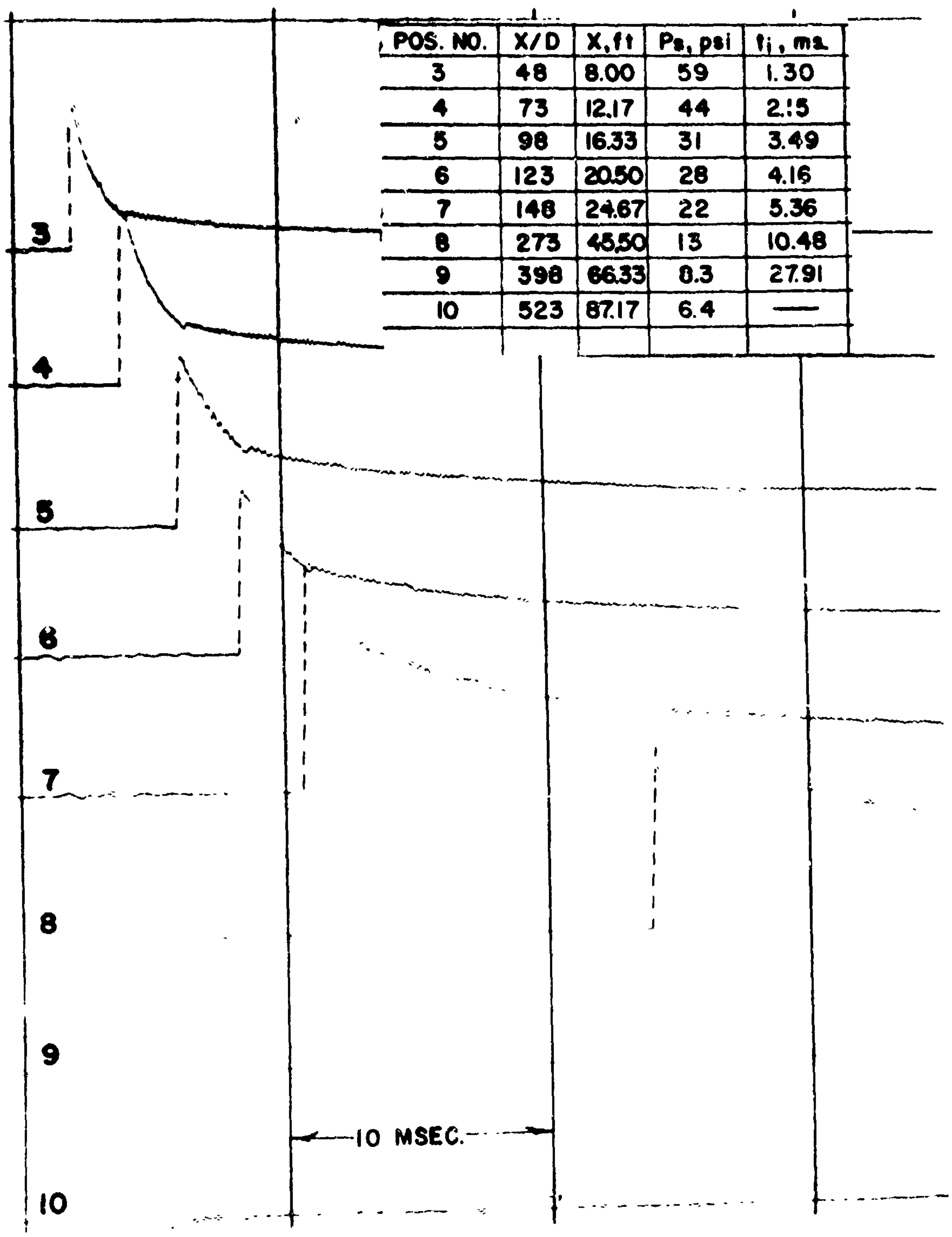

POS. NO.	X/D	X, ft	Ps, psi	t_i, ms.
3	48	8.00	59	1.30
4	73	12.17	44	2.15
5	98	16.33	31	3.49
6	123	20.50	28	4.16
7	148	24.67	22	5.36
8	273	45.50	13	10.48
9	398	66.33	8.3	27.91
10	523	87.17	6.4	—

FIG. 6 PRESSURE-TIME RECORDS FROM 2-INCH SHOCK TUBE - L_c = 2 INCHES

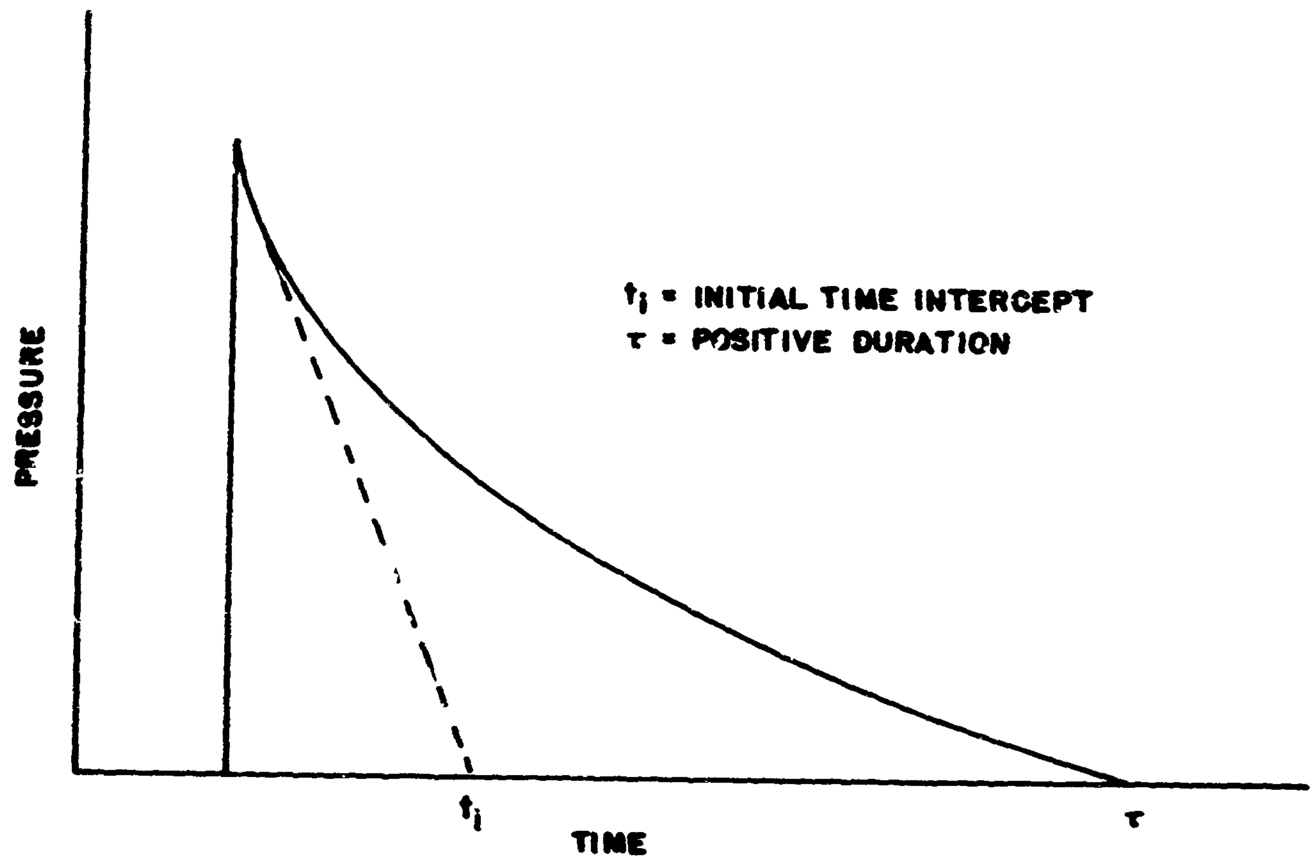

FIG. 7 PRESSURE-TIME WAVEFORM

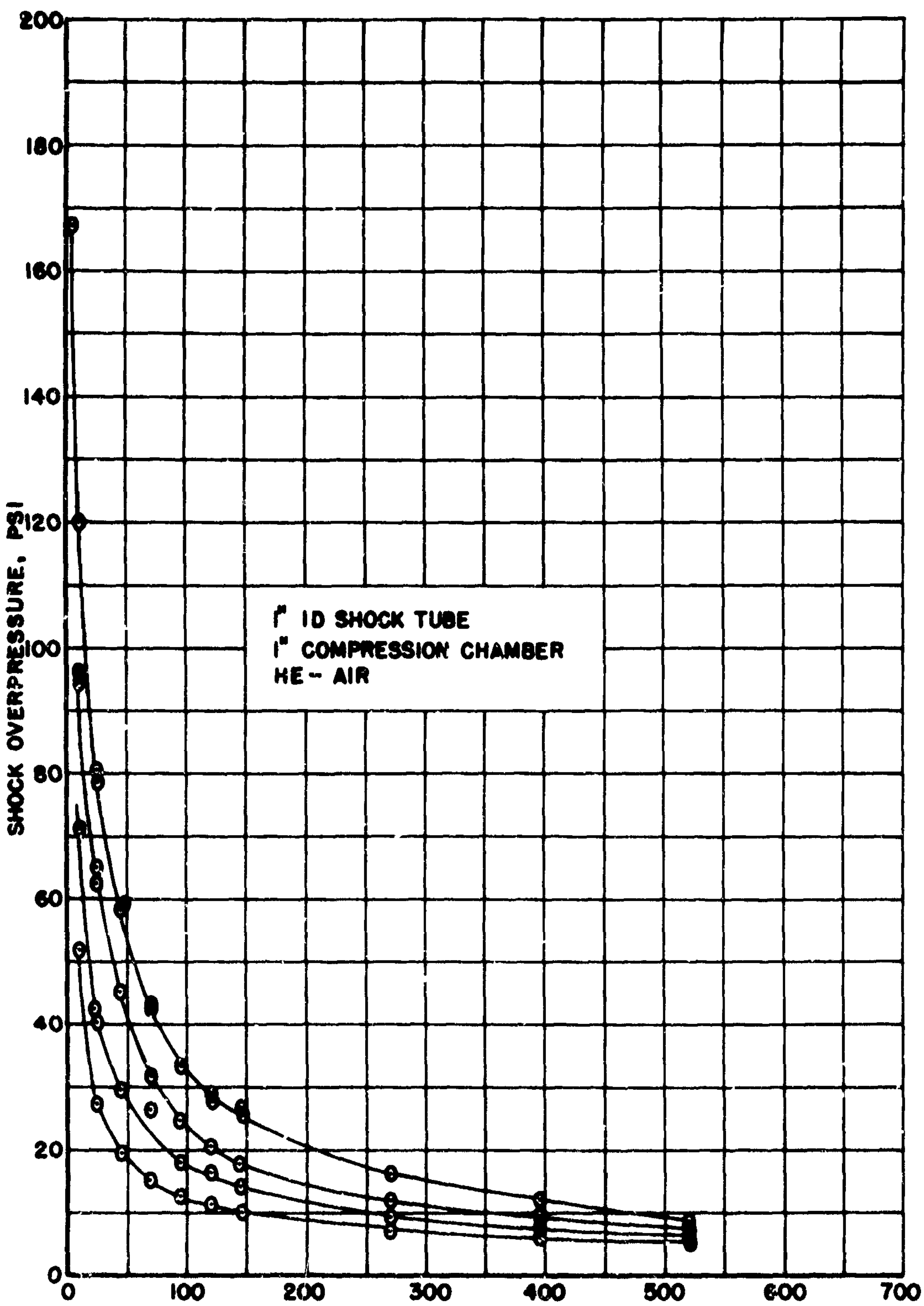

FIG. 8 PEAKED SHOCK WAVE ATTENUATION IN A 1-INCH SHOCK TUBE
L_C = 1 INCH

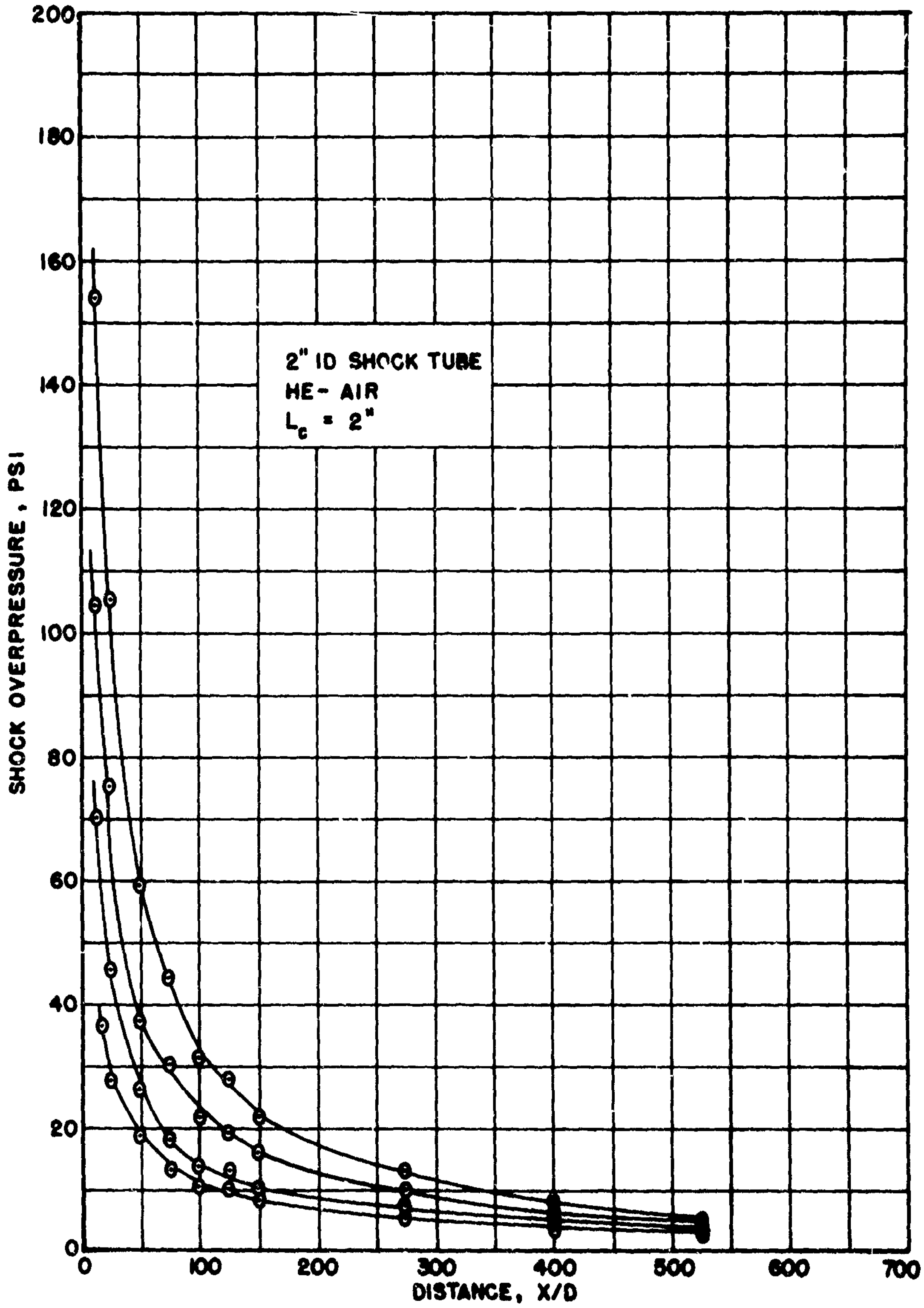

FIG. 9 PEAKED SHOCK WAVE ATTENUATION IN A 2-INCH SHOCK TUBE
L_C = 2 INCHES

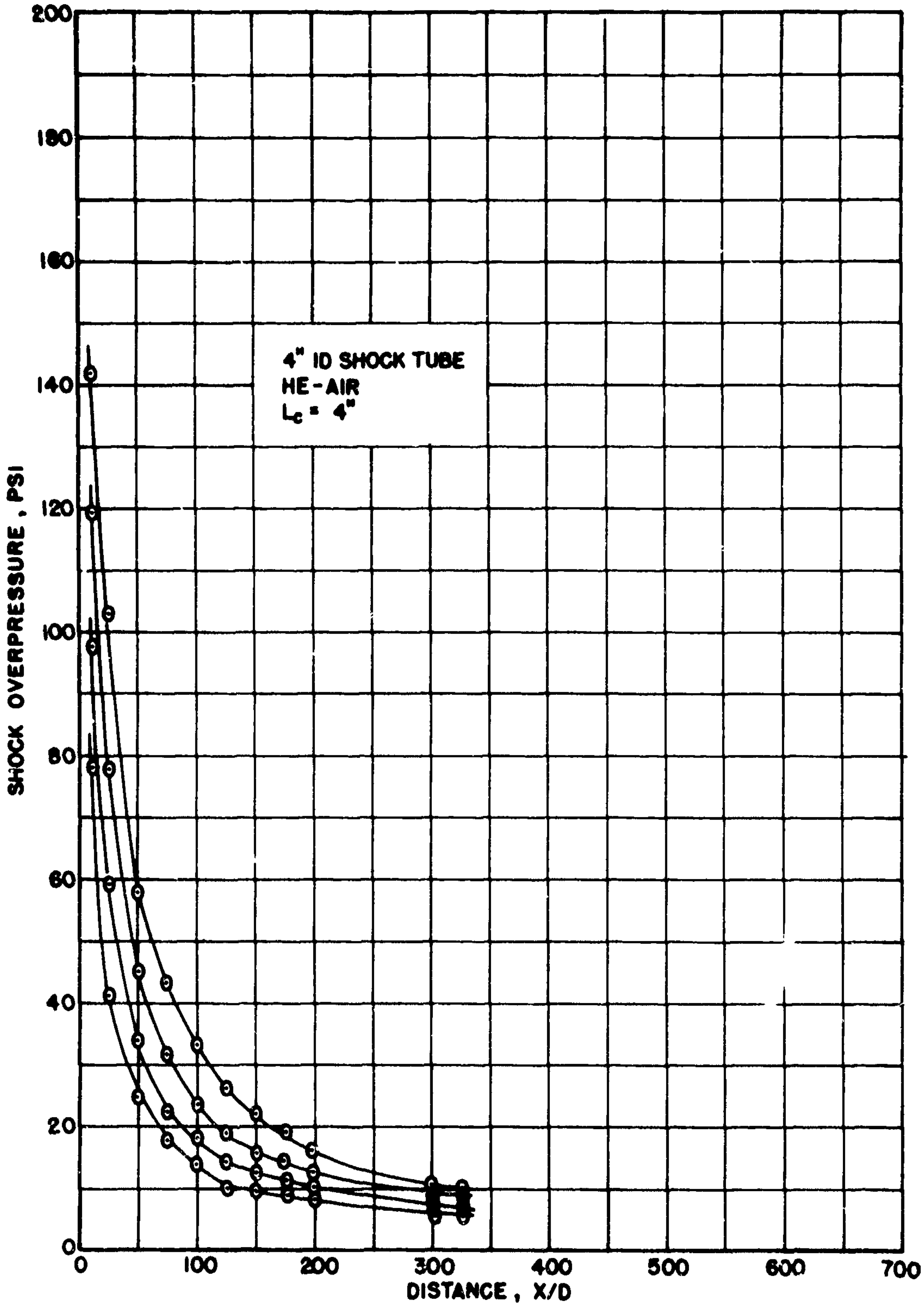

FIG. 10 PEAKED SHOCK WAVE ATTENUATION IN A 4-INCH SHOCK TUBE
L_c = 4 INCHES

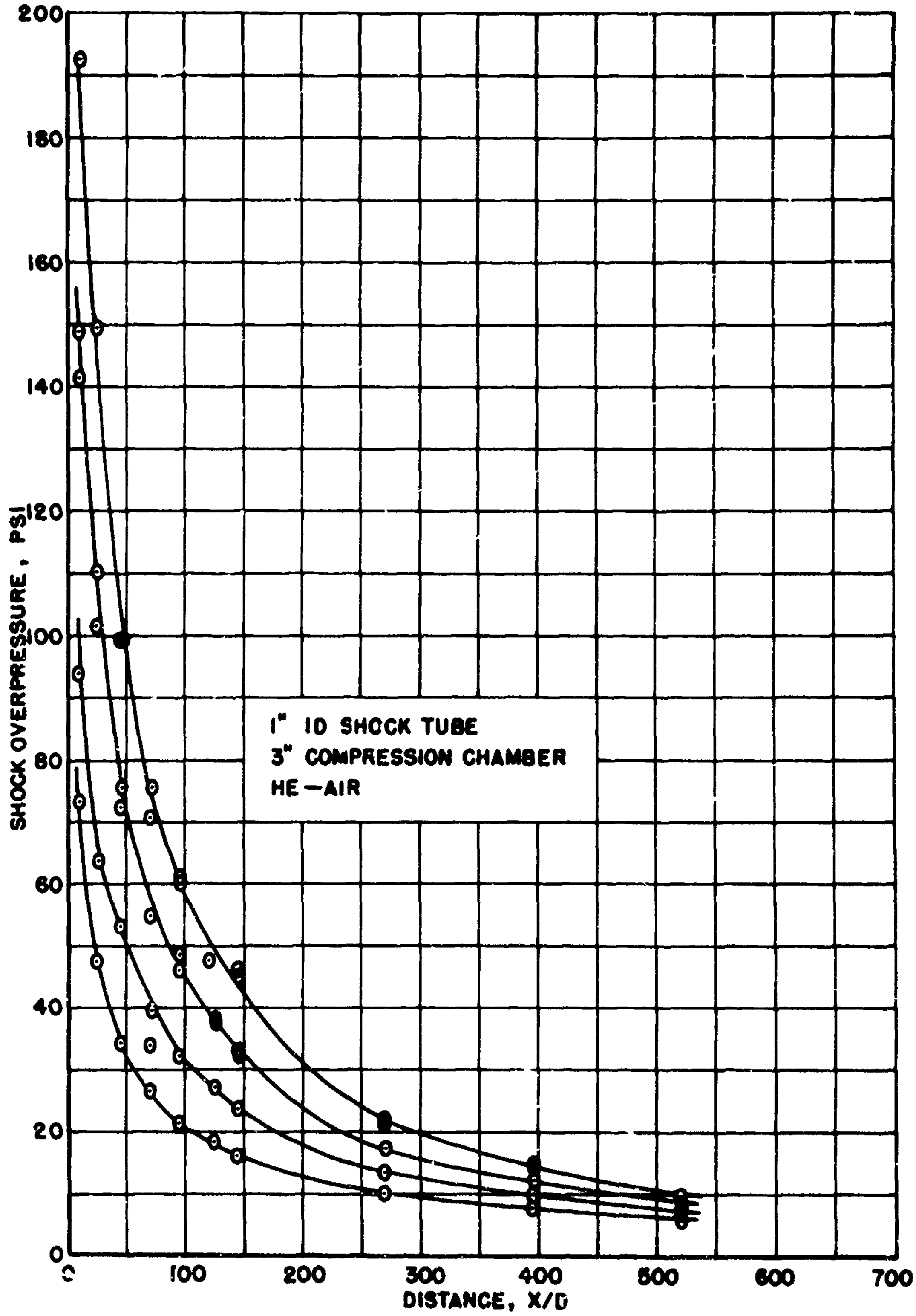

FIG. 11 PEAKED SHOCK WAVE ATTENUATION IN A 1-INCH SHOCK TUBE
L_C = 3 INCHES

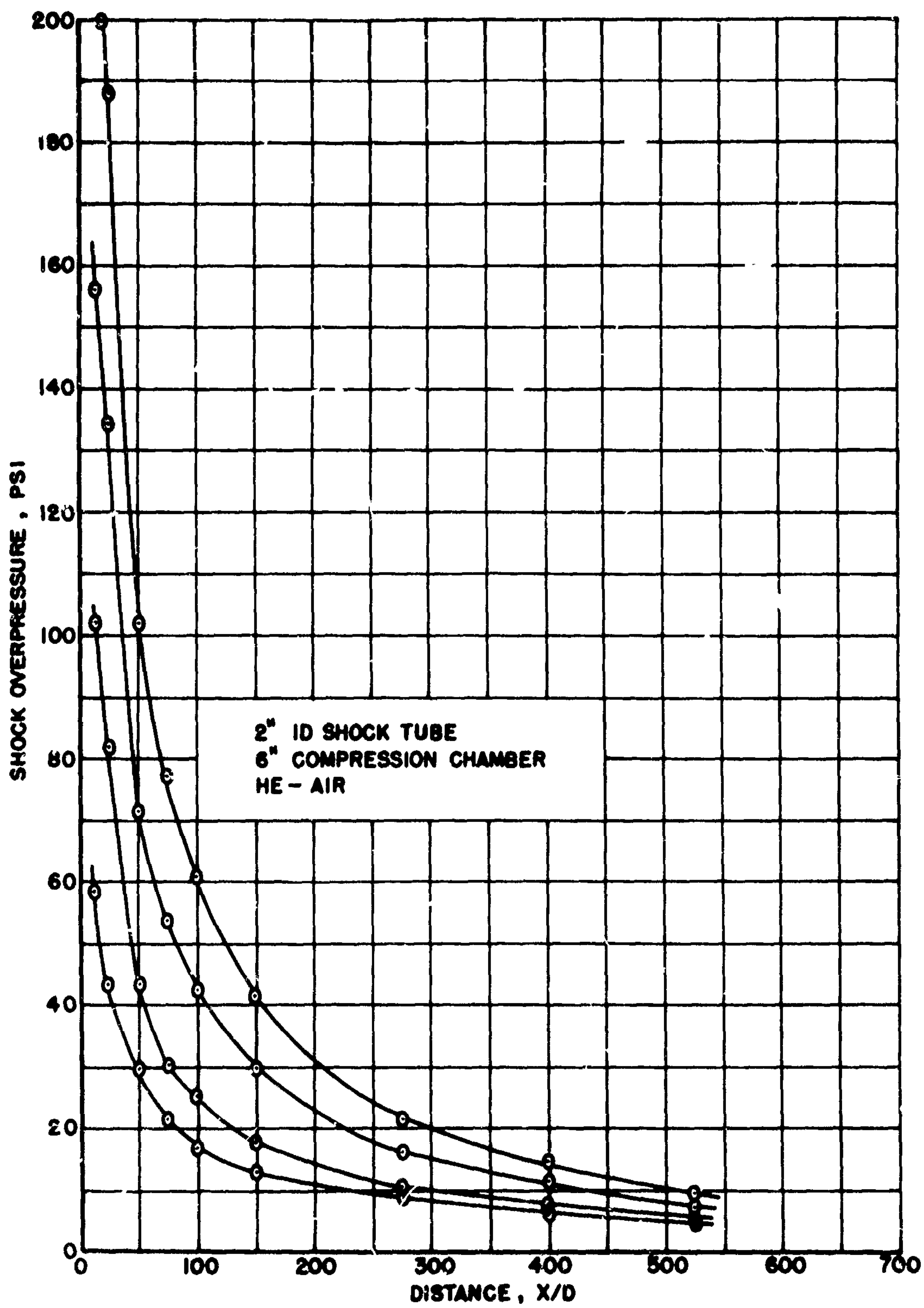

FIG. 12 PEAKED SHOCK WAVE ATTENUATION IN A 2-INCH SHOCK TUBE
L_C = 6 INCHES

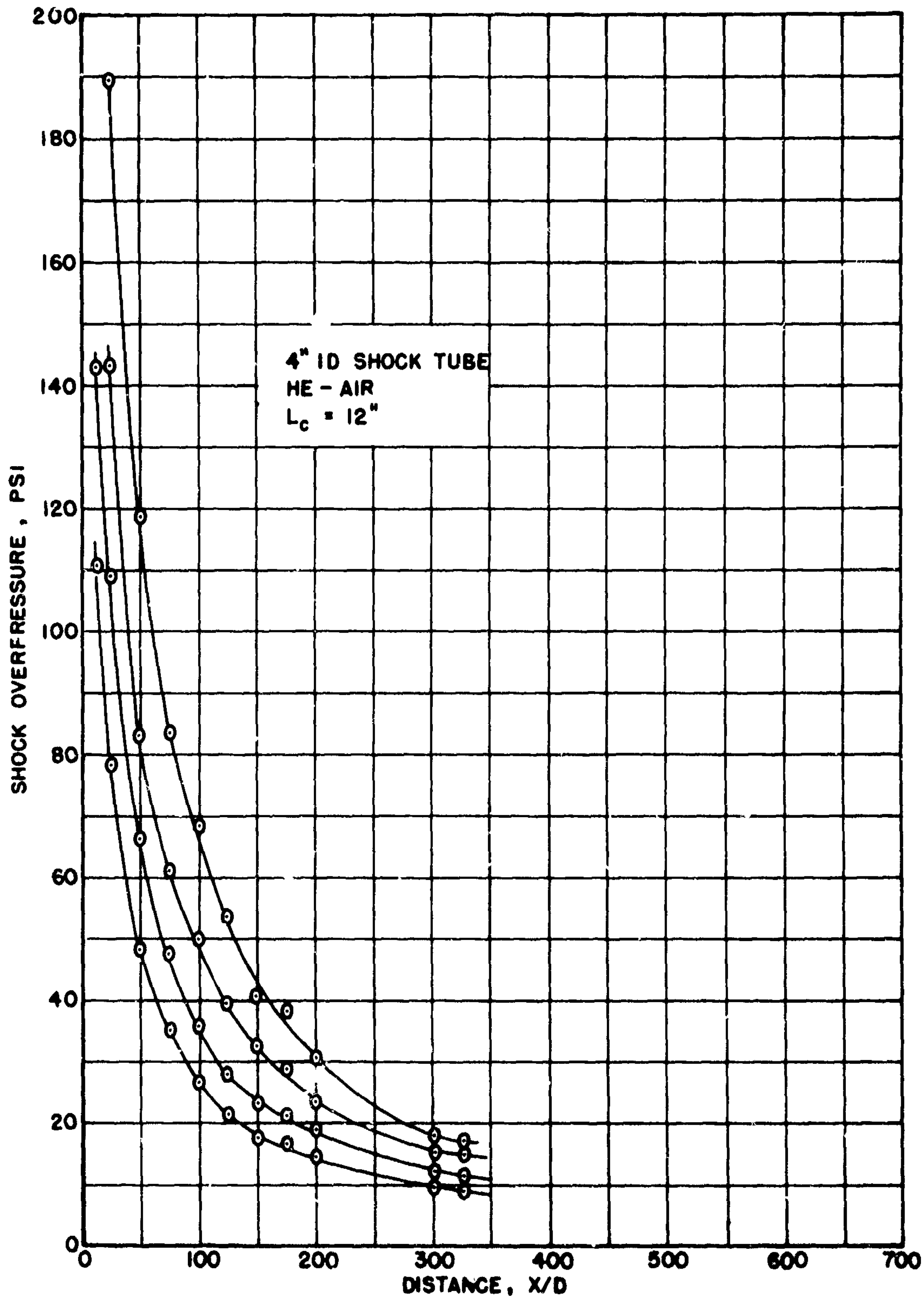

FIG. 13 PEAKED SHOCK WAVE ATTENUATION IN A 4 - INCH SHOCK TUBE
L_C = 12 INCHES

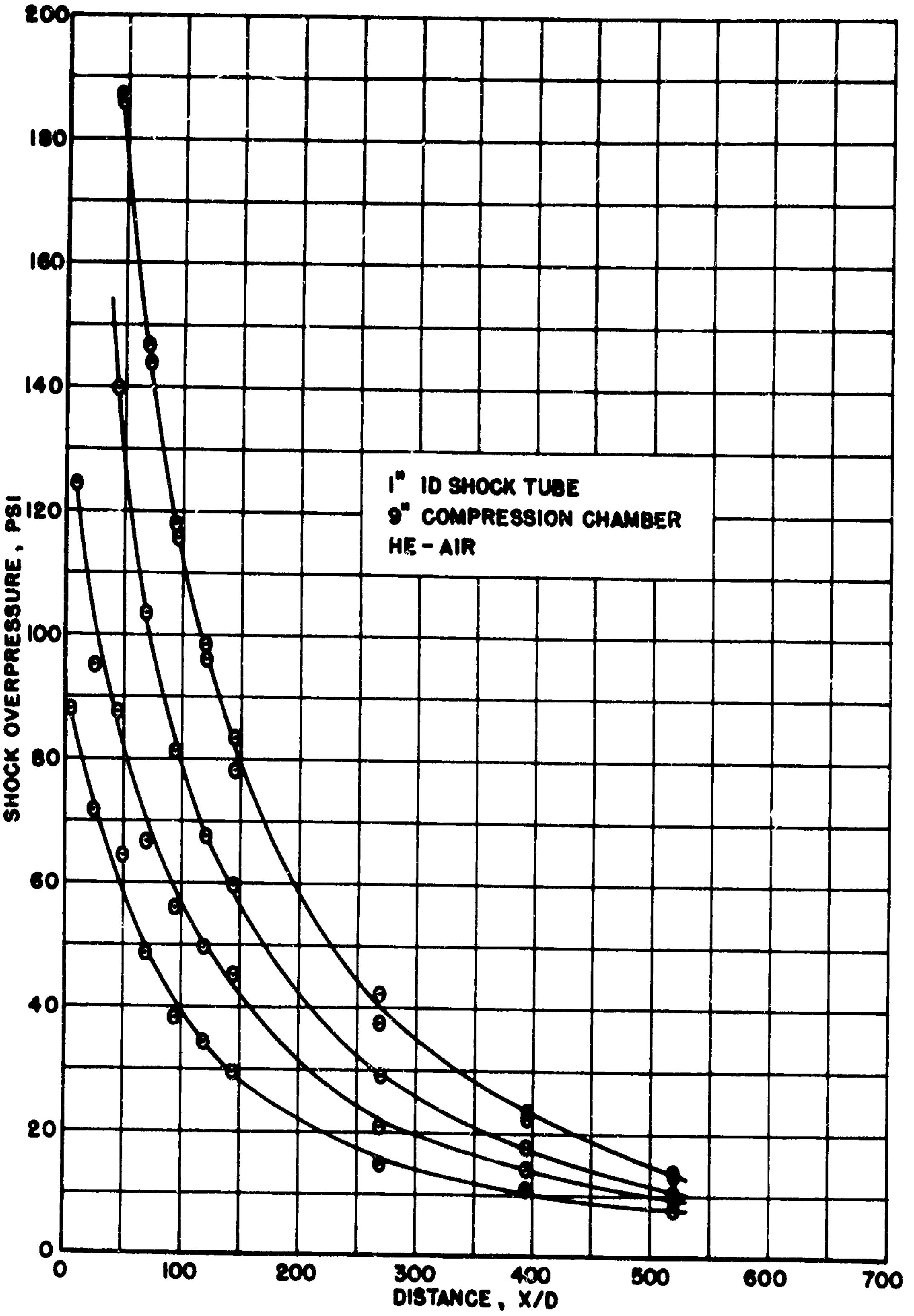

FIG. 14 PEAKED SHOCK WAVE ATTENUATION IN A 1-INCH SHOCK TUBE
L_C = 9 INCHES

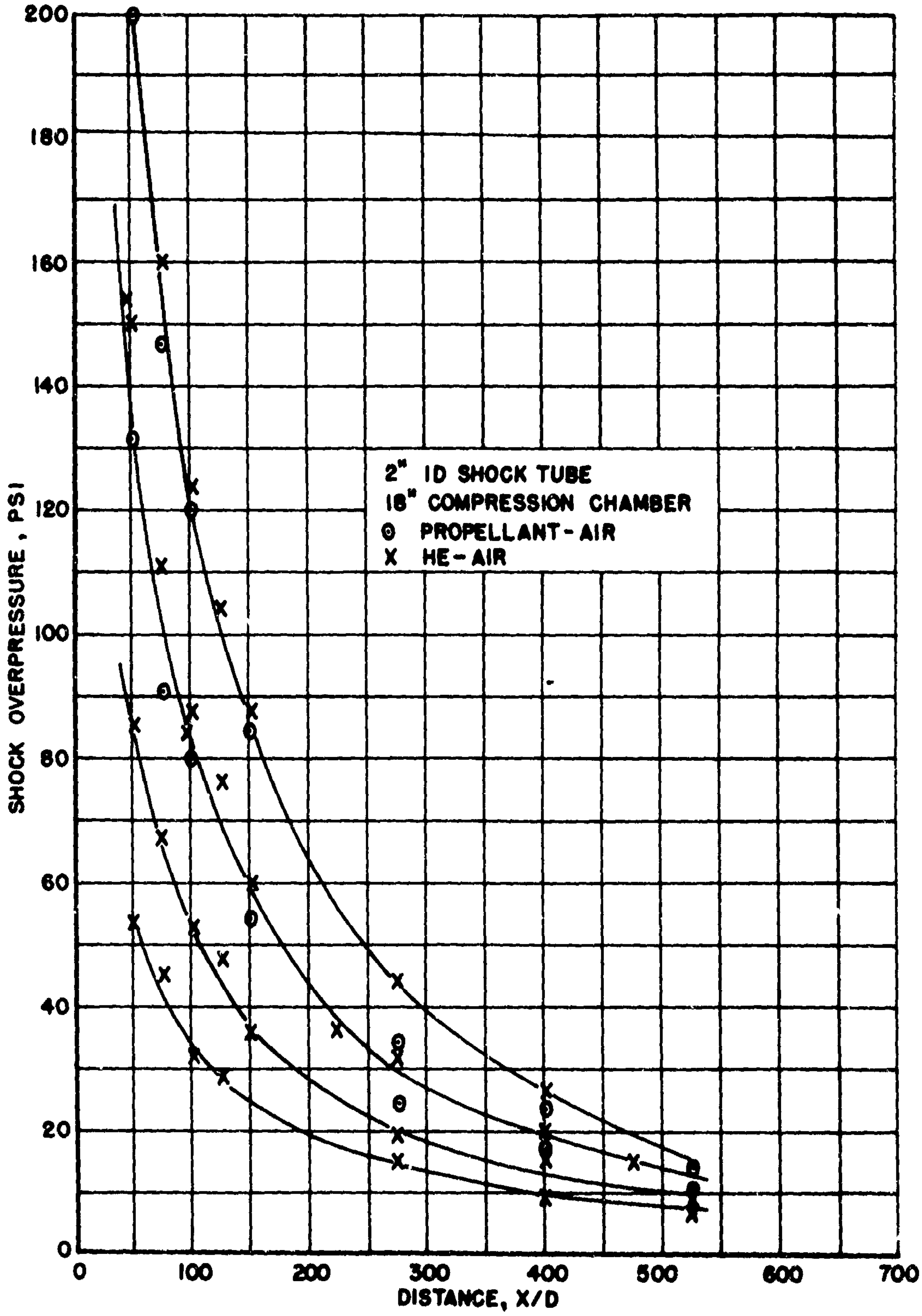

FIG. 15 PEAKED SHOCK WAVE ATTENUATION IN A 2-INCH SHOCK TUBE
L_C = 18 INCHES

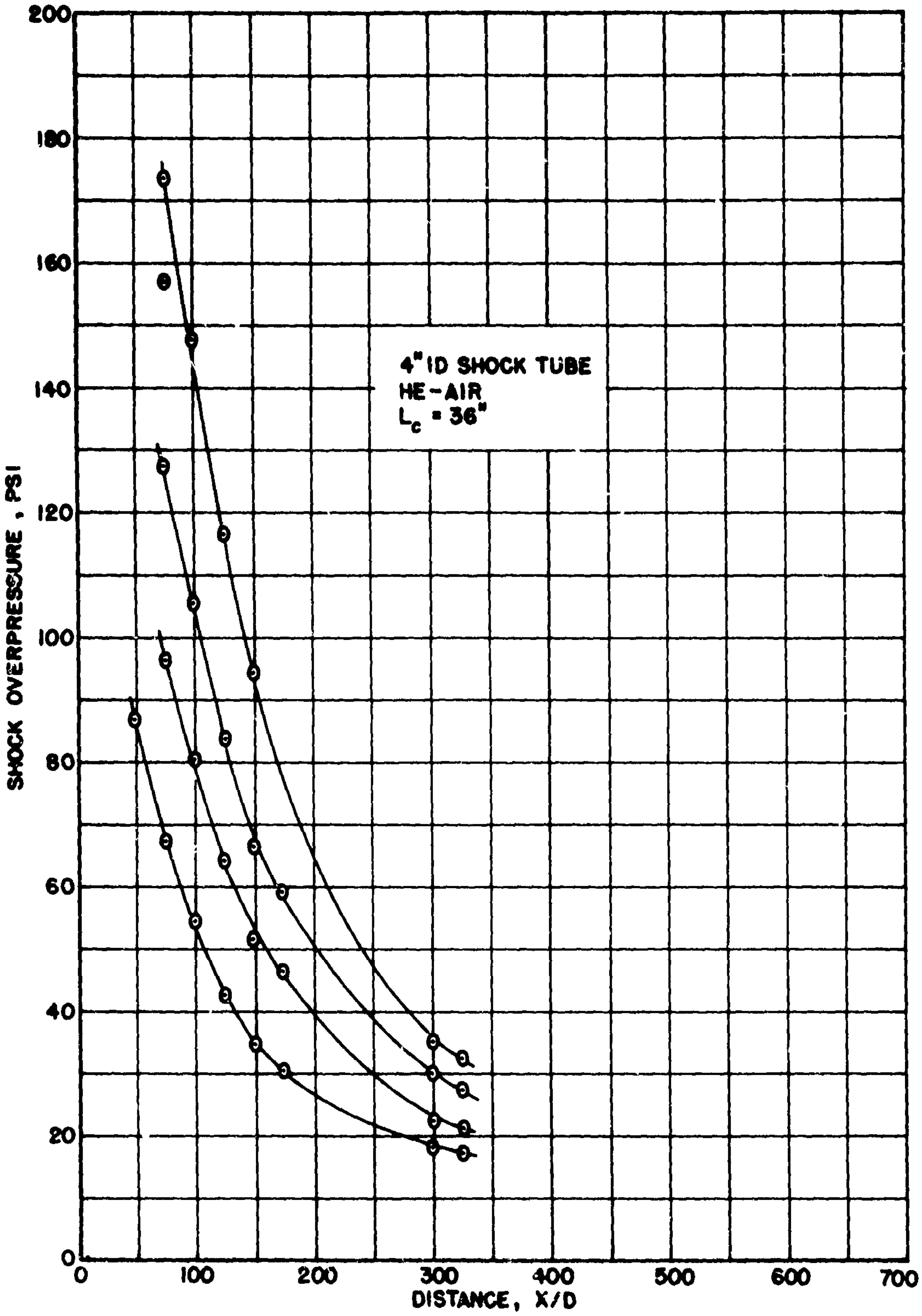

FIG. 16 PEAKED SHOCK WAVE ATTENUATION IN A 4-INCH SHOCK TUBE
L_C = 36 INCHES

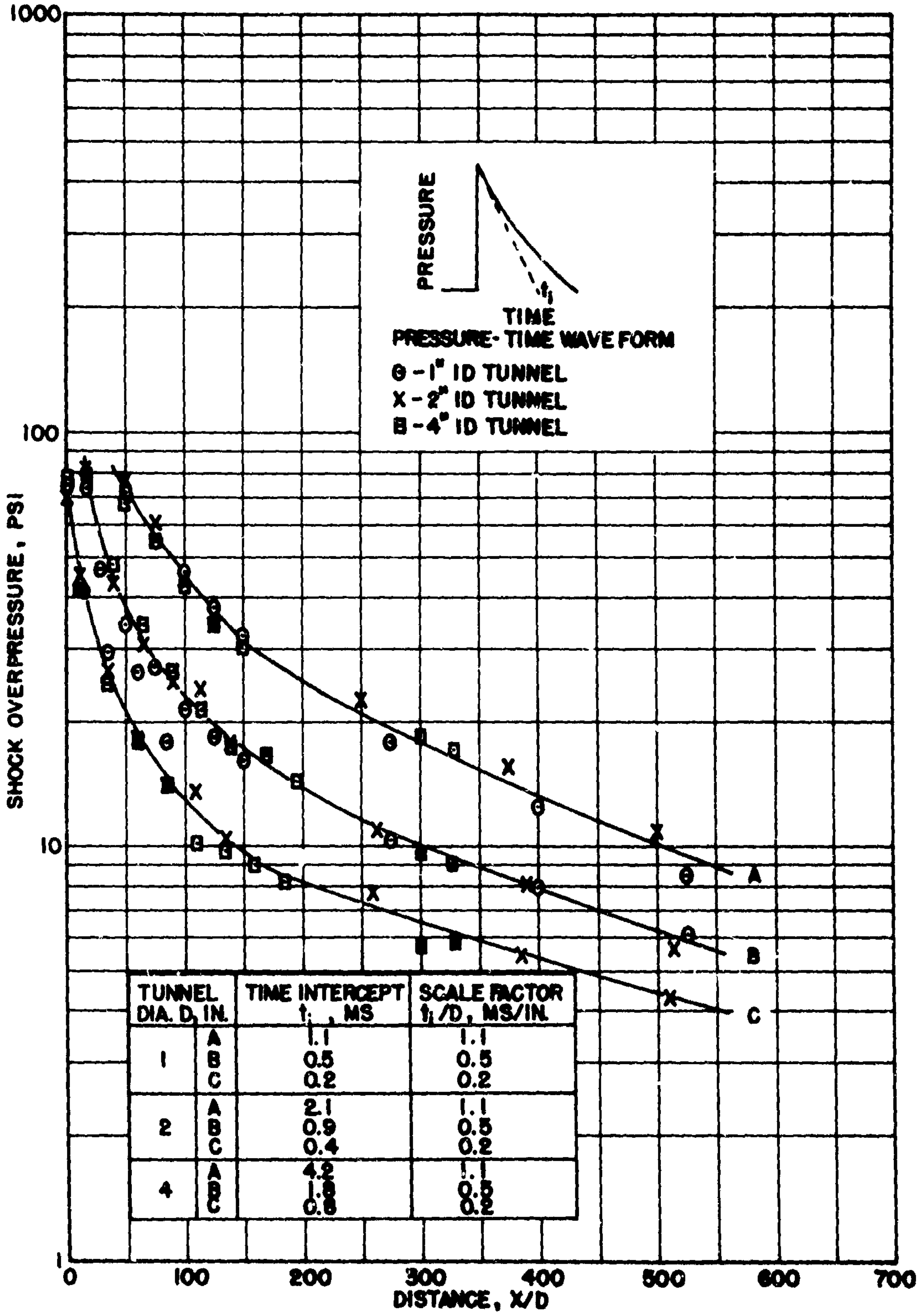

TUNNEL DIA. D, IN.		TIME INTERCEPT t_1, MS	SCALE FACTOR t_1/D, MS/IN.
1	A	1.1	1.1
	B	0.5	0.5
	C	0.2	0.2
2	A	2.1	1.1
	B	0.9	0.5
	C	0.4	0.2
4	A	4.2	1.1
	B	1.8	0.5
	C	0.8	0.2

FIG. 17 ATTENUATION OF 80 PSI INPUT SHOCK AS A FUNCTION OF SCALE FACTOR, t_1/D

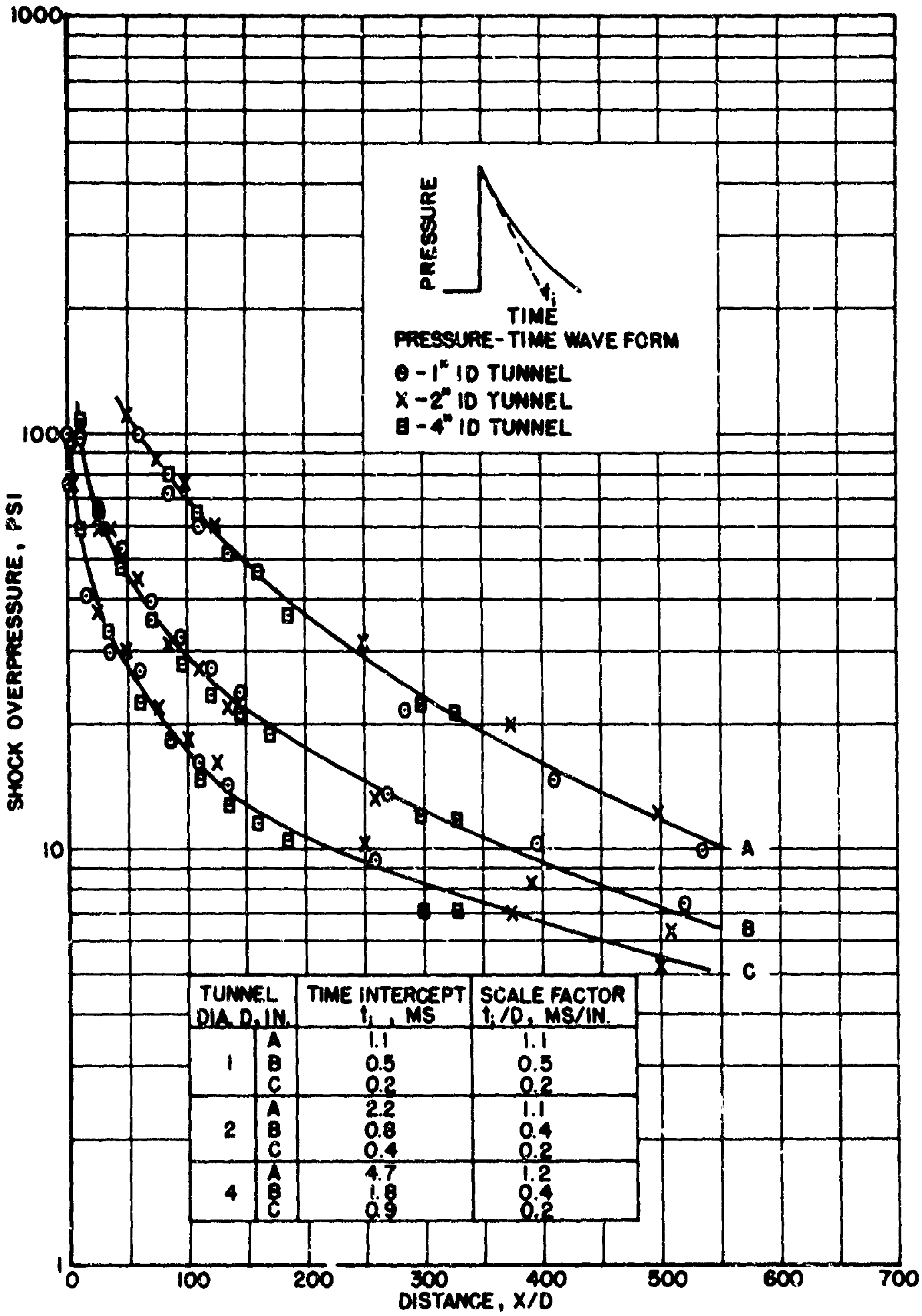

TUNNEL DIA. D, IN.		TIME INTERCEPT t_i, MS	SCALE FACTOR t_i/D, MS/IN.
1	A	1.1	1.1
	B	0.5	0.5
	C	0.2	0.2
2	A	2.2	1.1
	B	0.8	0.4
	C	0.4	0.2
4	A	4.7	1.2
	B	1.8	0.4
	C	0.9	0.2

FIG. 18 ATTENUATION OF 100 PSI INPUT SHOCK AS A FUNCTION OF SCALE FACTOR, t_i/D

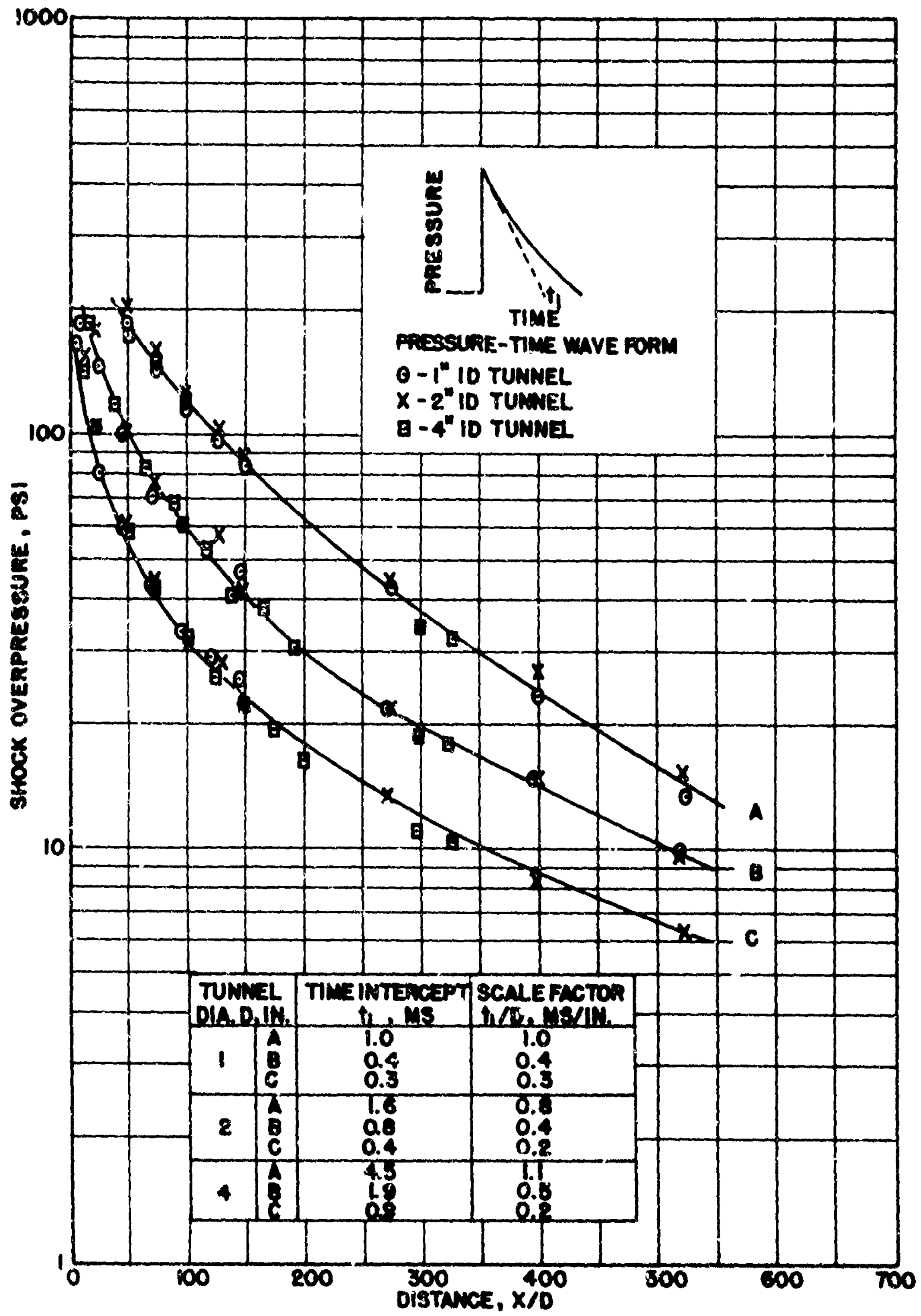

TUNNEL DIA. D, IN.		TIME INTERCEPT t_1, MS	SCALE FACTOR t_1/D, MS/IN.
1	A	1.0	1.0
	B	0.4	0.4
	C	0.3	0.3
2	A	1.6	0.8
	B	0.8	0.4
	C	0.4	0.2
4	A	4.5	1.1
	B	1.9	0.5
	C	0.9	0.2

FIG. 19 ATTENUATION OF 200 PSI INPUT SHOCK AS A FUNCTION OF SCALE FACTOR, t_1/D

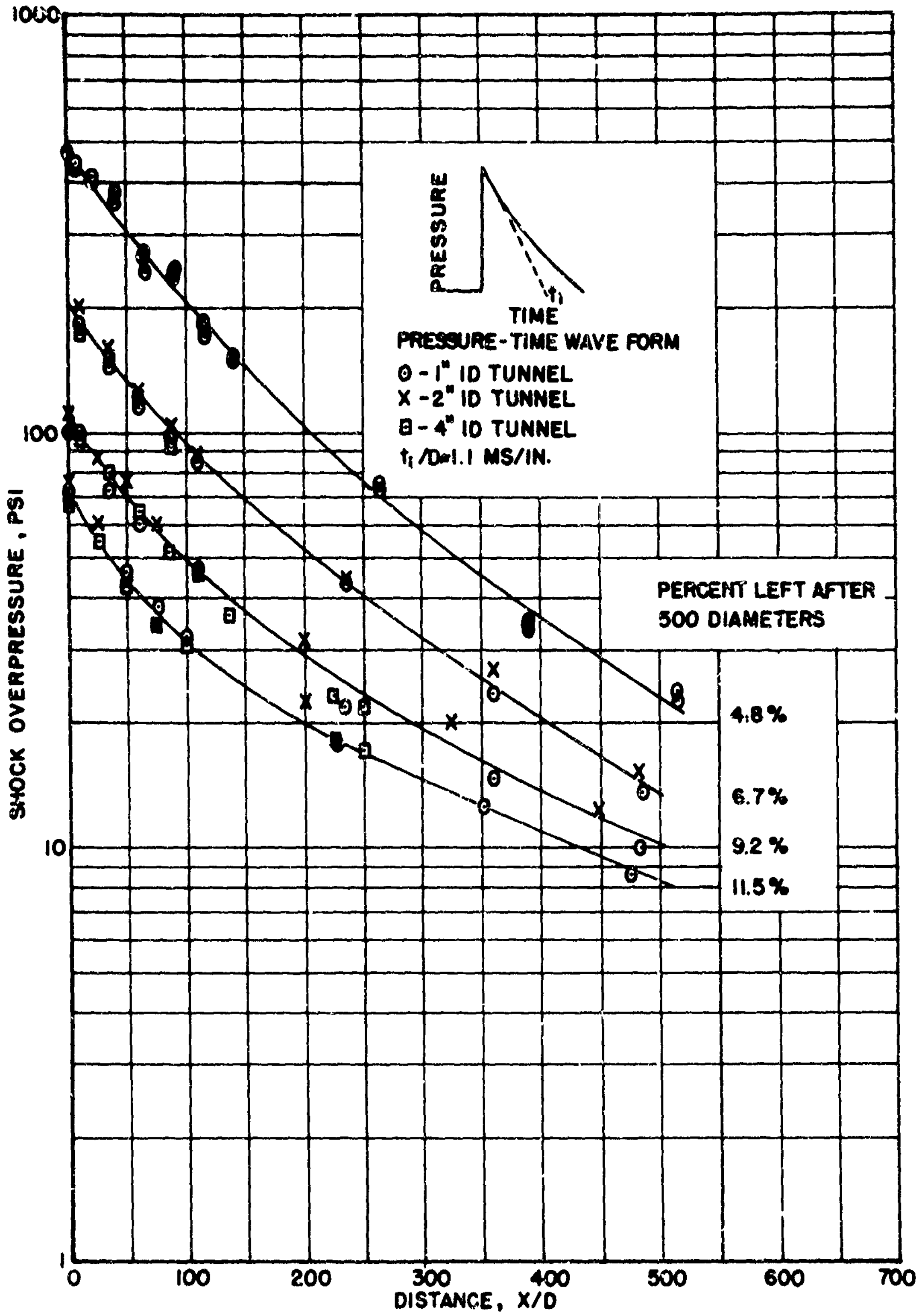

FIG. 20 ATTENUATION OF PEAKED SHOCK WAVES FOR CONSTANT SCALE FACTOR, t_1/D

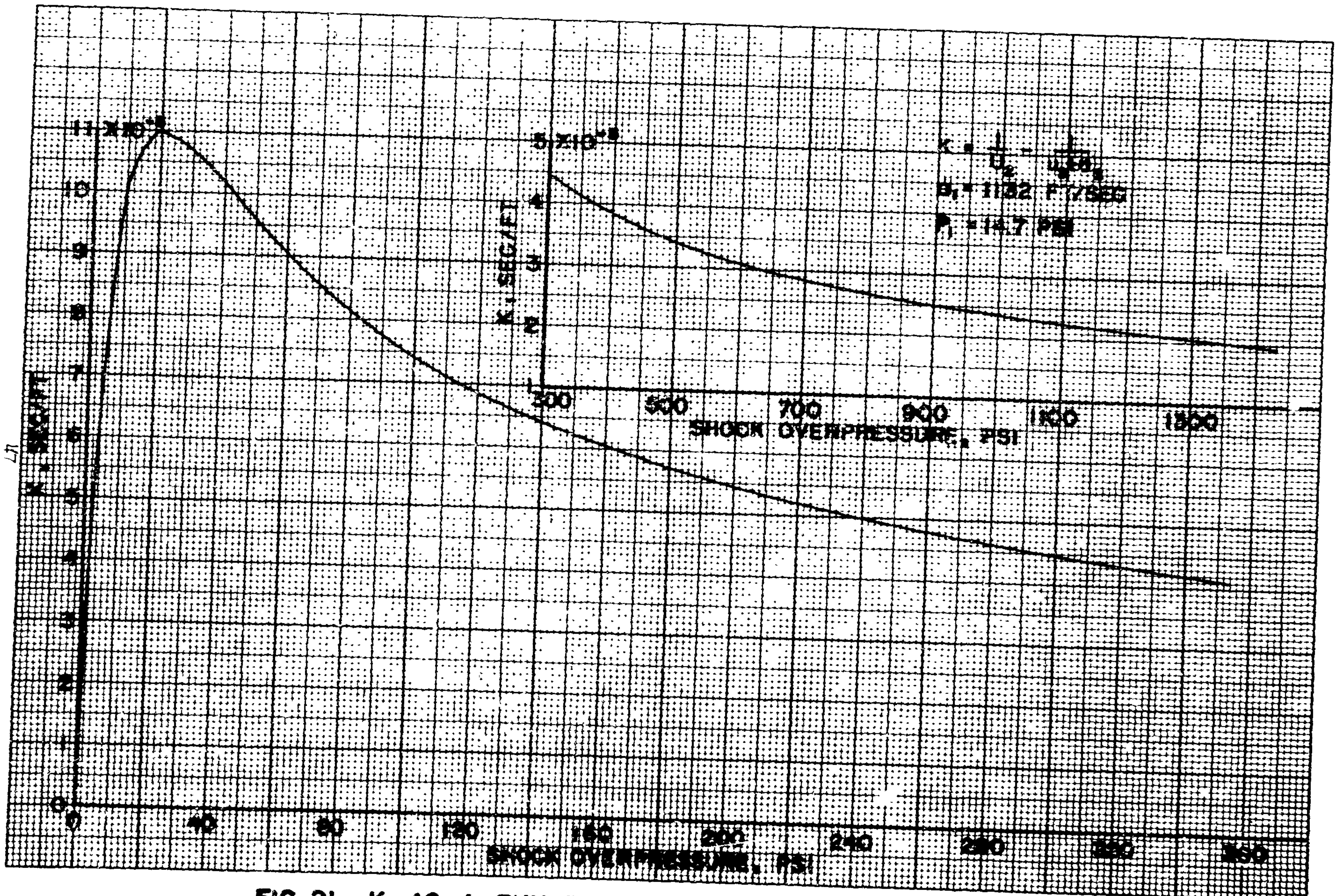

FIG. 21 K AS A FUNCTION OF SHOCK OVERPRESSURE

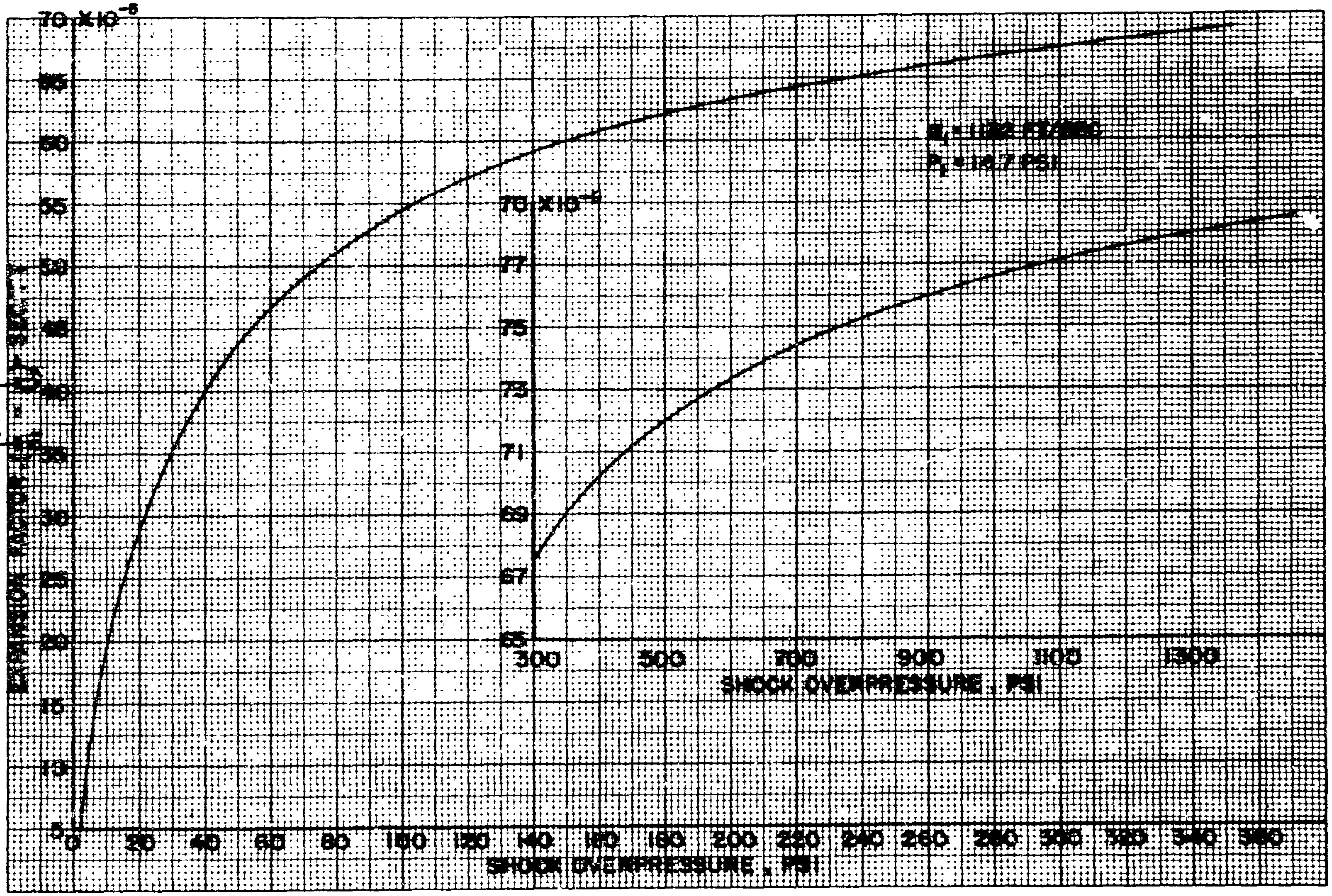

FIG. 22 EXPANSION FACTOR AS A FUNCTION OF OVERPRESSURE

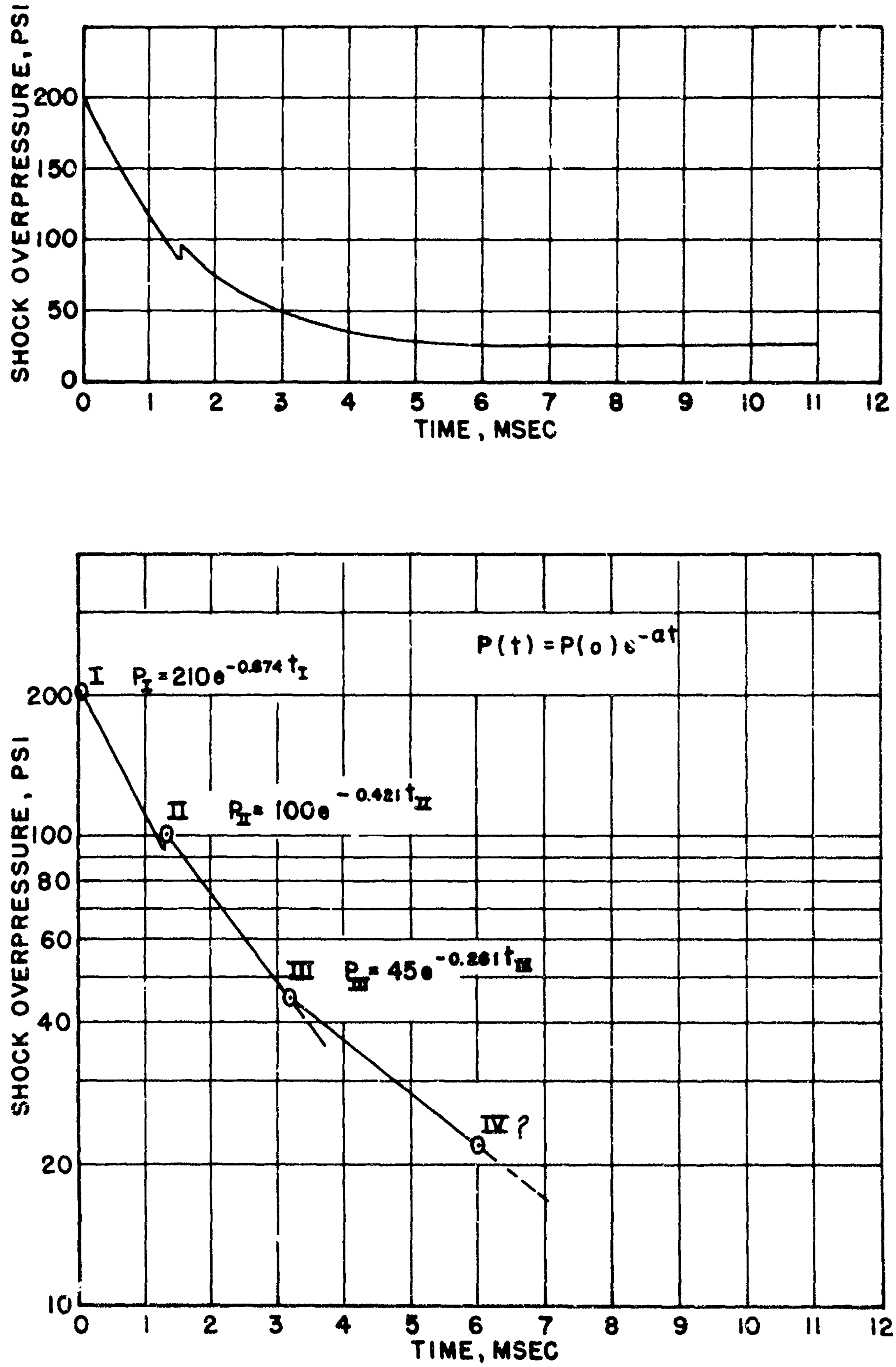

FIG. 23 DIVISION OF INPUT WAVE INTO SIMPLE EXPONENTIALS

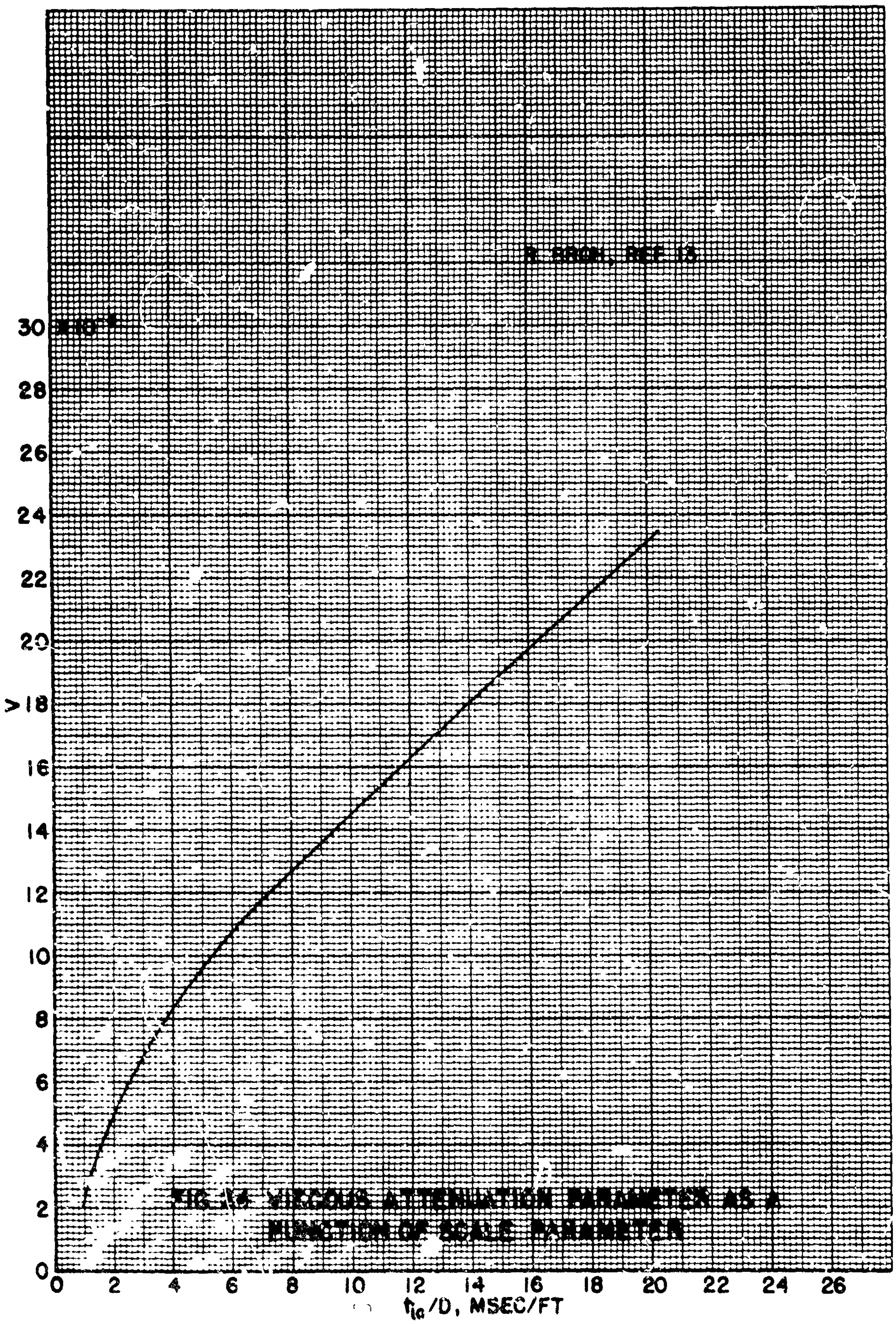

FIG. 16 VISCOUS ATTENUATION PARAMETER AS A FUNCTION OF SCALE PARAMETER

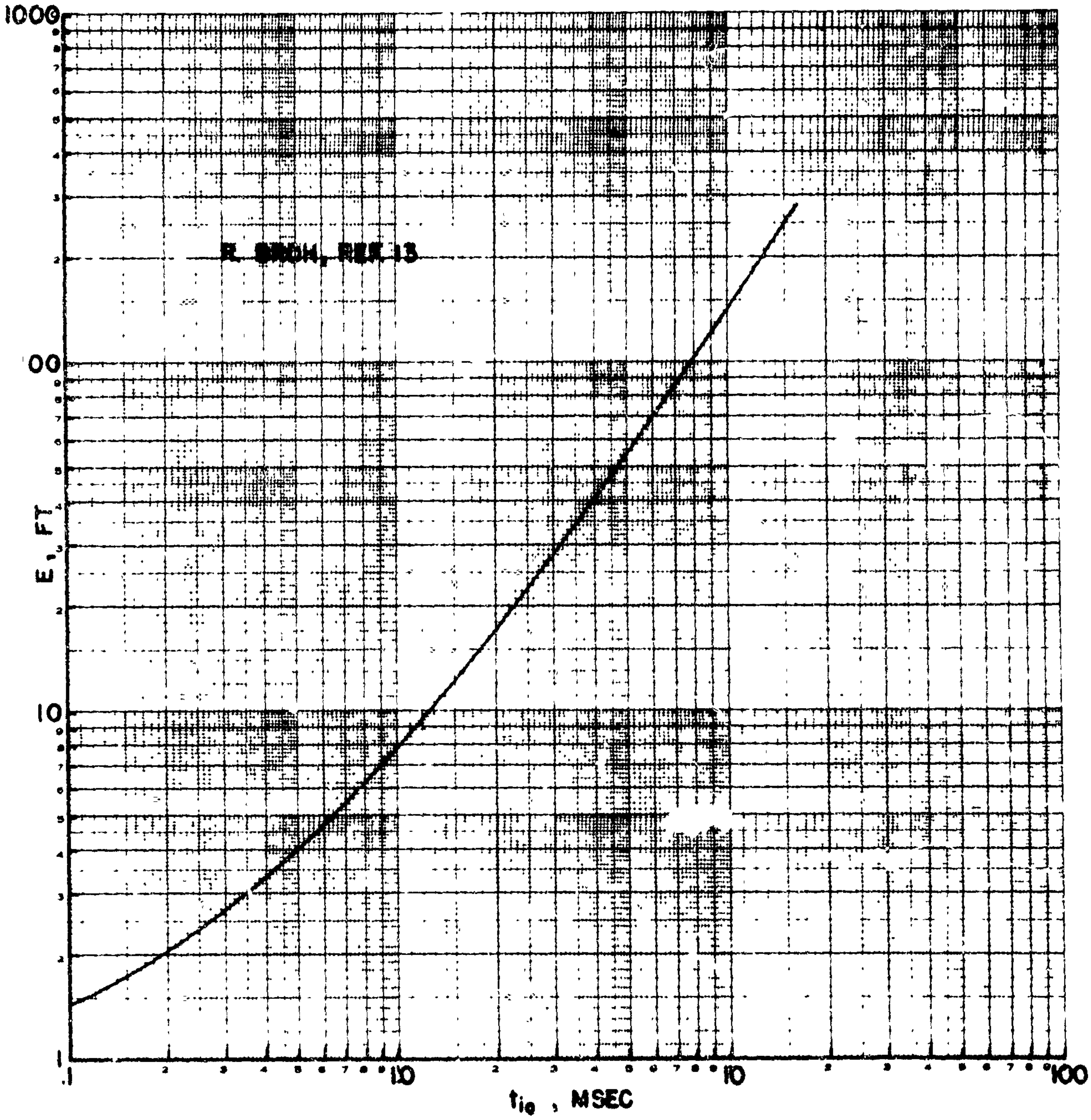

FIG. 25 RAREFACTION PARAMETER AS A FUNCTION OF TIME INTERCEPT

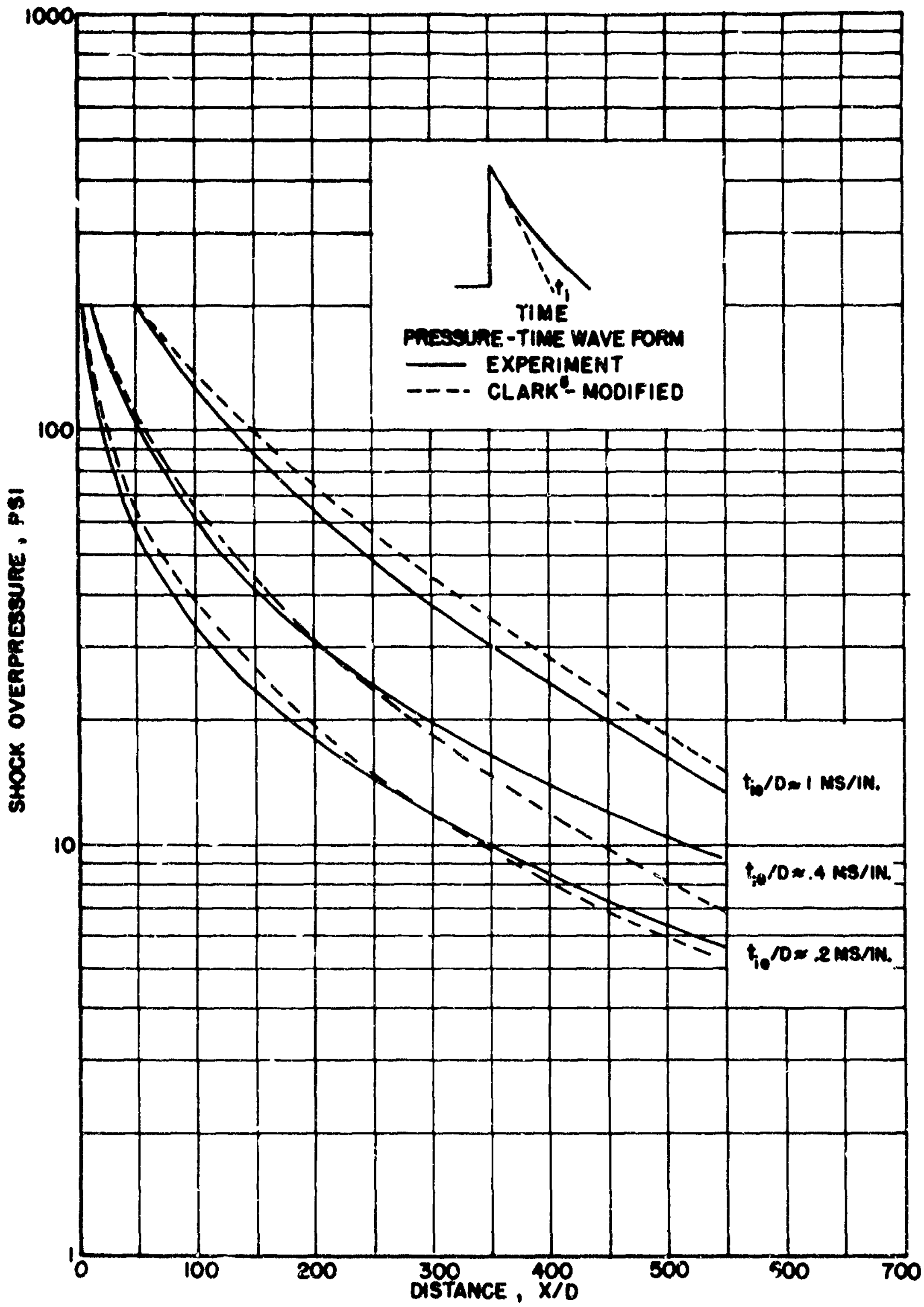

FIG. 26 COMPARISON OF DATA WITH THEORY

REFERENCES

1. Emrich, Raymond J. and Wheeler, Donald B., Jr. Wall Effects in Shock Tube Flow. The Physics of Fluids, Vol. 1, No. 1, pp. 14-23, January - February 1958.

2. Warren, A. Propagation of Blast Waves Along Tunnels. Fort Halstead, Sevenoaks, Kent, England, Armament Research and Development Establishment Report (MX) 27/58.

3. Glass, I. I. Shock Tubes, Part I: Theory and Performance of Simple Shock Tubes. University of Toronto, UTIA Review No. 12, Part I, May 1958.

4. Clark, Robert O. and Coulter, George A. Attenuation of Air Shock Waves in Tunnels. BRL Memorandum Report No. 1278, June 1960.

5. Clark, R. O. A Study of Shock Wave Attenuation in Tunnels. BRL Memorandum Report No. 1401, May 1962.

6. Teel, George (Editor). Information Summary of Blast Patterns in Tunnels and Chambers. Second Edition, BRL Memorandum Report No. 1390, March 1962.

7. Bleakney, Walker and Emrich, R. J. The Shock Tube. High Speed Problems of Aircraft and Experimental Methods. Vol. VIII, pp. 596-647, High Speed Aerodynamics and Jet Propulsion, Princeton University Press, 1961.

8. Melichar, Joseph F. Design of a High Pressure Propellant Driver Shock Tube. To be published as a BRL Memorandum Report.

9. Granath, Benjamin A. and Coulter, George A. BRL Shock Tube Pieozo-electric Blast Gages. BRL Technical Note No. 1478, August 1962.

10. Abrahams, Rodney R. A Multi-Channel Piezoelectric Recording System. BRL Memorandum Report No. 1650, May 1965.

11. Clark, R. O. Theory for Viscous Shock Attenuation in Ducts Based on the Kinetic Theory of Gases Experimentally Verified to a Shock Strength of 68. Kirtland Air Force Base, New Mexico, AFWL TR 64-204, July 1966.

12. Ethridge, Noel. A Procedure for Reading and Smoothing Pressure-Time Data from HE and Nuclear Explosions. BRL Memorandum Report No. 1691, September 1965.

13. Broh, Robert. Development of an Analytical Expression for the Attenuation of Shock Waves in Tunnels. To be published as a BRL Memorandum Report.

APPENDIX A

PRESSURE-TIME RECORDS

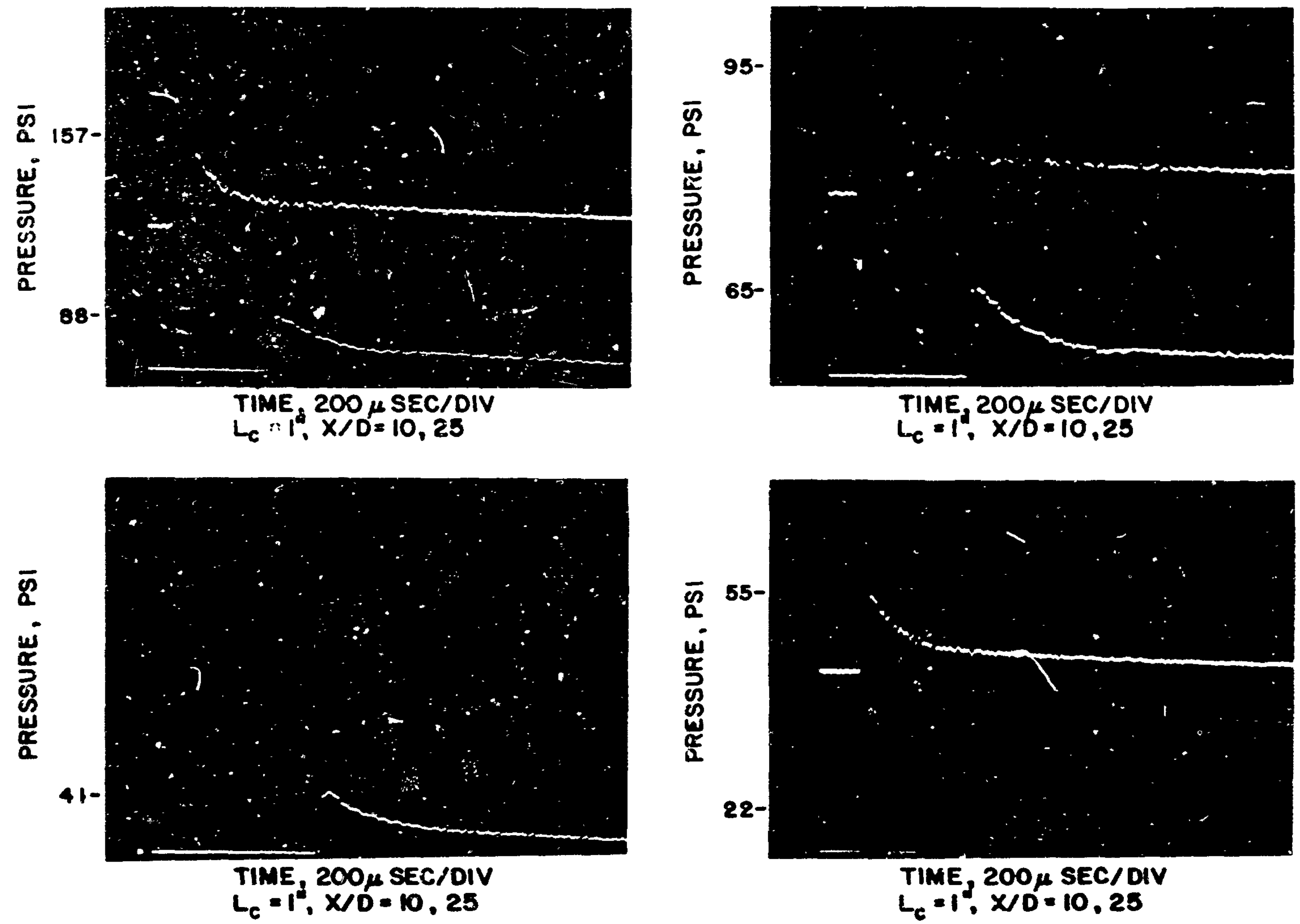

FIG. A-1A PRESSURE - TIME RECORDS FROM 1-INCH SHOCK TUBE - HELIUM DRIVER

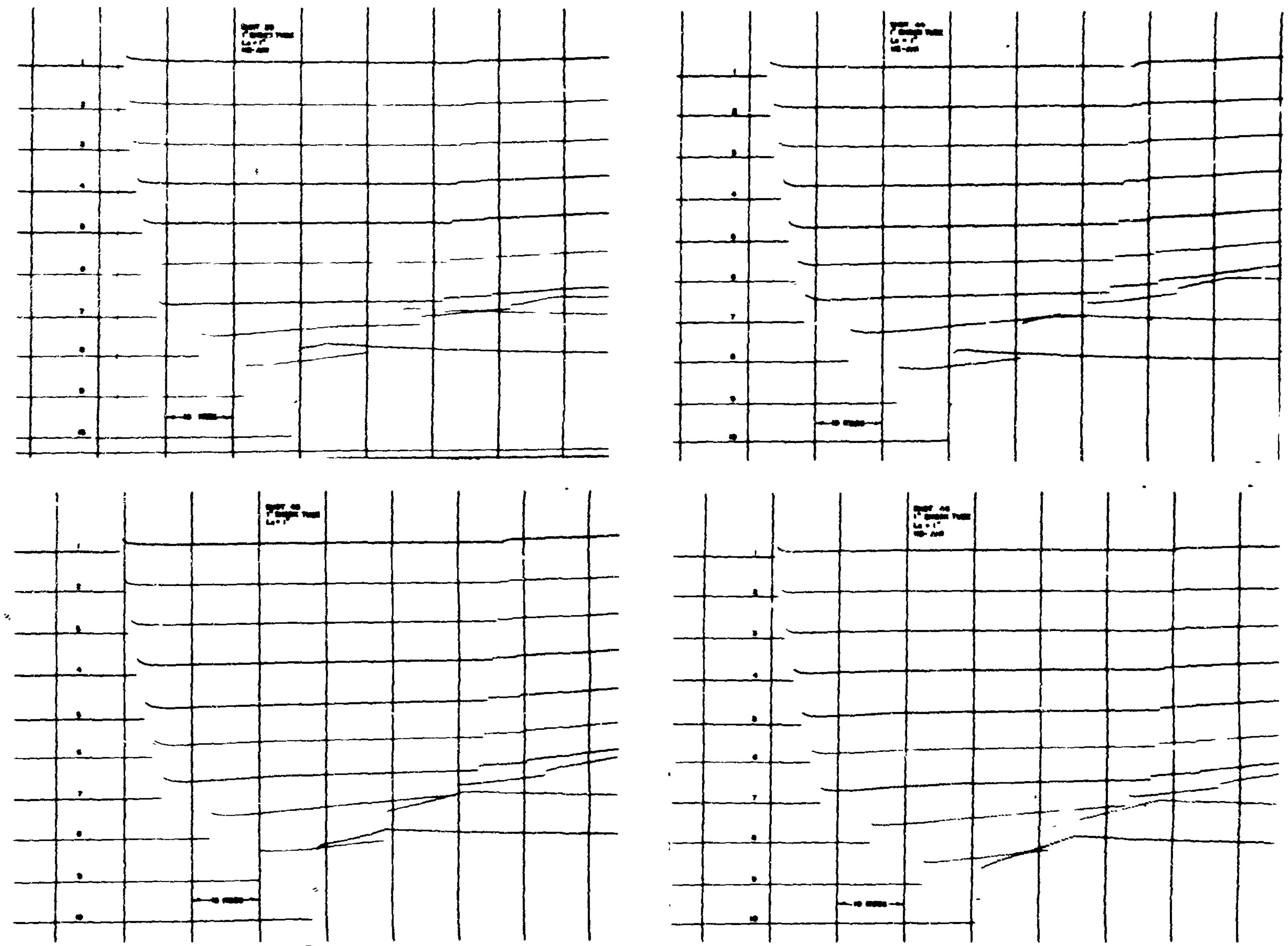

FIG. A-1A (CONTD)

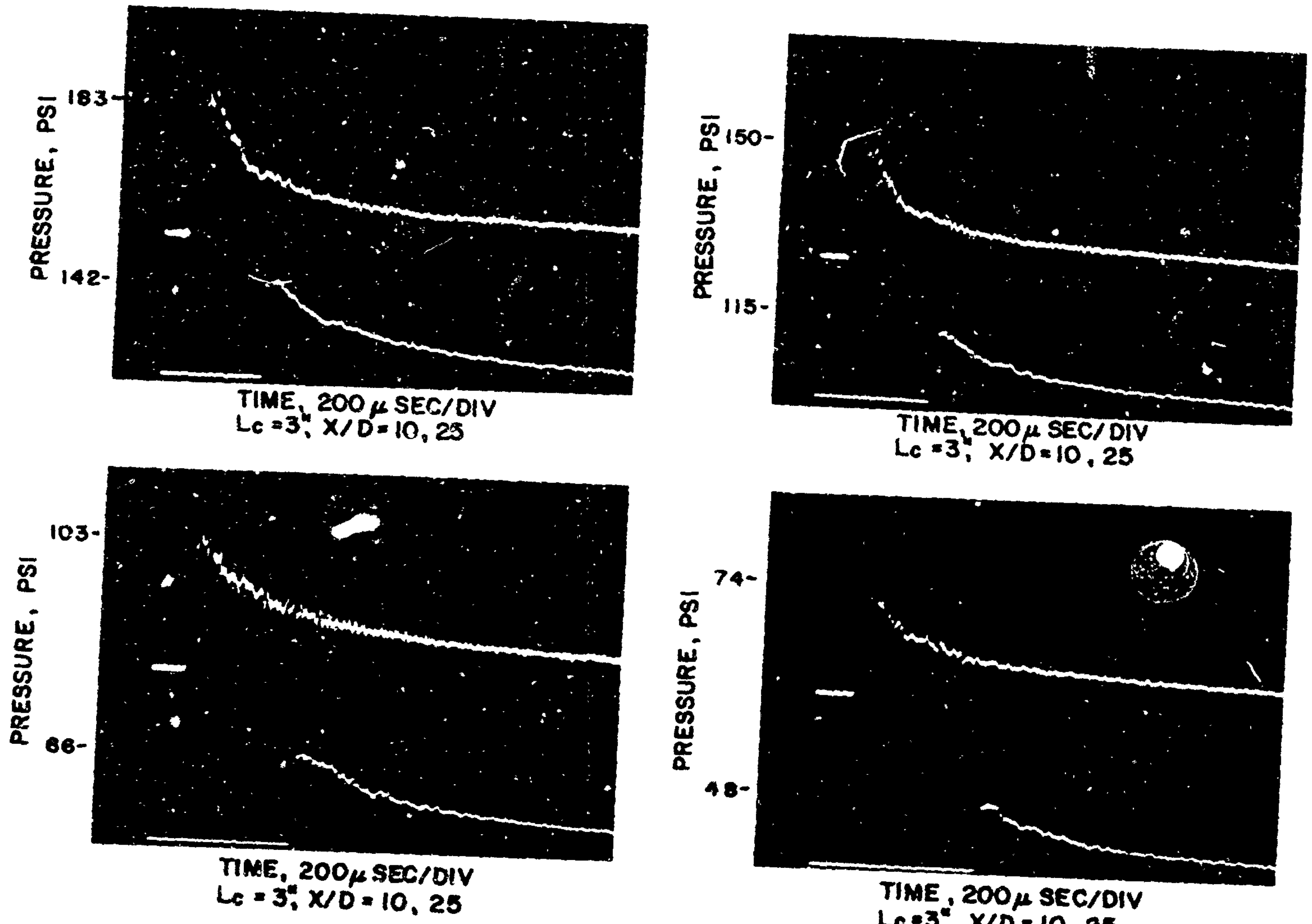

FIG. A-1B PRESSURE-TIME RECORDS FROM 1-INCH SHOCK TUBE-HELIUM DRIVER

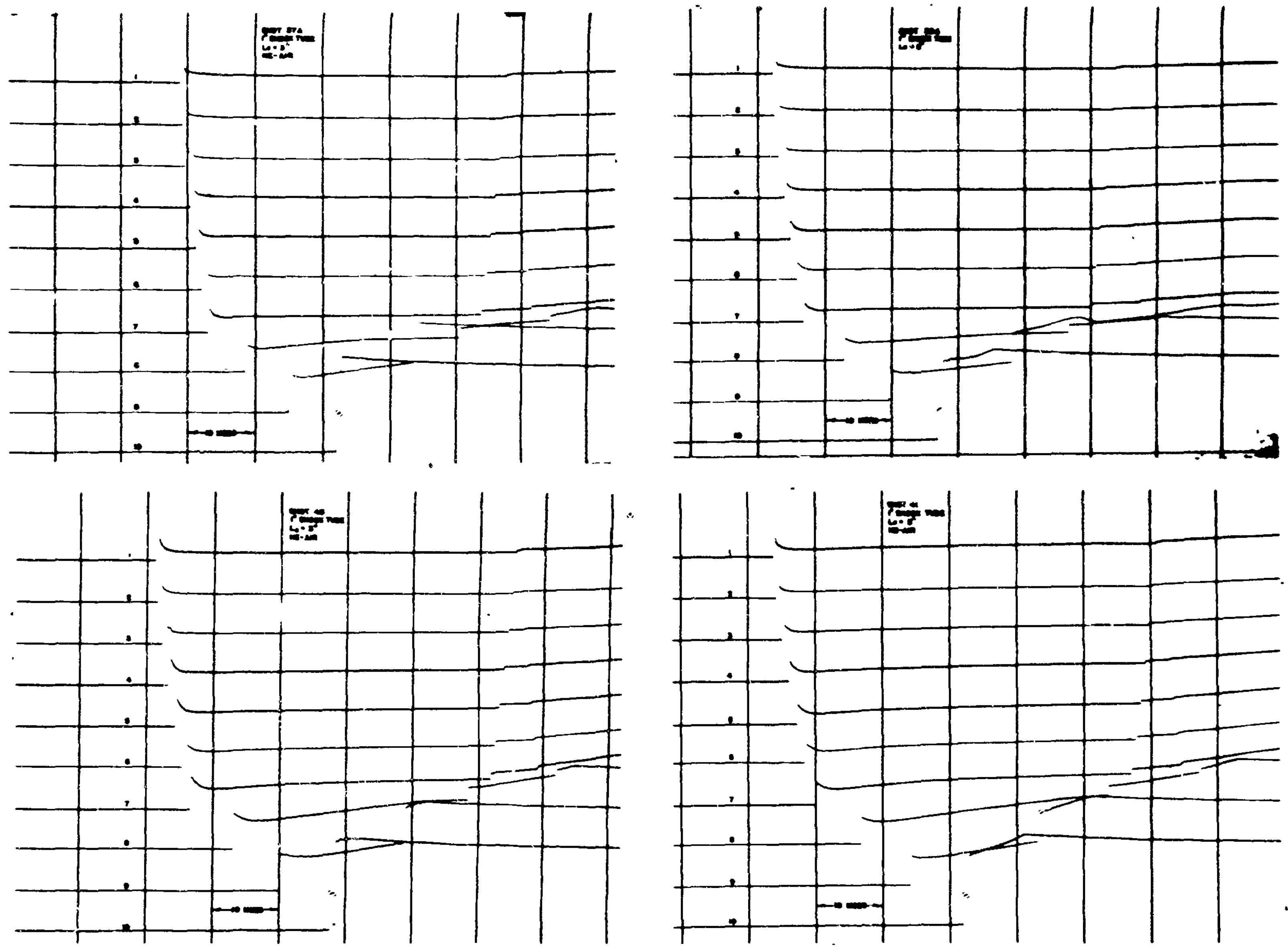

FIG. A-1B (CONTD)

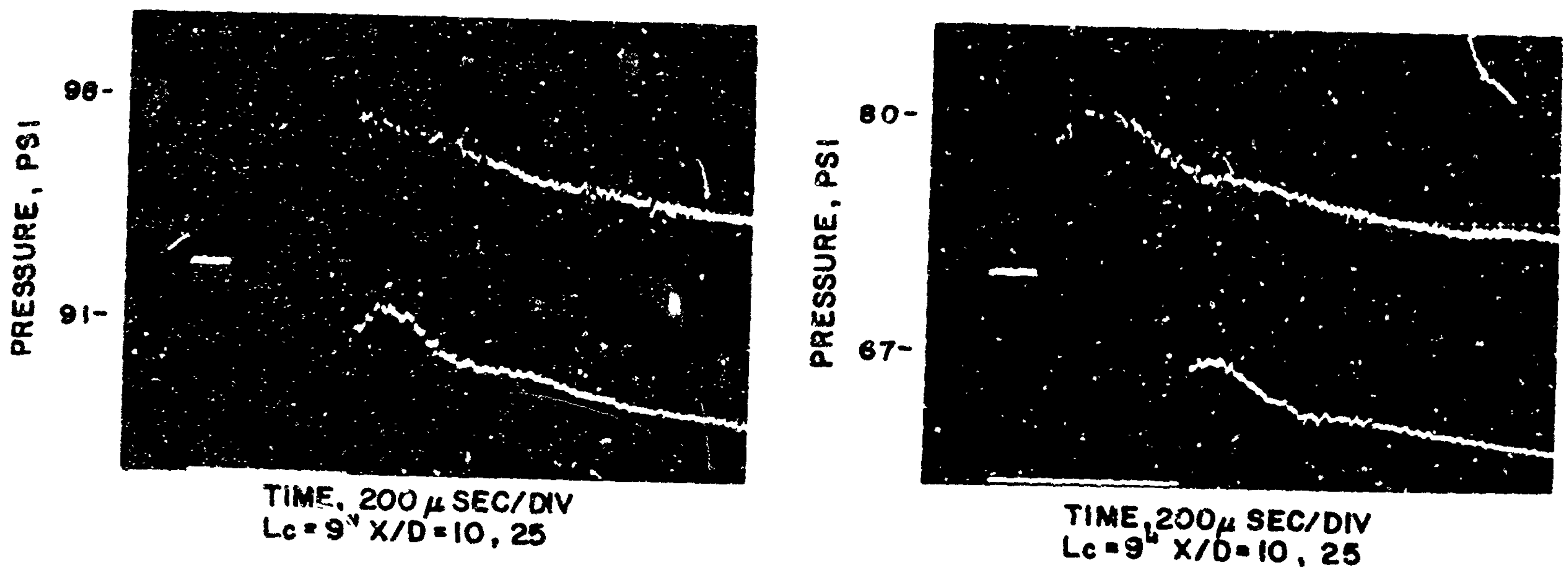

FIG.A-1C PRESSURE - TIME RECORDS FROM 1-INCH SHOCK TUBE - HELIUM DRIVER

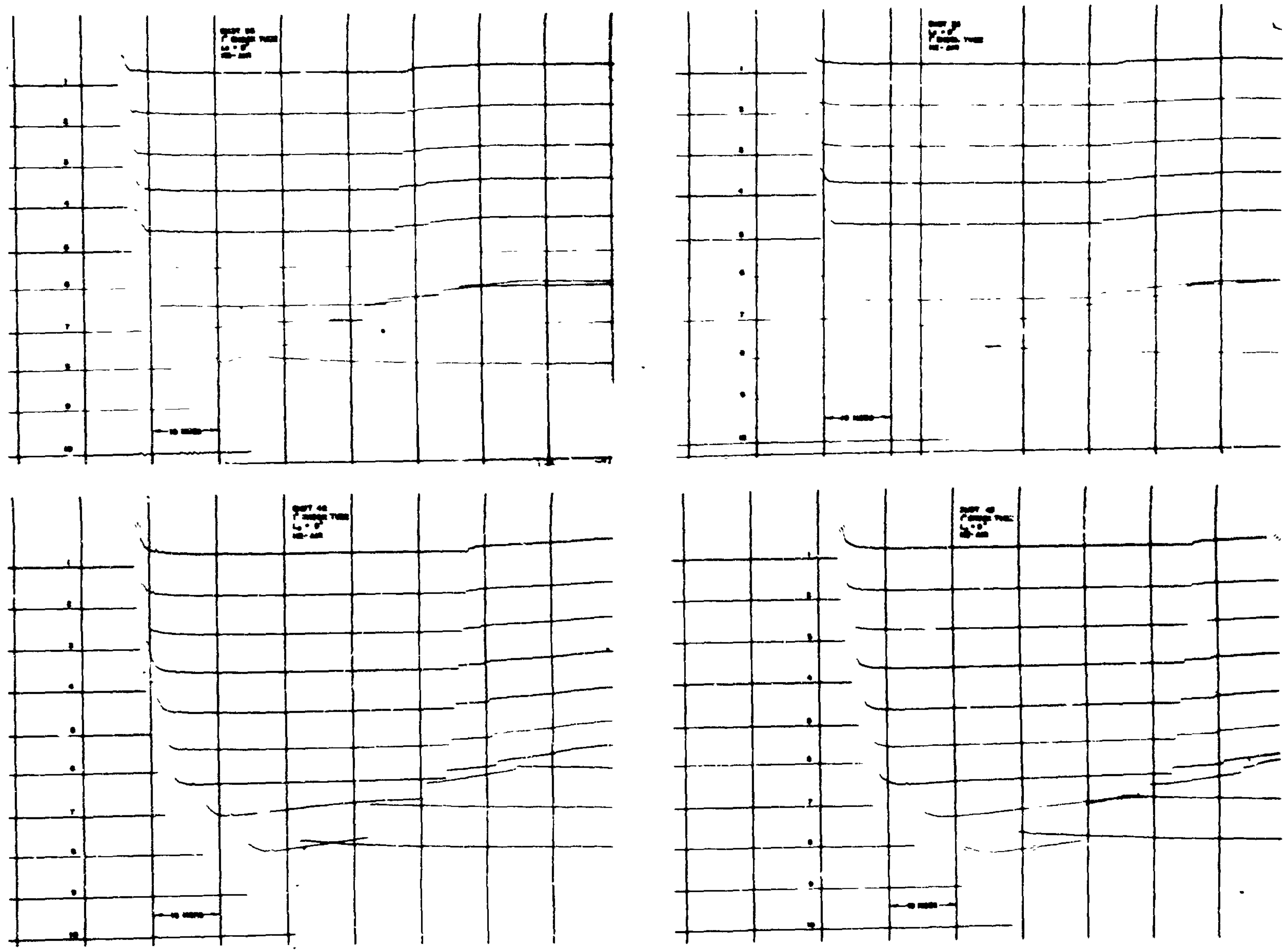

FIG. A-1C (CONTD)

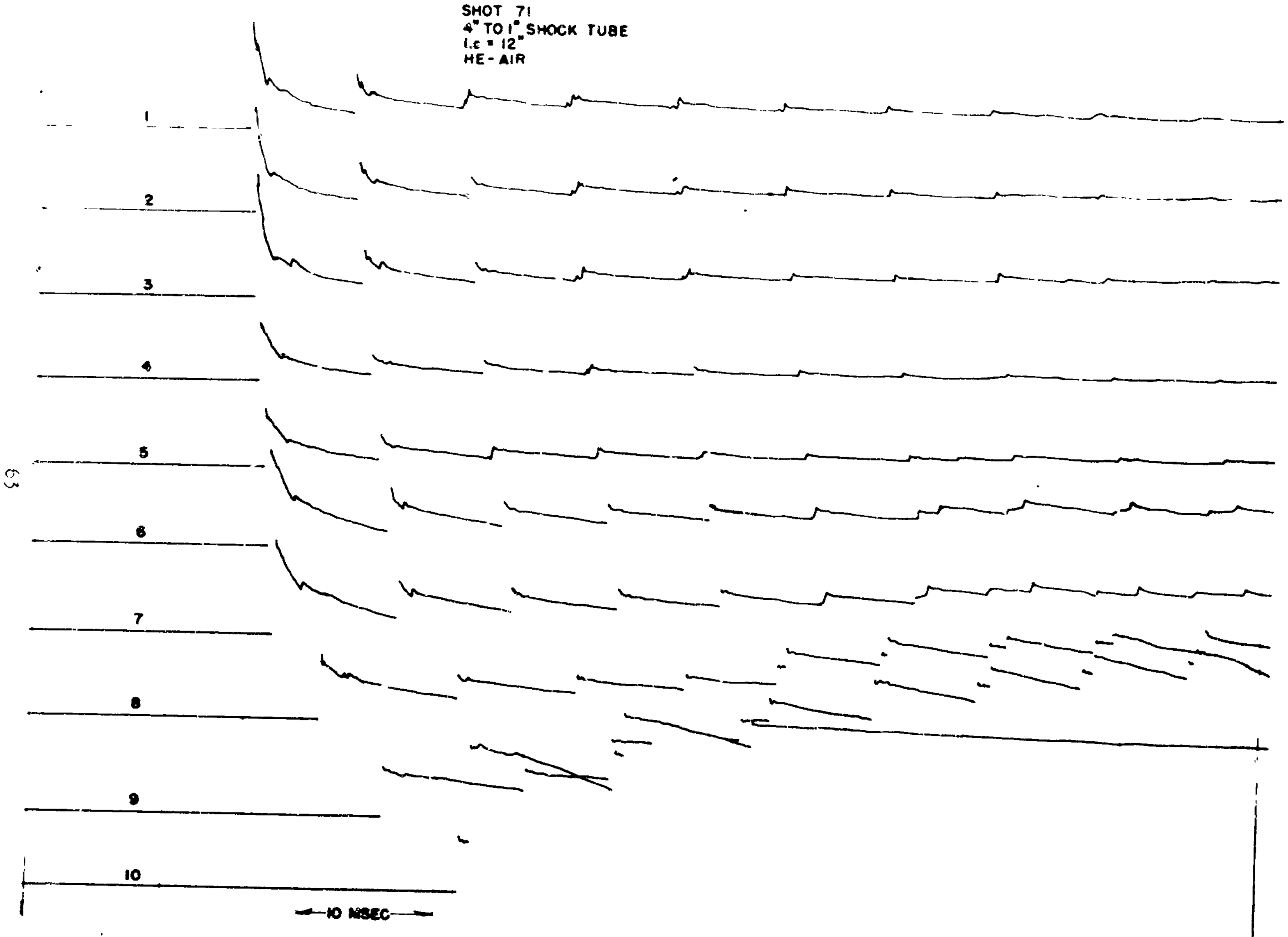

FIG. A-2 PRESSURE-TIME RECORDS FROM 1-INCH SHOCK TUBE-DISCONTINUOUS AREA CHANGE-16:1

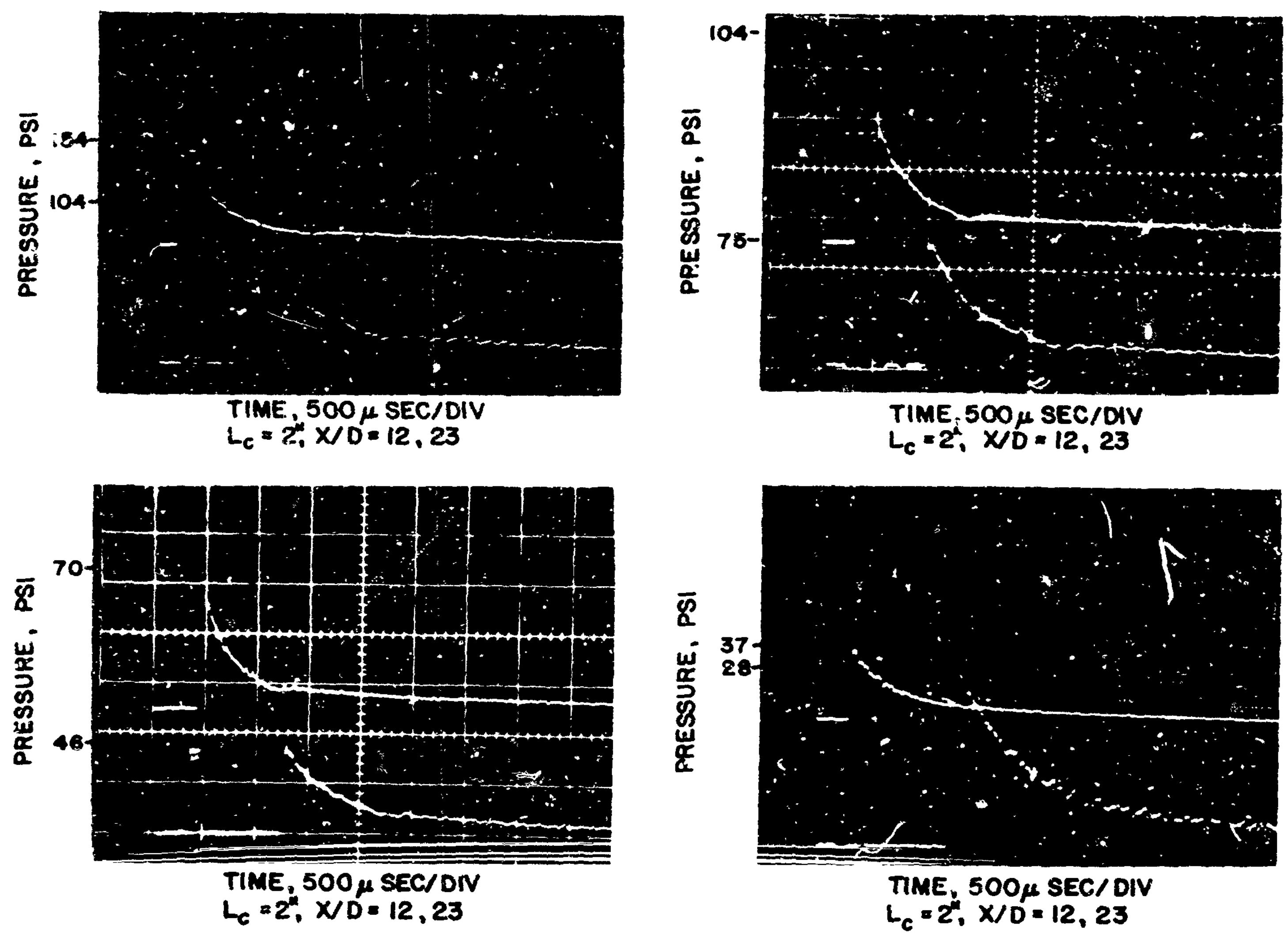

FIG. A-3A PRESSURE-TIME RECORDS FROM 2-INCH SHOCK TUBE-HELIUM DRIVER

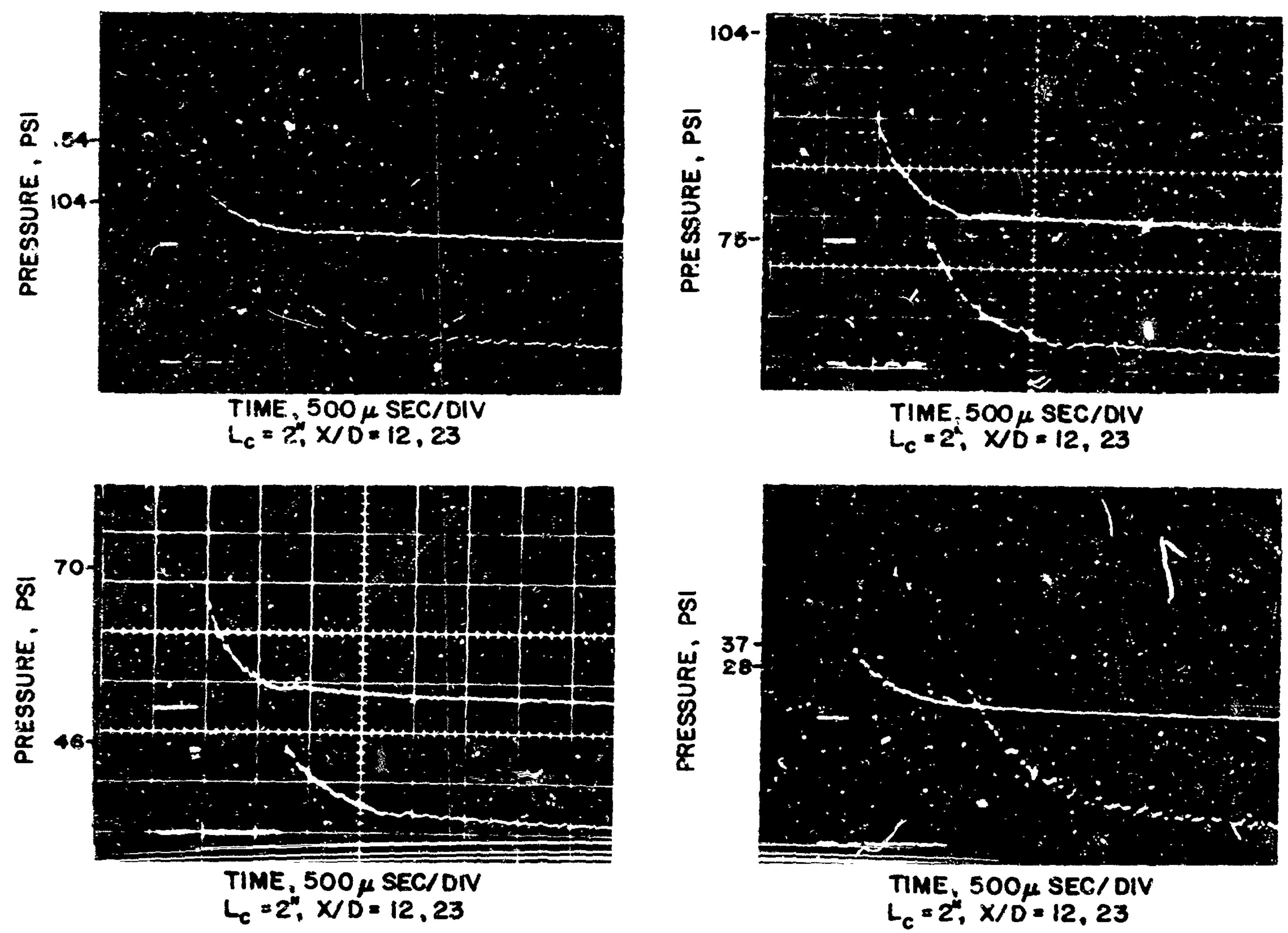

FIG. A-3A PRESSURE-TIME RECORDS FROM 2-INCH SHOCK TUBE-HELIUM DRIVER

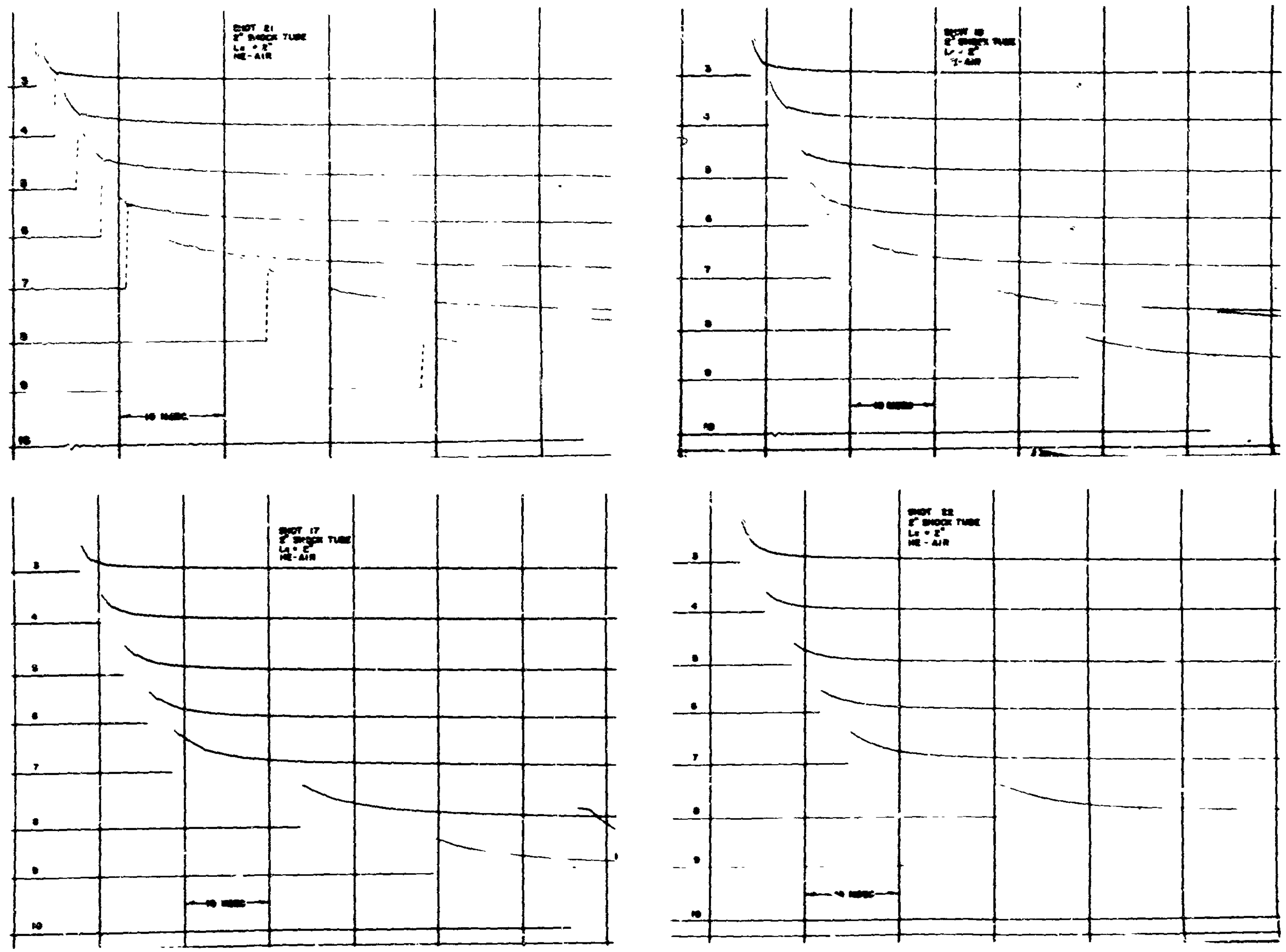

FIG. A-3 A (CONTD)

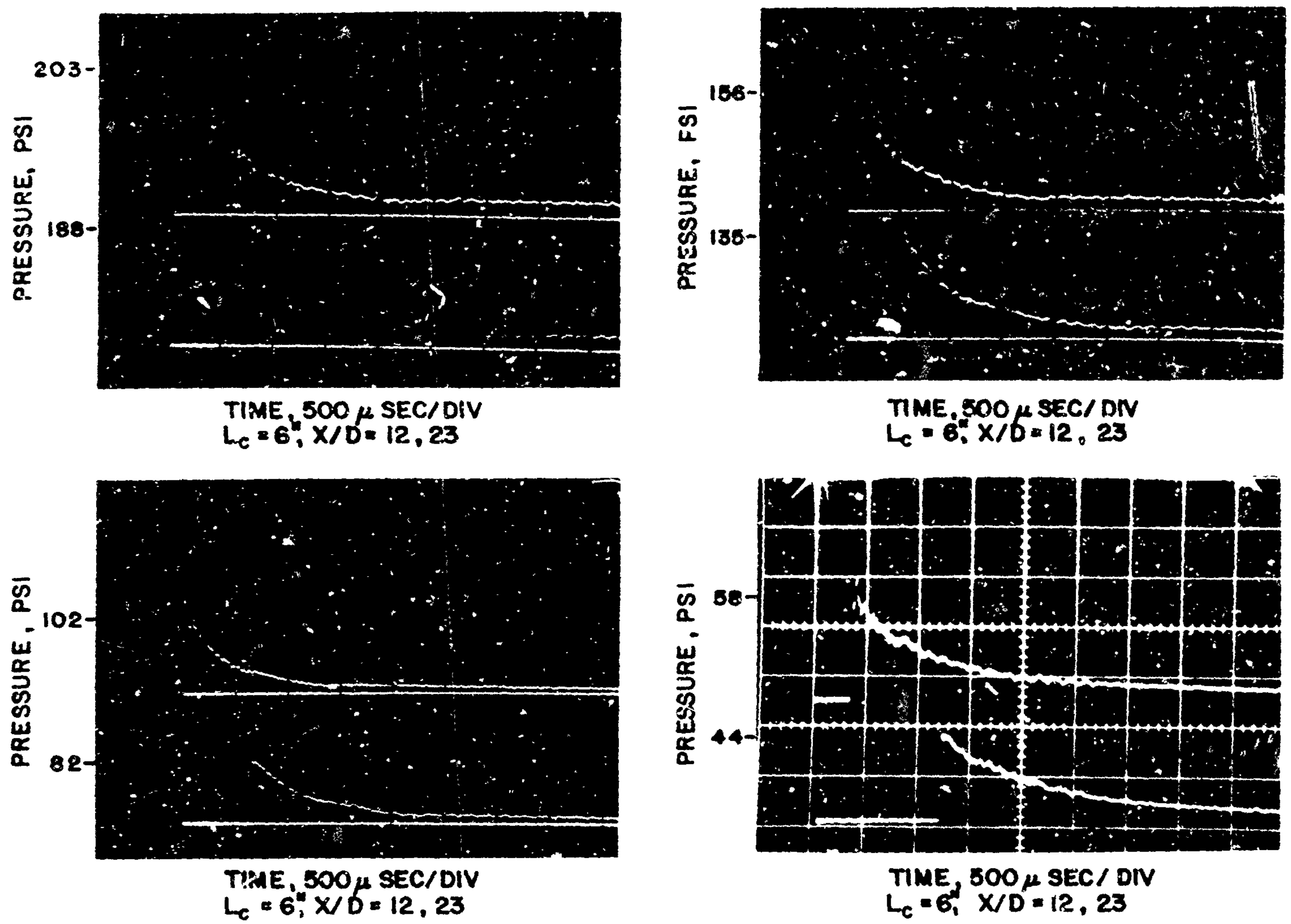

FIG. A-3B PRESSURE-TIME RECORDS FROM 2-INCH SHOCK TUBE-HELIUM DRIVER

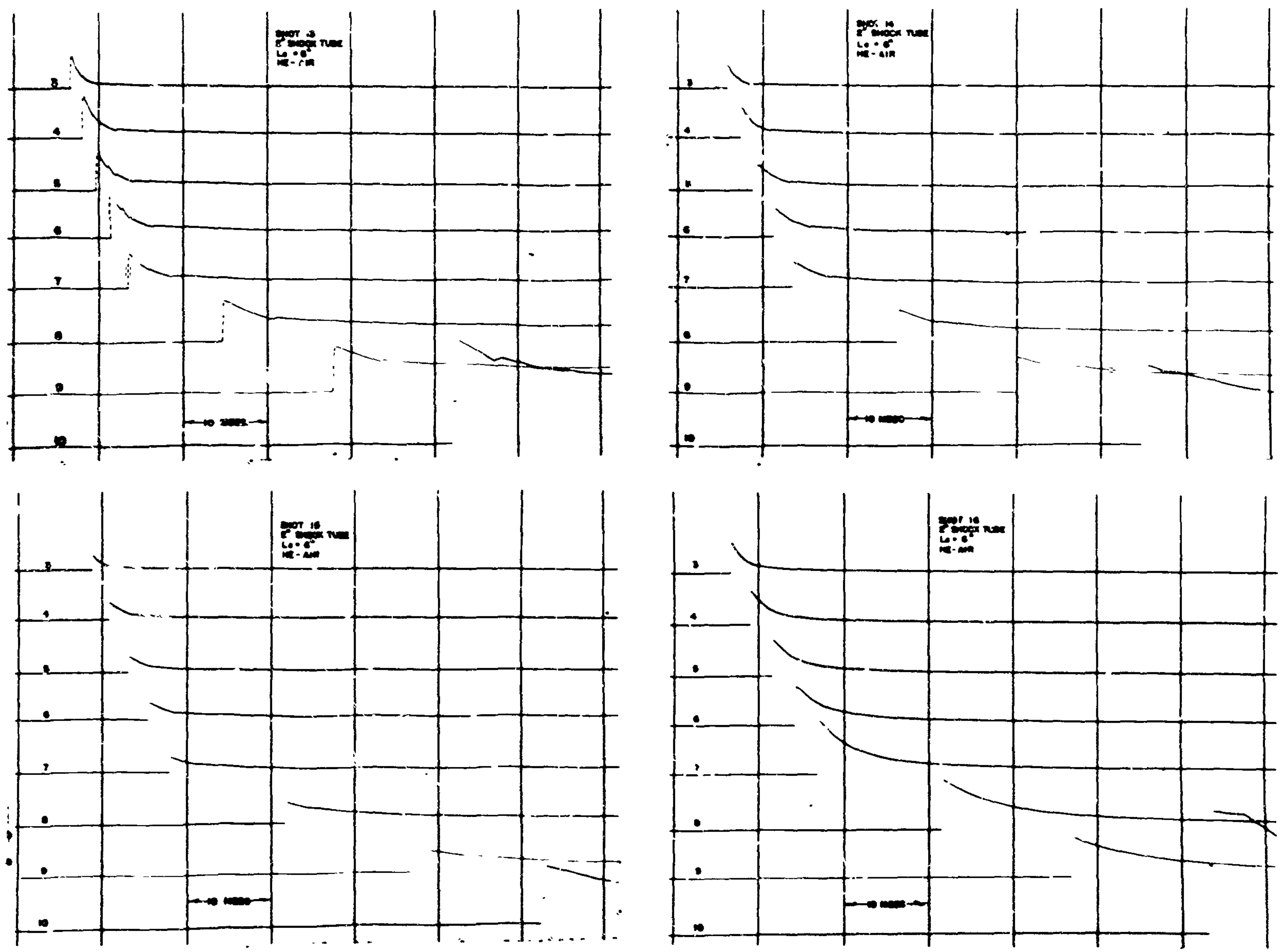

FIG. A-3B (CONTD)

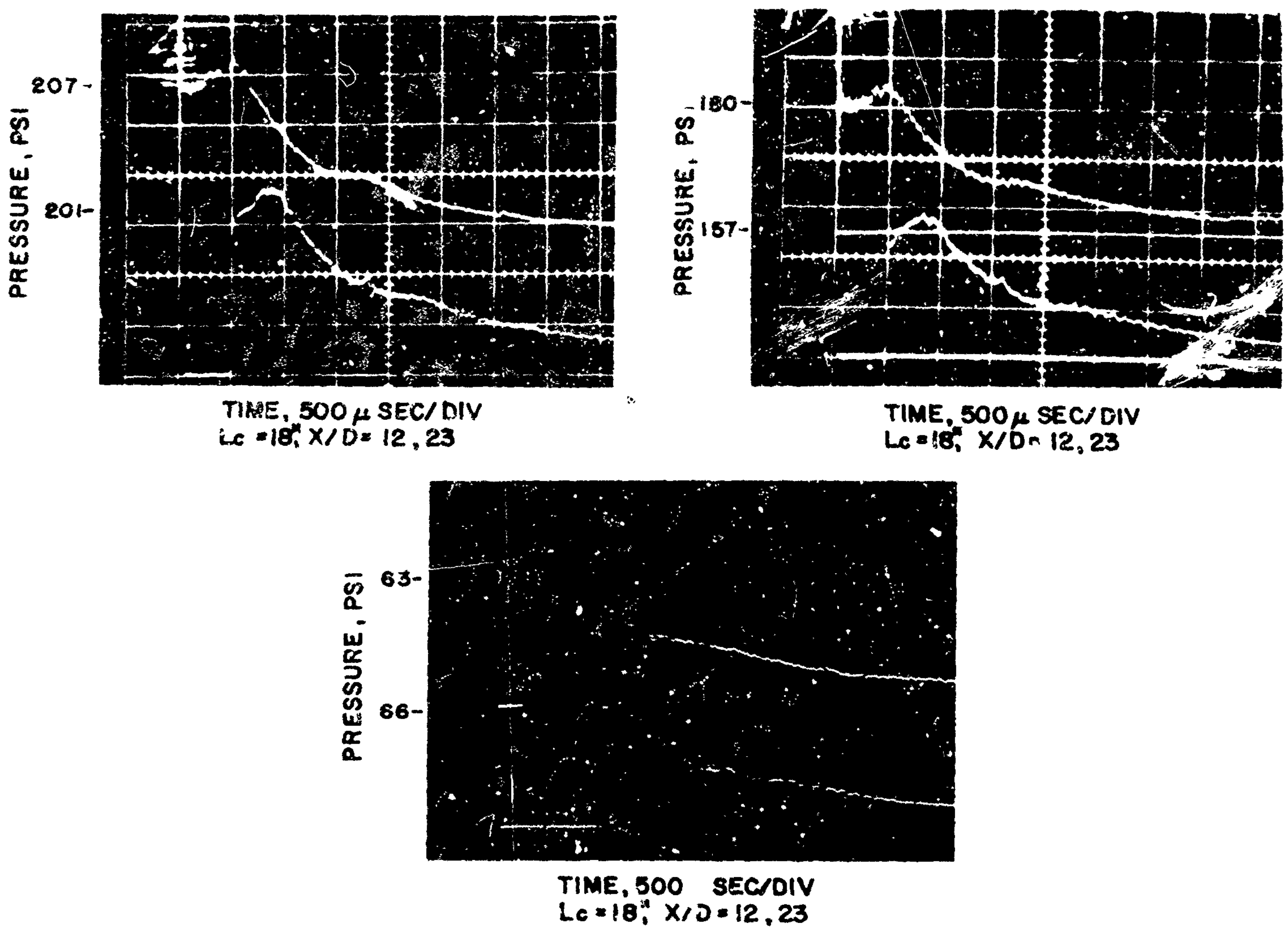

FIG. A-3C PRESSURE - TIME RECORDS FROM 2-INCH SHOCK TUBE - HELIUM DRIVER

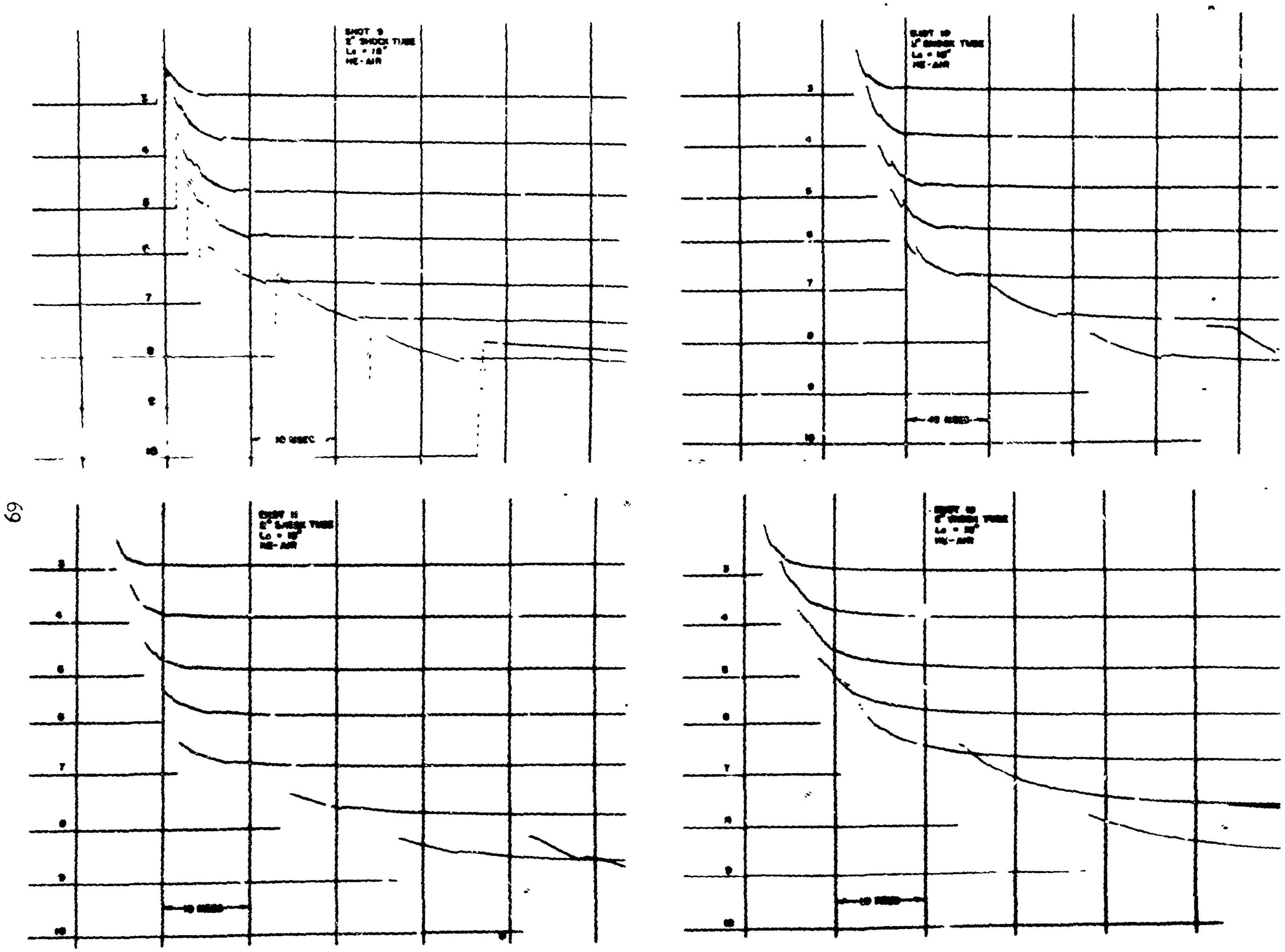

FIG. A-3 C (CONTD)

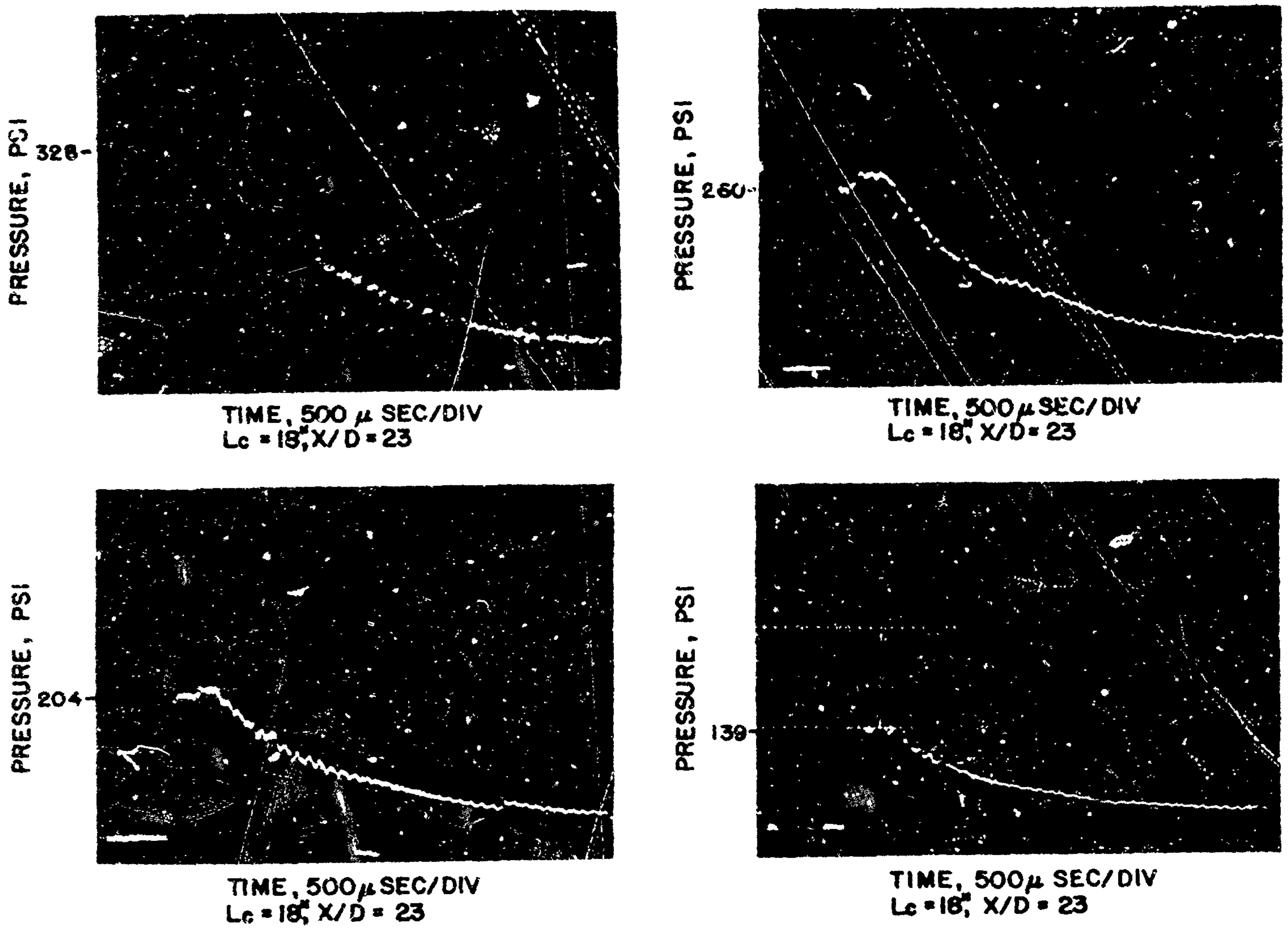

FIG. A-4 PRESSURE-TIME RECORDS FROM 2-INCH SHOCK TUBE - M-9 PROPELLANT DRIVER

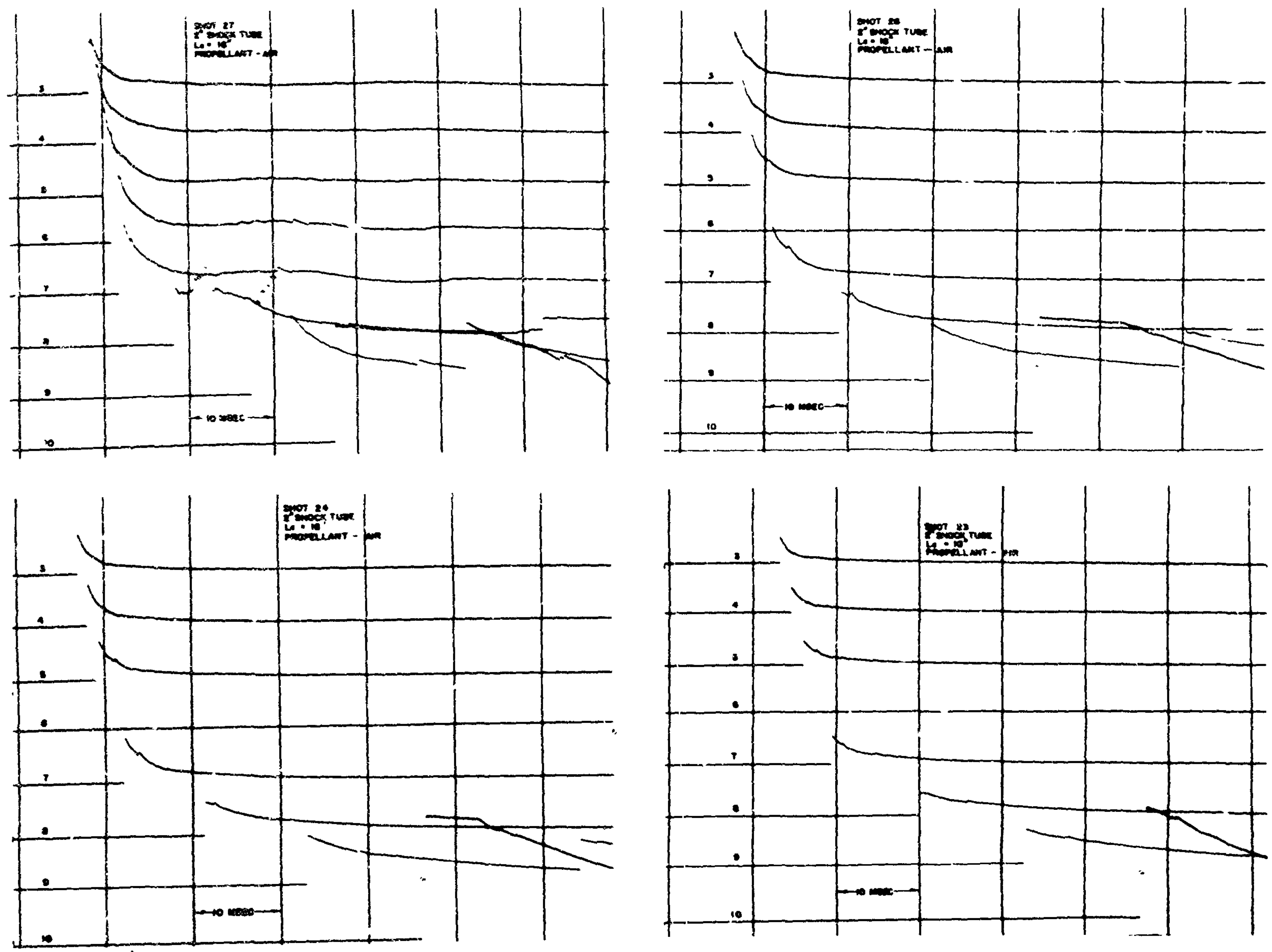
SHOT 27
2" SHOCK TUBE
PROPELLANT - AIR
10 MSEC
SHOT 26
2" SHOCK TUBE
PROPELLANT — AIR
10 MSEC
SHOT 24
2" SHOCK TUBE
PROPELLANT - AIR
10 MSEC
SHOT 23
2" SHOCK TUBE
10 MSEC

FIG. A-4 (CONTD)

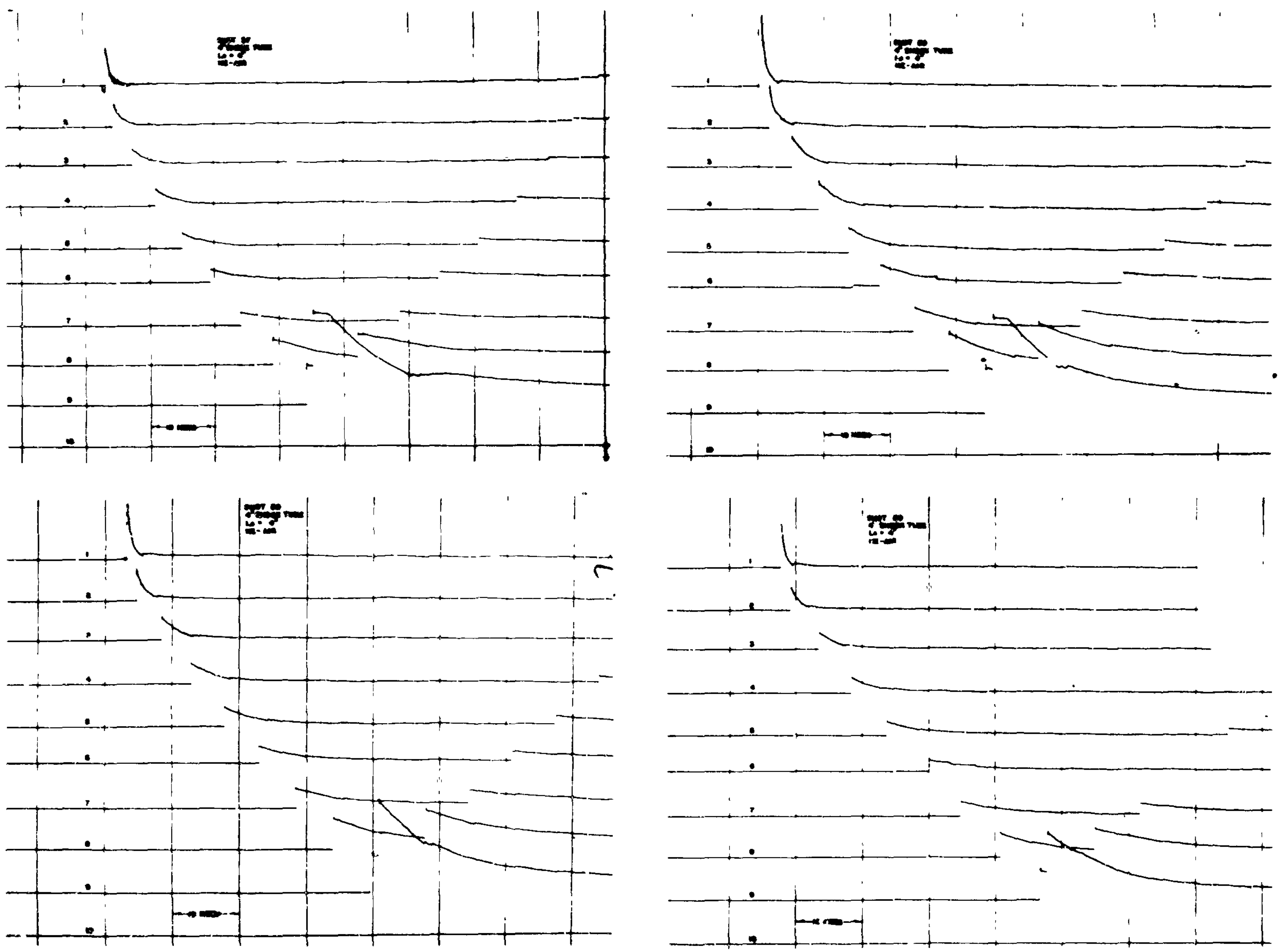

FIG. A-5A PRESSURE-TIME RECORDS FROM 4-INCH SHOCK TUBE - HELIUM DRIVER

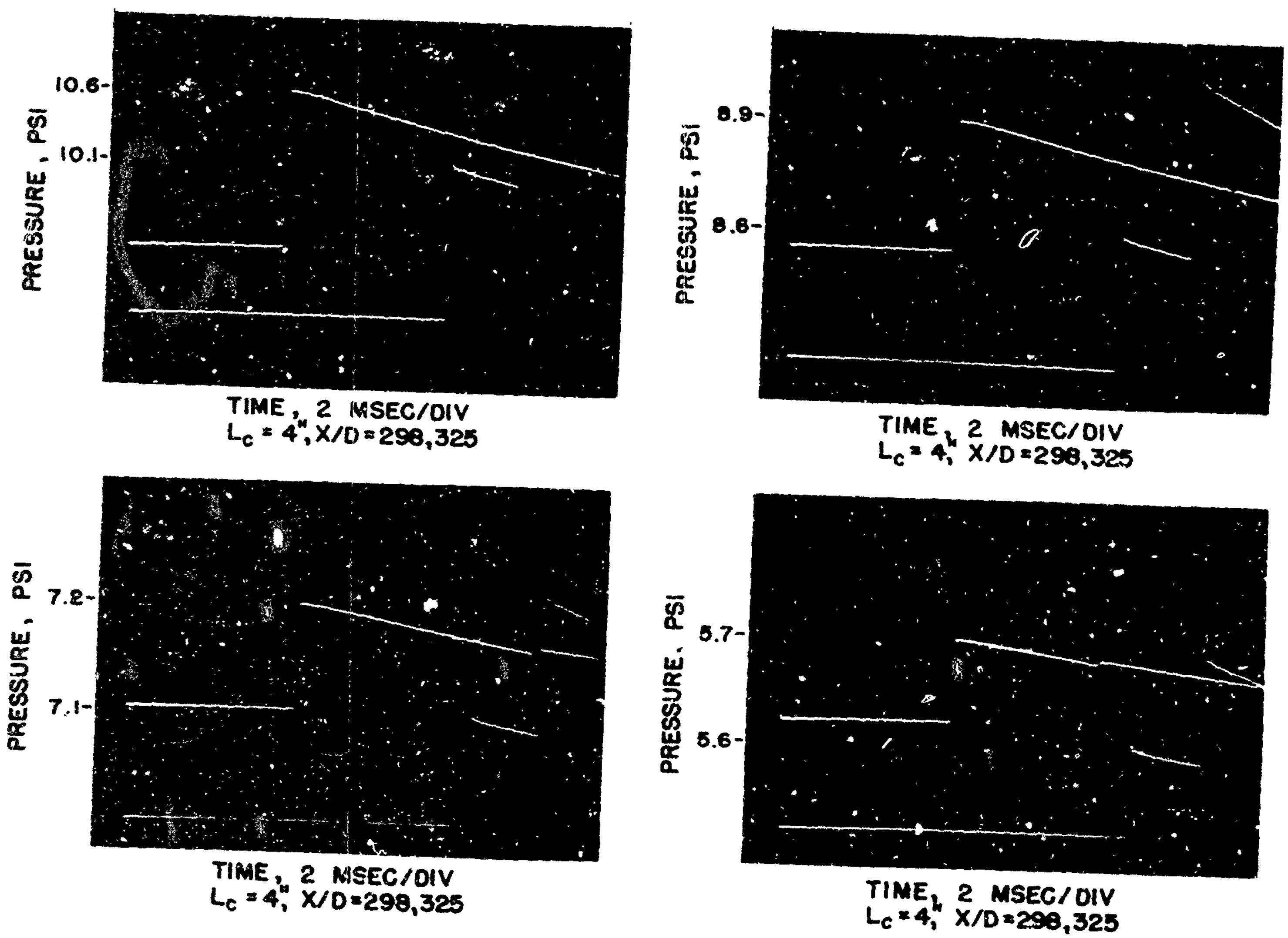

FIG. A-5A (Contd) POSITIONS 10 AND 11

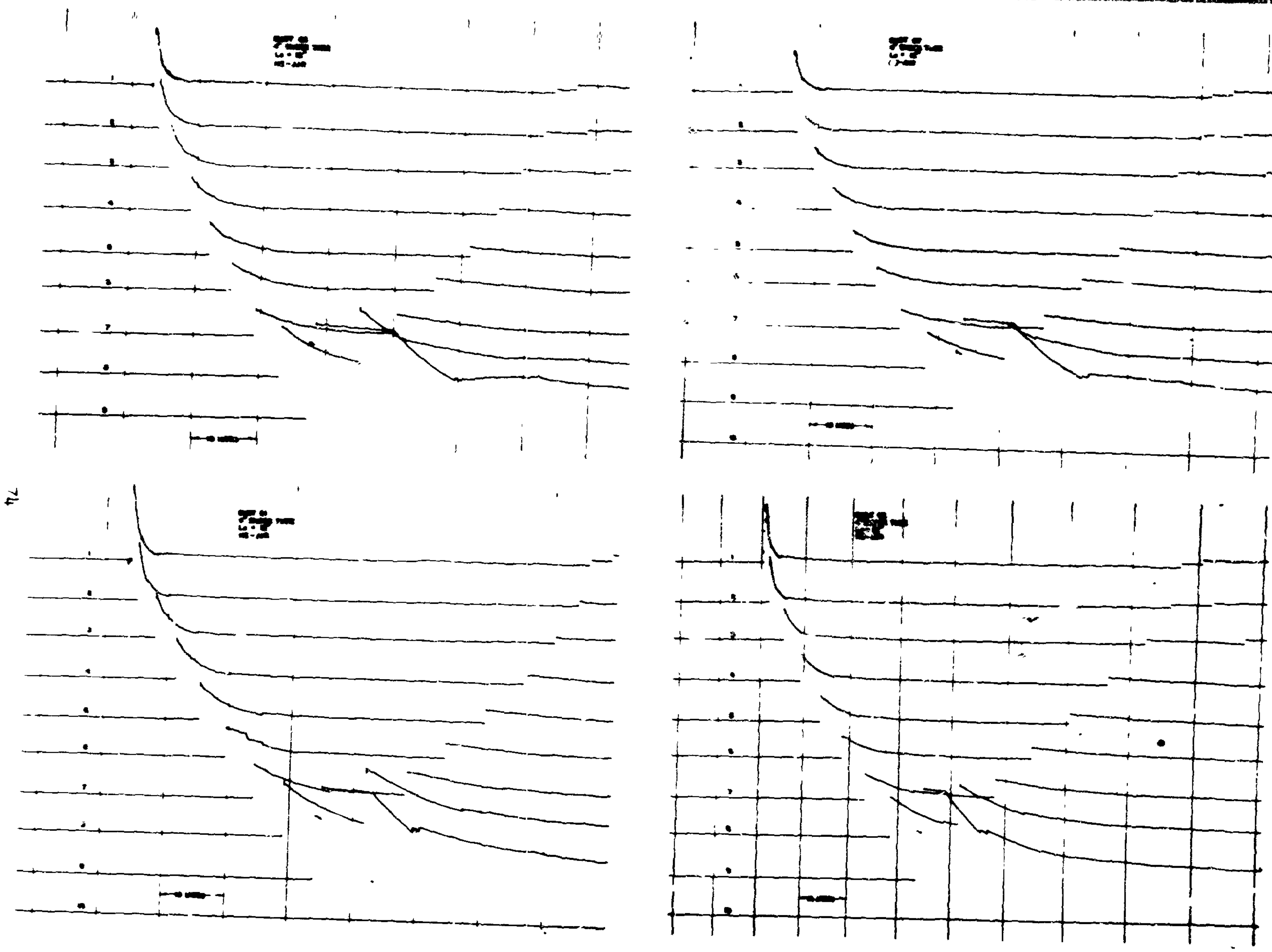

FIG. A-5B PRESSURE-TIME RECORDS FROM 4-INCH SHOCK TUBE - HELIUM DRIVER

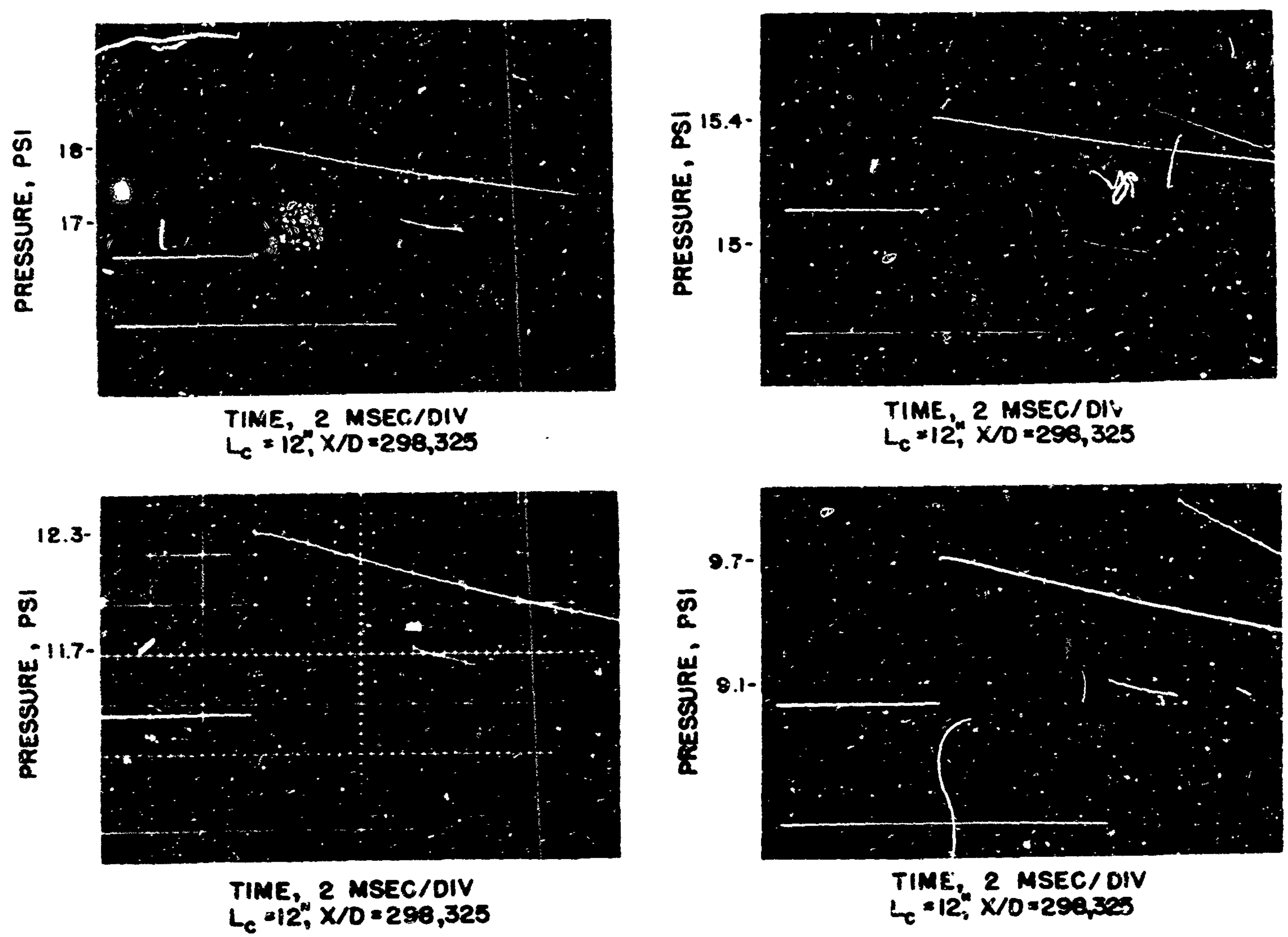

FIG. A-5B (Contd) POSITIONS 10 AND 11

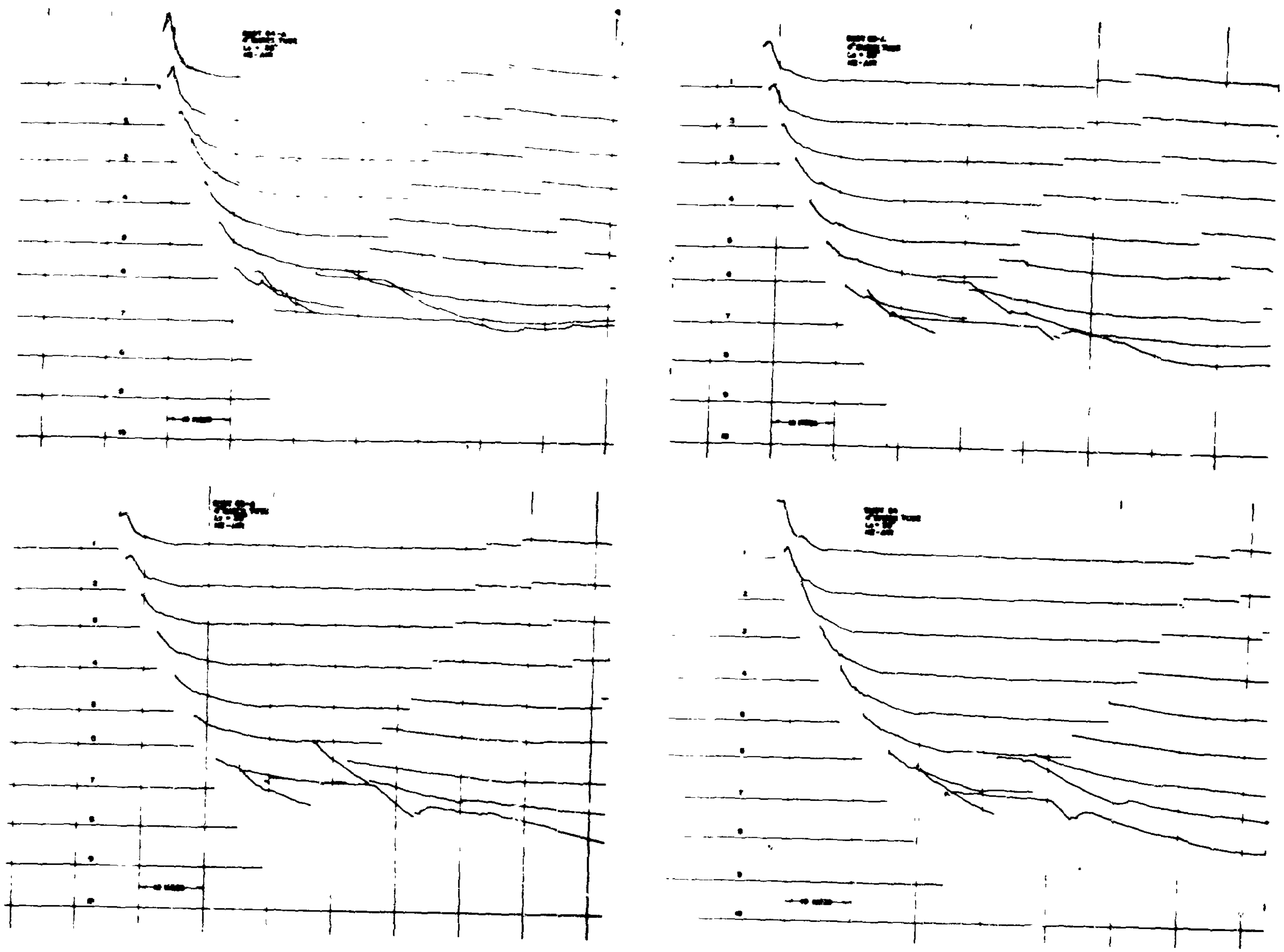

FIG. A-5C PRESSURE-TIME RECORDS FROM 4-INCH SHOCK TUBE - HELIUM DRIVER

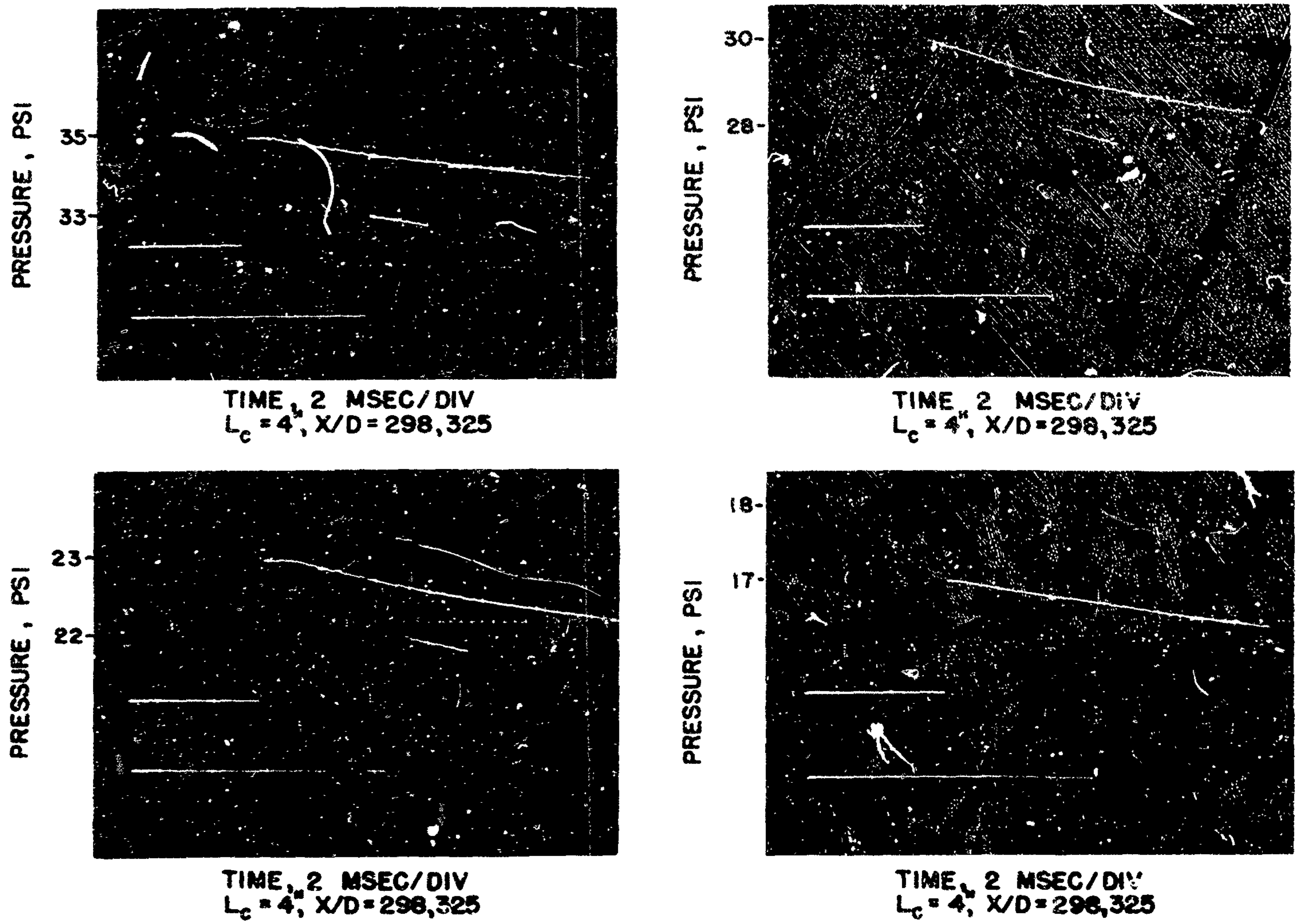

FIG. A-5C (Contd) POSITIONS 10 AND 11

APPENDIX B

TABLES OF ATTENUATION DATA

TABLE B-I

ATTENUATION OF PEAKED SHOCK WAVES IN 1-INCH SHOCK TUBE - HELIUM DRIVER

Shot No.			Shot 39		Shot 44		Shot 45		Shot 46		
Pos No.	$\frac{X}{D}$	X, ft.	P_s, psi	t_i, ms	P_s, psi	t_i, ms	P_s, psi	t_i, ms	P_s, psi	t_i, ms	L_c, in.
1	10	0.83	157	0.34	95	0.42	80	0.36	55	0.47	
2	25	2.08	88	0.46	65	0.59	41	0.47	27	0.84	
3	45	3.75	59	0.83	45	0.84	30	1.25	20	1.32	
4	70	5.83	43	1.56	32	1.36	27	2.29	15	3.03	
5	95	7.92	33	4.15	25	2.09	18	4.01	13	4.18	1
6	120	10.00	28	5.56	21	7.74	16	5.62	11	4.86	
7	145	11.99	27	7.11	18	9.94	14	7.08	10	7.35	
8	270	22.50	16	19.3	12	22.5	10	33.9	7	11.6	
9	395	32.92	12	-	9.7	58.0	8.1	24.6	6.4	29.0	
10	520	43.33	8.8	-	7.4	-	6.2	-	5.2	-	
Shot No.			Shot 37A		Shot 38A		Shot 40		Shot 41		
1	10	0.83	183	0.41	150	0.47	103	0.71	74	0.45	
2	25	2.08	142	0.62	115	0.63	66	0.73	48	0.58	
3	45	3.75	100	1.13	76	1.15	53	1.04	34	1.26	
4	70	5.83	71	1.49	55	1.46	40	1.77	27	1.95	3
5	95	7.92	60	1.80	49	1.88	32	2.40	21	2.96	
6	120	10.00	43	2.42	38	2.41	28	3.28	18	4.76	
7	145	11.99	46	2.67	33	3.40	24	4.09	16	5.86	
8	270	22.50	22	5.97	17	8.16	14	8.75	10	9.83	
9	395	32.92	15	28.3	12	19.8	10	26.1	8	18.4	
10	520	43.33	9.9	-	8.2	-	7.5	-	6.1	-	
Shot No.			Shot 35		Shot 36		Shot 42		Shot 43		
1	10	0.83	191	Step	166	Step	98	Step	80	Step	
2	25	2.08	192	0.90	161	-	91	0.78	67	0.76	
3	45	3.75	187	1.26	140	1.15	88	0.89	64	0.93	
4	70	5.83	147	1.31	104	1.36	67	1.71	49	2.07	
5	95	7.92	118	1.41	81	1.41	56	1.76	38	2.28	9
6	120	10.00	98	1.99	68	2.44	50	2.08	34	2.75	
7	145	11.99	78	1.88	60	3.12	45	2.33	30	2.95	
8	270	22.50	38	3.85	29	4.37	21	5.08	15	5.65	
9	395	32.92	23	9.56	18	8.69	14	14.7	11	16.6	
10	520	43.33	14	-	11	-	10	-	8.1	-	

TABLE B-II

ATTENUATION OF PEAKED SHOCK WAVES IN 1-INCH SHOCK TUBE - DISCONTINUOUS AREA CHANGE - 16:1

Shot No.			Shot 71			
Pos. No.	$\frac{X}{D}$	X, ft	P_s, psi	t_i, ms	L_c, in.	Remarks
1A	5	0.42	466	1.07		A 15° cone was used to
1	10	0.83	436	1.71		smoothly converge the
2	25	2.08	404	1.21		area of the 4" shock tube
3	45	3.75	396	1.28	12	to the 1" shock tube. The
4	70	5.83	270	2.17		distance of travel is
5	95	7.92	239	2.62		measured from the
6	120	10.00	181	3.26		beginning of the 1" section.
7	145	11.99	151	3.48		
8	270	22.50	77	4.78		
9	395	32.92	34	7.34		
10	520	43.33	23	12.40		

TABLE B-III

ATTENUATION OF PEAKED SHOCK WAVES IN 2-INCH SHOCK TUBE - HELIUM DRIVER

Shot No.			Shot 21		Shot 18		Shot 17		Shot 22		
Pos. No.	$\frac{X}{D}$	X,ft.	P_s, psi	t_1,ms	P_s, psi	t_1, ms	P_s,psi	t_1,ms	P_s,psi	t_1,ms	L_c, in.
1	12	2.00	154	0.42	104	0.35	70	0.35	37	0.68	
2	23	3.83	104	0.75	75	0.70	46	0.72	28	1.03	
3	48	8.00	59	1.30	37	1.58	27	1.92	18	2.11	
4	73	12.17	44	2.15	30	2.37	18	2.65	14	2.76	
5	98	16.33	31	3.49	22	3.68	14	3.59	11	4.11	2
6	123	20.50	28	4.16	19	4.84	14	4.63	10	4.58	
7	148	24.67	22	5.36	16	5.68	10	4.88	8.7	5.61	
8	273	45.50	13	10.48	10	9.54	8	14.30	5.9	12.40	
9	398	66.33	8.3	27.91	6.9	11.80	5.4	15.20	4.3	13.10	
10	523	87.17	6.4	-	5.2	-	4.3	-	3.4	-	
Shot No.			**Shot 13**		**Shot 14**		**Shot 15**		**Shot 16**		
1	12	2.00	203	Step	156	Step	102	0.52	58	0.99	
2	23	3.83	188	0.70	135	0.81	82	0.79	44	1.04	
3	48	8.00	102	1.26	72	1.31	44	1.46	30	2.16	
4	73	12.17	77	2.46	54	2.31	31	2.71	22	3.31	
5	98	16.33	61	2.93	43	3.56	25	4.17	17	4.81	6
6	123	20.50	58	3.40	39	4.24	24	4.77	17	6.49	
7	148	24.67	41	3.82	30	5.14	18	6.35	13	6.61	
8	273	45.50	22	11.34	16	12.37	11	11.02	9.1	10.94	
9	398	66.33	15	15.85	11	16.99	8.1	13.24	6.3	11.11	
10	523	87.17	9.5	-	7.5	-	5.6	-	4.7	-	
Shot No.			**Shot 9**		**Shot 10**		**Shot 11**		**Shot 19**		
1	12	2.00	207	Step	180	Step	-	-	63	Step	
2	23	3.83	201	Step	151	Step	-	-	66	Step	
3	48	8.00	203	1.67	150	1.37	103	1.51	53	1.67	
4	73	12.17	160	2.20	111	2.23	77	2.11	45	2.54	18
5	98	16.33	124	2.99	88	2.77	61	2.53	32	5.71	
6	123	20.50	104	3.66	76	3.78	46	3.80	29	6.50	
7	148	24.67	88	3.66	60	4.02	34	4.64	24	8.23	
8	273	45.50	44	7.59	32	10.23	23	13.41	15	13.03	
9	398	66.33	27	14.23	20	15.66	16	16.00	9.2	20.34	
10	523	87.17	15.5	-	12	-	11	-	6.7	-	

TABLE B-IV

ATTENUATION OF PEAKED SHOCK WAVES IN 2-INCH
SHOCK TUBE - M-9 PROPELLANT DRIVER

Shot No.			Shot 27		Shot 26		Shot 24		Shot 23		
Pos. No.	$\frac{X}{D}$	X, ft.	P_s, psi	t_1, ms	P_s, psi	t_1, ms	P_s, psi	t_1, ms	P_s, psi	t_1, ms	L_c, in.
1	12	2.00	-	-	-	-	-	-		-	
2	23	3.83	328	Step	260	Step	204	Step	139	Step	
3	48	8.00	309	Step	255	2.72	201	1.51	132	1.54	
4	73	12.17	392	1.76	214	1.55	147	1.87	91	2.09	
5	98	16.33	362	1.91	168	1.99	120	2.29	80	2.87	18
6	123	20.50	345	2.01	-	-	-	-	-	-	
7	148	24.67	243	1.39	111	3.11	84	3.67	54	3.74	
8	273	45.50	80	5.43	45	11.34	34	10.15	24	12.46	
9	398	66.33	55	-	29	13.04	23	13.49	17	13.43	
10	523	87.17	37	-	17	-	14	-	11	-	

TABLE B-V

ATTENUATION OF PEAKED SHOCK WAVES IN
4-INCH SHOCK TUBE - HELIUM DRIVER

Shot No.			Shot 57		Shot 58		Shot 59		Shot 60		
Pos. No.	$\frac{X}{D}$	X, ft.	P_s, psi	t_i, ms	P_s, psi	t_i, ms	P_s, psi	t_i, ms	P_s, psi	t_i, ms	L_c, in.
1	12	4.00	142	0.91	119	0.91	98	0.56	78	0.70	
2	23	7.67	103	1.50	78	1.49	60	1.33	41	1.46	
3	48	16.00	58	2.67	45	2.93	34	3.10	25	3.51	
4	73	24.33	43	3.61	32	4.73	23	5.07	18	5.11	
5	98	32.67	33	5.87	24	6.06	18	6.19	14	6.22	
6	123	41.00	26	8.39	19	8.78	15	8.46	10	9.04	4
7	148	49.33	22	11.10	16	10.67	13	10.74	9.8	11.01	
8	173	57.67	19	12.60	14	12.14	12	11.81	9.1	11.51	
9	198	66.00	16	23.60	13	15.97	10	16.77	8.2	18.15	
10	298	99.33	11	-	8.9	-	7.2	-	5.7	-	
11	325	108.33	10	-	8.6	-	7.1	-	5.6	-	
Shot No.			Shot 66		Shot 67		Shot 61		Shot 62		
1	12	4.00	195	Step	155	Step	143	1.39	111	1.07	
2	23	7.67	190	1.94	143	1.74	109	1.82	79	1.65	
3	48	16.00	119	2.84	83	2.95	66	2.89	48	2.90	
4	73	24.33	84	3.93	61	4.02	48	4.24	35	4.24	
5	98	32.67	68	4.77	50	5.57	36	6.48	27	6.42	12
6	123	41.00	54	6.44	39	7.57	28	9.25	21	9.40	
7	148	49.33	41	8.96	33	10.43	24	10.91	18	10.89	
8	173	57.67	38	10.46	29	10.54	21	11.66	17	11.37	
9	198	66.00	30	-	24	17.70	19	13.67	14	15.25	
10	298	99.33	18	-	15.4	-	12.3	-	9.7	-	
11	325	108.33	17	-	15.0	-	11.7	-	9.1	-	
Shot No.			Shot 64A		Shot 65A		Shot 63A		Shot 64		
1	12	4.00	212	Step	156	Step	130	Step	114	Step	
2	23	7.67	205	Step	158	Step	128	Step	95	Step	
3	48	16.00	187	Step	143	Step	117	Step	87	2.94	
4	73	24.33	174	4.49	127	4.85	97	4.71	67	4.20	
5	98	32.67	148	4.92	105	5.00	81	5.19	54	5.17	36
6	123	41.00	116	5.59	84	6.24	64	6.58	43	7.75	
7	148	49.33	94	7.59	66	8.91	52	9.30	35	9.73	
8	173	57.67	-	-	60	-	46	9.75	31	11.26	
9	198	66.00	38	-	38	-	38	17.00	-	13.93	
10	298	99.33	35	-	30	-	23	-	18	-	
11	325	108.33	33	-	28	-	22	-	17	-	

Unclassified

Security Classification

DOCUMENT CONTROL DATA - R&D

(Security classification of title, body of abstract and indexing annotation must be entered when the overall report is classified)

1 ORIGINATING ACTIVITY (Corporate author) U.S. Army Ballistic Research Laboratories Aberdeen Proving Ground, Maryland	2a REPORT SECURITY CLASSIFICATION Unclassified 2b GROUP

3 REPORT TITLE

ATTENUATION OF PEAKED AIR SHOCK WAVES IN SMOOTH TUNNELS

4 DESCRIPTIVE NOTES (Type of report and inclusive dates)

5 AUTHOR(S) (Last name, first name, initial)

Coulter, George A.

6 REPORT DATE	7a TOTAL NO OF PAGES	7b NO OF REFS
November 1966	92	13

8a CONTRACT OR GRANT NO	9a ORIGINATOR'S REPORT NUMBER(S) Memorandum Report No. 1809
b PROJECT NO c DASA NWER Sub-Task 13.111 d	9b OTHER REPORT NO(S) (Any other numbers that may be assigned this report)

10 AVAILABILITY/LIMITATION NOTICES

Distribution of this document is unlimited.

11 SUPPLEMENTARY NOTES	12 SPONSORING MILITARY ACTIVITY USAMC, Washington, D.C. DASA, Washington, D.C.

13 ABSTRACT

The attenuation of shock-front pressure for peaked air shock waves was measured along straight smooth-wall test sections of 1-, 2-, and 4-inch inside diameter shock tubes over travel distances up to 520-tunnel diameters. Shock overpressure between 50 and 450 psi for an ambient pressure of 1 atmosphere were produced by the use of helium or by burning M-9 propellant in the driver section of shock tubes. The lengths of the shock tube driver sections were changed to vary the shape of the shock waveform which caused the shock-front pressure to attenuate differently with distance. Pressure-time records are shown from piezoelectric pressure gages placed at ten test positions along the shock tube.

Unclassified
Security Classification

14. KEY WORDS	LINK A		LINK B		LINK C	
	ROLE	WT	ROLE	WT	ROLE	WT
Shock Tubes						
Blast Wave Attenuation						
One Dimensional Expansion						
Protective Structure Design						

INSTRUCTIONS

1. ORIGINATING ACTIVITY: Enter the name and address of the contractor, subcontractor, grantee, Department of Defense activity or other organization (*corporate author*) issuing the report.

2a. REPORT SECURITY CLASSIFICATION: Enter the overall security classification of the report. Indicate whether "Restricted Data" is included. Marking is to be in accordance with appropriate security regulations.

2b. GROUP: Automatic downgrading is specified in DoD Directive 5200.10 and Armed Forces Industrial Manual. Enter the group number. Also, when applicable, show that optional markings have been used for Group 3 and Group 4 as authorized.

3. REPORT TITLE: Enter the complete report title in all capital letters. Titles in all cases should be unclassified. If a meaningful title cannot be selected without classification, show title classification in all capitals in parenthesis immediately following the title.

4. DESCRIPTIVE NOTES: If appropriate, enter the type of report, e.g., interim, progress, summary, annual, or final. Give the inclusive dates when a specific reporting period is covered.

5. AUTHOR(S): Enter the name(s) of author(s) as shown on or in the report. Enter last name, first name, middle initial. If military, show rank and branch of service. The name of the principal author is an absolute minimum requirement.

6. REPORT DATE: Enter the date of the report as day, month, year; or month, year. If more than one date appears on the report, use date of publication.

7a. TOTAL NUMBER OF PAGES: The total page count should follow normal pagination procedures, i.e., enter the number of pages containing information.

7b. NUMBER OF REFERENCES: Enter the total number of references cited in the report.

8a. CONTRACT OR GRANT NUMBER: If appropriate, enter the applicable number of the contract or grant under which the report was written.

8b, 8c, & 8d. PROJECT NUMBER: Enter the appropriate military department identification, such as project number, subproject number, system numbers, task number, etc.

9a. ORIGINATOR'S REPORT NUMBER(S): Enter the official report number by which the document will be identified and controlled by the originating activity. This number must be unique to this report.

9b. OTHER REPORT NUMBER(S): If the report has been assigned any other report numbers (*either by the originator or by the sponsor*), also enter this number(s).

10. AVAILABILITY/LIMITATION NOTICES: Enter any limitations on further dissemination of the report, other than those imposed by security classification, using standard statements such as:

(1) "Qualified requesters may obtain copies of this report from DDC."

(2) "Foreign announcement and dissemination of this report by DDC is not authorized."

(3) "U. S. Government agencies may obtain copies of this report directly from DDC. Other qualified DDC users shall request through ______."

(4) "U. S. military agencies may obtain copies of this report directly from DDC. Other qualified users shall request through ______."

(5) "All distribution of this report is controlled. Qualified DDC users shall request through ______."

If the report has been furnished to the Office of Technical Services, Department of Commerce, for sale to the public, indicate this fact and enter the price, if known.

11. SUPPLEMENTARY NOTES: Use for additional explanatory notes.

12. SPONSORING MILITARY ACTIVITY: Enter the name of the departmental project office or laboratory sponsoring (*paying for*) the research and development. Include address.

13. ABSTRACT: Enter an abstract giving a brief and factual summary of the document indicative of the report, even though it may also appear elsewhere in the body of the technical report. If additional space is required, a continuation sheet shall be attached.

It is highly desirable that the abstract of classified reports be unclassified. Each paragraph of the abstract shall end with an indication of the military security classification of the information in the paragraph, represented as *(TS)*, *(S)*, *(C)*, or *(U)*.

There is no limitation on the length of the abstract. However, the suggested length is from 150 to 225 words.

14. KEY WORDS: Key words are technically meaningful terms or short phrases that characterize a report and may be used as index entries for cataloging the report. Key words must be selected so that no security classification is required. Identifiers, such as equipment model designation, trade name, military project code name, geographic location, may be used as key words but will be followed by an indication of technical context. The assignment of links, rules, and weights is optional.